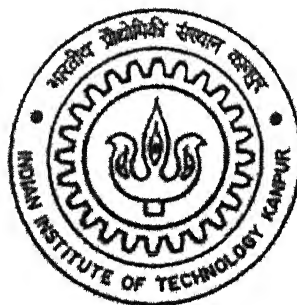# SOME STUDIES ON SEDIMENT CONSOLIDATION OF FLUIDIZED FLY ASH

by

M. RAJA SEKHAR

to the

Department of Civil Engineering

INDIAN INSTITUTE OF TECHNOLOGY

KANPUR – 208016, INDIA

July 2002

SOME STUDIES ON SEDIMENT CONSOLIDATION OF FLUIDIZED FLY ASH
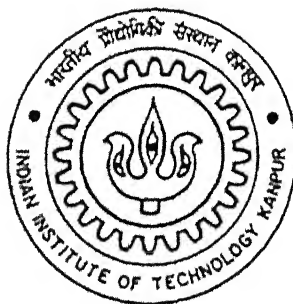
A Thesis
Submitted in Partial Fulfillment of the Requirements
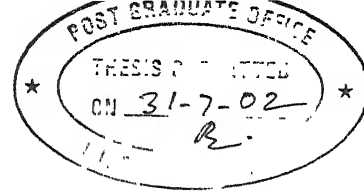*for the Degree of*

MASTER OF TECHNOLOGY

by

M. RAJA SEKHAR

to the
Department of Civil Engineering
INDIAN INSTITUTE OF TECHNOLOGY
KANPUR – 208016, INDIA

July 2002

CERTIFICATE

It is certified that the work contained in this thesis entitled, *"Some Studies on Sediment Consolidation of Fluidized Fly Ash"* by Sri **M. Raja Sekhar** has been carried out under our supervision and the same has not been submitted elsewhere for the award of any degree.

(A. Ghosh)

Scientist

Central Building Research institute

Roorkee-247667

(M.R. Madhav)

Professor

Department of Civil Engineering

I.I.T. Kanpur-208016

INDIAN INSTITUTE OF TECHNOLOGY

KANPUR – 208106.

JULY 2002

ABSTRACT

Most of the fly ash produced by Thermal Power Plants is disposed off in slurry form into ash ponds / lagoons / ash dykes. Fly ash released into the ponds undergoes sedimentation process, excess water is drained out, resulting in a very soft deposit. The fly ash particles come in contact and are ready to transfer stresses to each other. The soft deposit then undergoes consolidation, under its own weight, accompanied with large strains. The engineering properties of this sedimented and consolidated fly ash deposit could be very different from those based on compacted samples about which considerable literature exists. This thesis work presents experimental studies conducted to simulate the sedimentation and consolidation process of fluidized fly ash in ash ponds. A series of compressibility, consolidation and collapsible tests are conducted on the fly ash samples collected from the sedimented and consolidated deposits. Results show a pseudo-overconsolidation effect, compressibility increasing with stress and the collapse potential to be of the order of 0.5% for sedimented and consolidated fly ash samples. A new theory is proposed to estimate the variations of void ratio, unit weight and effective stress with depth in a natural sedimented and consolidated bed. A parametric study quantifies the effects due to variations in initial depositional void ratio, e_i, initial stress, σ'_o, rate of deposition, V, compression index, C_c, secondary compression index, C_α, specific gravity, G_s and time for sedimentation and consolidation, T_o.

ACKNOWLEDGEMENT

Keshava, Sreedhar, Satish, Mr. Sastry and Mr. Sarat Das for their cooperation during the course of this study.

I am also thankful to my classmates Neha Jain, Imran, Habib, Ajay, Avinash and others for their help and friendly nature during my stay at IIT, Kanpur.

I appreciate my friends Ravinder, Bhavani Sankar, Behra, Desai, Raghu, Kaustubh, Sandeep, and all others for their direct or indirect help during the course of study and stay at IIT, Kanpur.

M. Raja Sekhar

CONTENTS

LIST OF FIGURES

Fly Ash

LIST OF TABLES

LIST OF SYMBOLS

a	Ratio of natural water content (w_n)/liquid limit (w_L)
C_c	Compression index
C_{c_o}	Compression index at initial depositional void ratio (e_i)
C_s	Swell index
C_p	Collapse potential
C_α	Secondary compression index
e_i	Initial depositional void ratio
e_o	Natural void ratio of the fly ash sample
$e_{avg.}$	Average void ratio
Δe	Total change in void ratio
Δe_p	Primary compression
Δe_s	Secondary compression index
G_s	Specific gravity of solids
h	Depth of the deposit prior to sedimentation
H	Total thickness of the deposit after consolidation (final state)
H_o	Total thickness of the deposit prior to sedimentation
H_i	Initial thickness of the sample
ΔH_1 & ΔH_2	Vertical strains before and after flooding the dry sample with water
PI	Plasticity index
t	Time
t_e	Time required to achieve an infinitesimal initial effective stress, σ_o'
T_o	Time for sedimentation and consolidation
T_i^* & T_{i+1}^*	Normalized times for i^{th} & $(i+1)^{th}$ layers
V	Rate of deposition
V_f	Final sediment volume
V_s	Volume of solids
w_f	Final water content
w_i	Initial water content
w_s	Weight of solids
w_w	Weight of water

z	Depth of the deposit after consolidation (final state)
$\Delta \bar{z}_i$	Normalized depth of ith layer
Δz_i	Thickness of layer 'i'
γ_w	Unit weight of water
γ_{bo}	Initial submerged unit weight of the deposit, at the time of deposition
γ_b	Submerged unit weight of the deposit i.e. after consolidation
γ_{b_i}	Submerged unit weight of layer 'i'
γ_{bi}	Initial submerged unit weight at time of deposition
$\bar{\gamma}'$	Average unit weight of the deposit
σ_o'	Infinitesimal initial effective stress
σ_h'	Effective stress on the layer at any depth prior to consolidation
σ_z'	Effective stress on the layer at any depth after consolidation
σ_{cs}'	Pseudo-overconsolidation pressure
σ_c'	Predetermined stress at which dry samples are flooded with water
μ	Slope of e vs. $\log(\sigma')$ curve

CHAPTER 1

INTRODUCTION

1.1 GENERAL

In India, the major portion, nearly 73% of power generation is based on Thermal Power Plants (TPPs) of which 90% use pulverized coal as fuel, as it is the major source of energy in India, the remaining comprising of diesel, wind, gas, and steam. The coal that is used in India has relatively low calorific value of about 2500 Kcal/kg to 3500 Kcal/kg and with ash content of about 40 to 50%, which is higher in comparison to that from coal used in other countries namely U.S.A, Germany, Canada and U.K. Even by washing the coal, the ash content may not be reduced considerably as the impurities in Indian coal are mainly embedded within the structure of the coal rather than on the surface. On an average, the rate of ash production in a 1000 MW Power Plant is of the order of about 5000 tonnes per day.

The non-combustible minerals in coal result in the formation of coal ash, which has two principal components namely Bottom ash and Fly ash. The powdered coal is conveyed by air to a furnace where the carbon is ignited in an atmosphere of 1040 to 1150 °C. The non-combustible minerals become molten as they are carried through the firing zone by the air stream / flue gas. The molten minerals solidify in this moving air stream and become the "finely divided powdered residue" known as fly ash, which is spherical in shape (Fig. 1.1). The fly ash produced is collected in electrostatic precipitator hoppers or silos. A general flow diagram of fly ash production is presented in Fig. 1.2. The bottom ash is collected at the bottom of the boilers/furnaces.

Because of variations in coals from different sources, as well as differences in the design of coal-fired boilers, not all fly ashes are the same. There can also be substantial variations in the quality of fly ash obtained from different TPPs depending on the pulverization process, type of coal used, operation of the boiler, etc. Fly ash that is produced from the burning of anthracite or bituminous coal is typically pozzolanic and is referred to as a Class F fly ash if it meets the requirement that the percentage of major oxides ($Al_2O_3 + SiO_2 + Fe_2O_3$) $\geq 70 \%$ (ASTM C618).
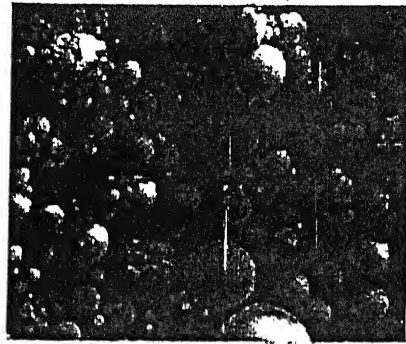
Fig 1.1 Spherical Shape of FA Particles
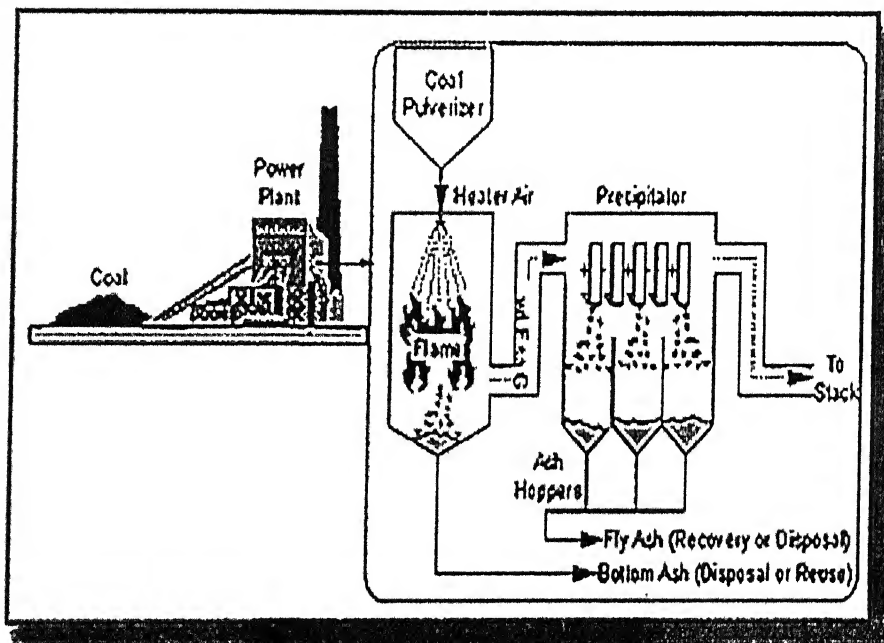
Fig. 1.2 General Flow Diagram of Fly ash Production

Fly ash that is produced from the burning of lignite or sub bituminous coal, in addition to having pozzolanic properties, also has some self-cementing properties

(ability to harden and gain strength in the presence of water alone). When this fly ash meets the requirement that the percentage of major oxides < 70 % (ASTM C618), it is referred as Class C fly ash. Most Class C fly ashes have self-cementing properties.

1.2 PHYSICAL PROPERTIES

Fly ash consists of fine, powdery particles that are predominantly spherical in shape, either solid or hollow, and mostly glassy (amorphous) in nature. The carbonaceous material in fly ash is composed of angular particles. The particle size distribution of most bituminous coal fly ashes is generally similar to that of silt (less than a 0.075 mm or No. 200 sieve). Although sub-bituminous coal fly ashes are also silt-sized, they are generally slightly coarser than bituminous coal fly ashes (DiGioia *et al.*, 1972). The low specific gravity of fly ash 1.9 to 2.3 (Pandian *et al.,* 1998) as compared to soils (2.65-2.8) is an attractive property for its use in geotechnical engineering applications as light weight fill.

The colour of fly ash can vary from tan to gray to black, depending on the amount of unburnt carbon in the ash. The lighter the color, the lower the carbon content. Lignite or sub bituminous fly ashes are usually light tan to buff in color, indicating relatively low amounts of carbon as well as the presence of some lime or calcium. Bituminous fly ashes are usually some shade of gray, with the lighter shades of gray generally indicating a higher quality of ash.

1.3 CHEMICAL PROPERTIES

The chemical properties of fly ash are influenced to a great extent by those of the coal and the techniques used for handling and storage. There are basically four types of coal, each of which varies in terms of its heat value, chemical composition, ash content, and geological origin. The four types of coal are anthracite, bituminous, sub-bituminous, and lignite. In addition to being handled in a dry, conditioned, or wet form, fly ash is also sometimes classified according to the type of coal from which the ash was derived. The following table shows the chemical compositions of fly ashes based on coal types. The chief difference between Class F and Class C fly ashes is in the amount of calcium, silica, alumina, and iron contents in the ash. In Class F fly ash, total calcium content typically ranges from 1 to 12 percent, mostly in the form of calcium

hydroxide, calcium sulfate, and as glassy components in combination with silica and alumina. In contrast, Class C fly ash may have reported calcium oxide contents as high as 30 to 40 percent. Another difference between Class F and Class C fly ashes is that the amount of alkalis (combined sodium and potassium) and sulfates (SO_4) are generally higher in the Class C fly ash than in the Class F fly ash.

Table 1. Normal Range of Chemical Composition for Fly Ash Produced from Different Coal Types (expressed as percent by weight).

Component	Bituminous	Sub bituminous	Lignite
SiO_2	20-60	40-60	15-45
Al_2O_3	5-35	20-30	10-25
Fe_2O_3	10-40	4-10	4-15
CaO	1-12	5-30	15-40
MgO	0-5	1-6	3-10
SO_3	0-4	0-2	0-10
Na_2O	0-4	0-2	0-6
K_2O	0-3	0-4	0-4
LOI	0-15	0-3	0-5

The loss on ignition (LOI), which is a measurement of the amount of unburnt carbon remaining in the fly ash, is one of the most significant chemical properties of fly ash, especially as an indicator of suitability for use as cement replacement in concrete.

1.4 DISPOSAL OF FLY ASH

Rapid increase in industrialization requires large amounts of electrical power, which in turn leads to production of huge amounts of fly ash as by-product. Disposal of this ash is a major concern and requires huge land area for its disposal the value of which cannot be compensated by money specially for a country like India, where land/population ratio is much less as compared to other countries. Usually fly ash is disposed by the following methods

1. Land disposal either in wet or dry form.

2. Sea/River disposal

3. Utilization of fly ash as construction material.

Among the various alternatives for disposal, wet disposal into Ash Ponds / Lagoons / Ash Dykes has been widely adopted by most TPPs. The bottom ash and fly ash as extracted are stored temporarily in silos, before transportation to the disposal areas, from which it can be used or disposed off in a wet or dry form. In the wet process, fly ash is mixed with 70 to 80% of water and then transported through pipes for storage into ponds or lagoons or ash dykes, where the ash particles settle by sedimentation process and the supernatant liquid is collected and let off into the nearby stream or river. Some of the liquid percolates into the ground and pollutes the ground water. This can be prevented by using liners or by providing infiltration galleries through which water is collected and disposed off into the nearby sea / river. It is estimated that for a 500 MW Power Plant an ash pond spreads over an area up to 10 km^2 and ash fills up to a height of 10 m in 5 years .The height may increase to 30-50 m with time. In many places total height of the ash ponds / deposits is > 30 m.

1.5 RECLAMATION OF FLY ASH DEPOSITS

Due to the scarcity of land and with the cost of land increasing day by day, it is essential to reclaim or improve these ash ponds so that they can be used for the construction of light and to medium heavy structures. These ash deposits have bearing capacity comparable to that of loose sandy deposit. As such lightweight building can be constructed without any stabilization measures (Ghosh et al., 1997). Generally the ash deposits placed in slurry form will be in a relatively soft and loose state with very low density and may lead to liquefaction during earthquake. Considerable research has been conducted to improve the density of these ash deposits such as blast densification, vacuum dewatering, vibro-compaction, vibro-floatation (Gandhi et al., 1999; Gandhi, 2000), stone columns (Madhav et al., 1999), chemical stabilization (Ghosh et al., 1999).

1.6 MOTIVATION FOR THE STUDY

Some studies were conducted on the compaction, compressibility and consolidation characteristics of compacted fly ash samples (Gray and Lin, 1972; Leonards and Bailey, 1982; Web and Hughes, 1987; Martin and Collins, 1990; Capco, 1990; Singh, 1994; Sinha, 1998), improvement of ash deposits (Gandhi et al., 1999;

Madhav *et al.*, 1999; Gandhi, 2000; Ghosh *et al.*, 1999), construction on abandoned fly ash beds (Ballisager *et al.*, 1981; Havukainen, 1983), reclamation of fly ash beds (Ghosh *et al.*, 1997). Skarzyska *et al.* (1989) studied the engineering characteristics of in situ fly ash (ash in storage ponds). Sridharan *et al.* (1996) studied the geotechnical characteristics of pond ash. Kolay (2000) studied the interaction of fly ash with water, characterization of lagoon ash and also collapse potential of compacted ash samples. Raza *et al.* (2000) presented a study on the effects of lime, surfactant and geo-fibre on compression index, coefficient of consolidation and permeability of compacted fly ash. But no literature is found on the consolidation and compressibility characteristics, collapse potential of sedimented fly ash deposits.

Myint *et al.* (1999) conducted a laboratory study on the consolidation process of slurry-like soil with radial drainage. Gibson *et al.* (1967) developed a most general governing equation for one-dimensional consolidation taking large strains into account. Gibson *et al.* (1981) and Lee *et al.* (1981) applied the above proposed theory to the consolidation process of normally consolidated and under consolidated deposits respectively. Koppula and Morgernstern (1982) studied the consolidation process of sedimenting clays. Saito *et al.* (2001) developed an analytical solution, based on Bjerrum's (1967) hypothesis, to determine the distribution of void ratio, unit weight etc. with depth. These studies gave the inspiration for developing a new theory to deduce the variation of void ratio, unit weight and effective stress with depth of a sedimented and consolidated fly ash deposit.

1.7 STRUCTURE OF THE THESIS

A brief review of existing literature pertaining to the studies on fly ash and consolidation models considering large / finite strains into account has been presented in chapter 2. Chapter 3 gives the details of the experiments performed on sedimentation and consolidation processes of fluidized fly ash and of compressibility and collapse potential of these sedimented fly ash deposits. Discussion of the results obtained from these studies is also presented here. Chapter 4 presents an analytical study on the variation of void ratio, unit weight and effective stress with depth of the fly ash deposits. Concluding remarks on the above studies are presented in chapter 5.

CHAPTER 2

LITERATURE REVIEW

2.1 GENERAL

A review of the existing literature on studies related to fly ash is presented in this chapter. First part of this chapter deals with the experimental studies conducted on fly ash as an engineering material, reclamation of fly ash beds, and consolidation with radial drainage. The second part deals with the analytical studies on consolidation of soft deposits under applied load and self-weight consolidation of dredged fill.

2.2 EXPERIMENTAL STUDIES

Gray and Lin (1972) presented a state-of-the art review of the engineering properties and utilization of compacted fly ash. Drained triaxial tests were conducted on fly ash compacted to maximum dry density (MDD). The friction angle varied from 38^0 to 43^0 and cohesion from $69 - 103$ kPa. Effects of degree of saturation, lime treatment, preliminary curing time and duration of load increment were studied. It was observed that partially saturated fly ash was considerably less compressible compared to saturated fly ash. The permeability of fly ash compacted to MDD ranged from 0.05×10^{-5} cm/sec to 8×10^{-5} cm/sec (impervious to poorly pervious). The compressibility behaviour of compacted fly ash was dependent on age hardening or pozzolanic properties. The compressibility of lime treated fly ash, either tested in long term loading or cured before testing, were comparable and less compared to untreated compacted fly ash. Long term field settlement of compacted fly ash cannot be predicted satisfactorily on the basis of standard short term laboratory consolidation tests as the pozzolanic behaviour tends to limit the extent of actual field settlement in the long run. However, the field evidence suggests that settlement is not a significant problem in compacted fly ash.

Ballisager and Sorenson (1981) presented an interesting study on the construction of 40,000 m^3 steel tank on a bed of sand and gravel resting directly on about 5 m of lagoon fly ash, deposited hydraulically with water content of 103% and unit weight of 13.8 kN/m^3. Self-cementing properties of the existing fly ash were

revealed partly through a preconsolidation pressure of 250 to 550 kN/m^3 in consolidation tests and partly as an effective cohesion of 11 to 14 kN/m^3 with a friction angle of 30^0 to 35^0 in drained triaxial tests. Settlement of the tank was recorded to be 159 mm corresponding to a modulus of compression of 2100 kN/m^2. As the hardening properties of the fly ash depend on the quality of fly ash, which in turn depends on the origin, combustion, etc., fly ash sedimented as lagoon ash was not a well-defined material.

Leonards and Bailey (1982) presented a study on fly ash as structural fill. The study included the evaluation of index and chemical properties, strength, compressibility and aging characteristics of compacted fly ash. Field tests such as static cone penetration and plate load tests were also conducted. Unconfined compressive strength values were 115 to 211 kN/m^2 for samples compacted to dry density of 9.6 to 10.2 kN/m^3 at moisture contents in the range 20% to 40%. Maximum dry density and optimum moisture content varied from 10.5 to 14.1 kN/m^3 and 17.5% to 39% respectively. Compression index of samples compacted to unit weight of 9.4 to 9.8 kN/m^3 at nearly 30% water content was 0.1. Samples exhibited collapse of about 0.45% on adding water at a particular stress level (400 kN/m^3). A series of plate load tests were performed, on plates of size 0.3×0.3 m and 0.6×0.6 m respectively, during the early stages of fill placement and in each case a compacted ash layer of thickness of at least three times the plate dimension was present beneath the bearing surface. Settlements from plate load test, on 0.3× 0.3 m plate, on compacted fly ash was 3.81 mm and on very dense sand was 6.35 mm at a stress level of 480 kN/m^3. Maximum bearing pressure from plate load test on 0.3×0.3 m was 1724 kN/m^3.

McLaren and Digioia (1987) reported that compression index, C_c, for normally consolidated fly ashes with void ratio in the range of 0.8±0.2, was in the range of 0.13±0.082. The coefficient of consolidation, C_v, of compacted fly ashes was in the range of 100 to 1000 m^2/year (Web and Hughes, 1987) and of undisturbed samples from fly ash reclamation fill in the range of 30 to 60 m^2/year (Capco, 1990). Martin et al., (1990) reported the compression and recompression indicies of six different fly ashes to range from 0.1 to 0.3 and 0.02 to 0.04 respectively.

Singh (1994) studied the engineering properties of compacted fly ash. The effects of adding lime to fly ash on its strength, maximum dry density and optimum moisture content were also investigated. Maximum dry density (MDD) and optimum moisture content (OMC) from Miniature compaction test were found to be 1.165 gm/cm^3 and 32.6% respectively. It was noticed that MDD decreases and OMC increases for fly ash – lime mixtures with increasing lime content. Unconfined compression tests performed on samples with varying calcium oxide (CaO) and curing period revealed that the lime fixation point was about 6%. It was observed that the compressibility of fly ash decreases with increase in storage/curing period after mixing with water. The stress-strain and volume change-strain behaviour of the compacted fly ash was shown to be sensitive to the applied confining stress.

Sridharan et al. (1996) studied the geotechnical characterization of pond ash. The fly ash stored in lagoons is known as pond ash. The lagoon or pond ash is more variable in composition than the fly ash. The degree of segregation depends on the distance of the sampling location from the discharge point. The specific gravity of the ash particles at the discharge zone is higher than that at the outflow point. The specific gravity of pond ash varied from 1.9 to 2.5. The dry density of pond ash tested under Standard Proctor Compactive effort ranged from 9.1 kN/m^3 to 14.9 kN/m^3 and the optimum moisture content from 18 to 45% (Skarzynska et al. 1989). The compressibility characteristics of fly ash depend on initial density, degree of saturation, self-hardening characteristics and pozzolanic activity. Partially saturated fly ashes were less compressible (Table2.1) compared to fully saturated ones (Yudbhir and Honjo, 1991; Skarzynska et al. 1989).

Pandian et al. (1997) studied the specific gravity of three Indian coal ashes (fly ash, pond ash, bottom ash) and the effects of crushing on specific gravity. The variation of specific gravity of coal ash was due to the combination of several factors such as gradation, particle shape and chemical composition. The specific gravity of larger particles was lower, may be due to the entrapped air in the particles most of which were cenospheres. The specific gravity of crushed particles was higher compared to uncrushed particles indicating removal of air during crushing. In most cases, fly ash has

a high specific gravity (1.9 – 2.3) compared to pond ash (1.6 -.1.9). Specific gravity of coal ash lies generally between 1.6-2.3.

Table 2.1 Values of Compression Index for Fly Ashes (after Yudbhir and Honjo, 1991)

Placement Void Ratio	Condition of placement	Compression Index, C_c	Comment
0.3-1.0	conditioned compacted	0.19-0.24	Very dense to medium dense
1.0-2.0	hydraulically placed	0.24-0.61	medium dense to loose
2.0-3.0	lagoon ashes / loose dumps	0.61-0.88	loose to very loose

Ghosh *et al.* (1997) presented an interesting study on geotechnical characteristics of fly ash pond. The site has been investigated over a depth of 10.8 m by (i) Boring and collecting undisturbed samples, (ii) Standard penetration tests, iii) Dynamic cone penetration tests, and (iv) Plate load tests. Direct shear tests conducted on undisturbed samples collected from different depths gave cohesion and friction angle in the ranges of 16 to 22 kPa and 34^0 to 36^0 respectively. The N values from standard penetration tests ranged between 4 and 7 while $N_{dyn.}$ values were in the range of 6 to 12 for depths of 11.0 m. Plate load tests on 30 cm and 45 cm square plates gave a bearing capacity of 300 kPa at a settlement of 25 mm. A full scale test on the foundation exhibited sudden collapse of the footing at a stress of 387.5 kPa. With these bearing pressures light loaded structures can be constructed without any treatment / improvement. But for medium to heavy structures the ash ponds need some type of ground treatment / improvement.

Sinha *et al.* (1998) studied the compressibility characteristics of compacted pond ash from two different locations of the same pond. It was observed that the compressibility characteristics were sensitive to density. Compression index values reported range from 0.12 to 0.31 and were found to be higher than those of other

10

compacted samples, even though the void ratios of these samples were smaller (0.7 – 1.2).

Sridharan and Prakash (1998) have shown that the liquid and plastic limits determined conventionally either by percussion cup or cone penetration method were arbitrary and strength-based water contents. The state of the soil-water system at conventional liquid limit does not correspond to a stress-free reference state. As such they proposed simple procedures to determine 'real liquid limit' of any soil. The term liquid limit qualitatively represents the maximum water holding capacity, which represents the stress-free reference state. This real liquid limit (settling limit) is the limiting water content between the liquid and semi-liquid states. Number of experiments was conducted to show clearly that the settling limit represents the maximum water-holding capacity of soils and that it corresponds to stress-free reference state.

Kaniraj and Havanagi (1999) studied the characteristics of fly ash-soil mixtures from Rajghat Thermal Power Plant, Delhi, India and Baumineral, Bochum, Germany and reported the physical and chemical properties of these ashes. The MDD and OMC were 10.52 kN/m^3 and 36.5% respectively for Rajghat fly ash and 14.18 kN/m^3 and 18.4% respectively for Baumineral fly ash. Unconfined compressive strength (UCS) of statically compacted Rajghat fly ash was 67.5 kN/m^3 while that of dynamically compacted Baumineral fly ash was 165.52%. It was observed that UCS of the fly ash-soil mixtures increases with increase in fly ash content. Compression Index (C_c) of statically compacted Rajghat fly ash was 0.072, the Swell Index (C_s) was 0.017, while the Coefficient of Consolidation (C_v) ranged 238 to 299 m^2/year. The compression of compacted fly ash fills was small and occurs very quickly as consolidation rates are very high.

Myint *et al.* (1999) presented an interesting laboratory study on one-dimensional compression of slurry-like soil with radial drainage under a vertical load. The average water content and bulk density of the slurry were 132% and 13.6 kN/m^3 respectively. Initial void ratio of the soil was 3.5, liquid and plastic limits were 73 and 27% respectively. A vertical load of 110 kPa was applied. The net additional pressure on the

slurry was about 105 kPa after the deduction due to side friction. Initially deformation of slurry occurred only due to the expulsion of excess water. During this period there was no change in excess pore water pressure and hence no gain in effective stress. Consolidation of the slurry was started once the soil particles came in contact with each other and attained the density of 14.26 kN/m^3, corresponding to a void ratio of 2.68, at which effective stress gain was just started. Vertical strain during the no pore pressure dissipation period was found to be as high as 19% in the laboratory and 26% in the field studies. As such, the deformation of slurry-like soils does not follow Terzaghi's consolidation theory in the initial stage. Been and Sills (1981) noticed in their experiments that other time and rate dependent processes exist which were not associated with changes in effective stress.

Kolay (2000) studied the consolidation and compressibility characteristics and collapse potential of compacted fly ash. The maximum dry density and optimum moisture content were found to be 11.4 kN/m^3 and 30.5% respectively. The compression index and swell index were 0.0382 and 0.0161 respectively. The collapse potential of fly ash, compacted at OMC, at normal stress varying from 200 to 400 kPa, was < 0.3% and decreases with increase in normal stress. Clemence and Fibnarr (1981) relate (Table 2.2) collapse potential with the severity on foundation.

Raza et al., (2000) studied the consolidation behaviour of treated compacted fly ash. The compression index of plain fly ash compacted to 76.5% of MDD is 0.1158. The compression index decreased initially with increase in lime content from 0.116 at 0% lime content to 0.072 at 1% lime content but increased to 0.0919 at 5% showing that 1% of lime content was the optimum value. Similarly it was found that the optimum percentages of surfactant and geo-fibre were 0.1% and 0.2% respectively. The reduction initial void ratio, compression index and settlement of plain fly ash treated and reinforced with optimum percentages of lime content, surfactant and geo-fibre were found to be 5.5%, 55.5% and 53.9% respectively over plain compacted fly ash. Consequent increases in coefficients of consolidation and permeability were 135% and 18% respectively.

Table 2.2 Collapse Potential Values in Relation to the Foundation Damage.

Collapse Potential	Severity of Problem
0-1	No problem
1-5	Moderate trouble
5-10	Trouble
10-20	Severe trouble
> 20	Very severe trouble

Ghosh and Bhatnagar (2000) conducted laboratory and full scale field tests on chemical stabilization, through grout columns, of fly ash beds. The grout columns comprised of about 85% fly ash and rest lime or gypsum or cement content. Three different mix designs were prepared in the laboratory and the columns of size 0.15 m diameter and 1.25 m deep were installed. Ultimate bearing capacity of virgin fly ash bed, stabilized beds of design mixes - mix-2, mix-3 and mix-4 were respectively 370, 380, 580 and 720 kN/m^3. Theoretical computation of ultimate bearing capacities using bulging theory and pile failure theory was found to be 574 kN/m^3 and 490 kN/m^3 respectively.

Madhav and Ghosh (2000) studied the reclamation of fly ash beds with granular piles. An experimental program has been taken up to study the effectiveness of stone columns. Load tests were conducted on small scale model beds prepared by reconsolidation technique. Settlement of unreinforced fly ash bed was about 19 mm under a stress of 60 kPa while that of reinforced bed was 7 mm under the same stress. A combined stone column raft system gave a settlement of 10 mm under the same average stress, about 50% reduction in settlement compared to that of untreated ground. Granular piles also increase the resistance to liquefaction. This can also be achieved through vibro-compaction, vibroreplacement and blast densification (Gandhi, 2000; Gandhi *et al.*, 1999).

2.3 ANALYTICAL STUDIES

Gibson *et al.,* (1967) derived the equation governing one-dimensional consolidation of a fully saturated clay layer with assumptions rather more general than those adopted in conventional theories. The limitation of small strain has not been imposed and the variations of permeability and compressibility with void ratio were considered. Following equation governing the variation of void ratio with depth and time was obtained.

$$\pm \left(\frac{\rho_s}{\rho_f} - 1 \right) \frac{d}{de} \left[\frac{k(e)}{1+e} \right] \frac{\partial e}{\partial z} + \frac{\partial}{\partial z} \left[\frac{k(e)}{\rho_f (1+e)} \frac{d\sigma'}{de} \frac{\partial e}{\partial z} \right] + \frac{\partial e}{\partial t} = 0 \qquad (2.1)$$

where ρ_f and ρ_s are the unit weights of the fluid and solid phases, $k(e)$ is the coefficient of permeability as a function of void ratio (e), z is the solid thickness of the material, σ' is the effective stress. '+' sign is taken when 'z' is measured against the gravity. The above theory was applied to study the finite nonlinear consolidation of thin homogeneous layers with the assumption that the stresses due to the self-weight of solids and pore fluid were negligible compared to those applied. The same was incorporated in the above equation by assuming that $\rho_s = \rho_f$.

Lee and Sills (1981) developed a consolidation model based on the theory proposed by Gibson *et al.,* (1967) and applied it to the consolidation of dredged fill during and after deposition. No restriction was made on the magnitude of strain and the boundaries were allowed to move as required during the consolidation process. While the coefficient of permeability 'k' increases with increasing void ratio and the coefficient of consolidation, C_F, was assumed to be constant and simplified Eq. 2.1 to

$$\frac{\partial e}{\partial t} = C_F \frac{\partial^2 e}{\partial z^2} \qquad (2.2)$$

where $C_F = -\dfrac{k}{\rho_f (1+e)} \dfrac{\partial \sigma'}{\partial e}$

and $\dfrac{k}{\rho_f} = k_o (1+e)$, k_o is permeability at initial void ratio.

Consolidation process for the following cases was studied.

1) Consolidation of a dredged fill due to self-weight.

14

2) Consolidation of a normally consolidated stratum due to surface loading.

The coefficient of secondary compression was defined in different ways (Mesri, 1973). Several definitions of the coefficient of secondary compression are

$$s_\alpha = \frac{\Delta s}{\Delta \log t}; \quad C_\alpha = \frac{\Delta e}{\Delta \log t}; \quad \varepsilon_\alpha = \frac{C_\alpha}{1+e}; \quad \varepsilon_{\alpha o} = \frac{C_\alpha}{1+e_o}; \quad \varepsilon_{\alpha i} = \frac{C_\alpha}{1+e_i}; \quad \varepsilon_{\alpha p} = \frac{C_\alpha}{1+e_p}$$

where s = settlement, e = void ratio, t=time, e_o=initial void ratio at natural water content, e_i= void ratio at the beginning of load increment and e_p=void ratio at the beginning of linear portion of e versus $\log(\sigma')$. Mesri and Godlewski (1977) studied the relationship of compressibility with respect to effective stress (σ') and time (t). The compressibility with respect to stress and time were expressed by compression index, C_c = $\Delta e/\Delta \log \sigma'$ and secondary compression index, $C_\alpha = \Delta e/\Delta \log t$, where e is the void ratio. One-dimensional compressibility data on Mexico City clay, Leda clay and New Haven organic clay silt were presented. The applied stress on Leda clay and organic clay silt varied from 1.68 – 3100 kN/m^2 and 1.9 – 860 kN/m^2 respectively. Relationship between C_α and C_c was examined from the plots of C_α versus C_c and data from variety of natural soils. The values of the ratio C_α/ C_c were in the range of 0.025 – 0.10. It was also observed that C_α may increase, decrease or remain constant with time depending on the shape of e versus $\log \sigma'$ curve.

Gibson et al., (1981) studied the finite strain consolidation of saturated thick, homogeneous soil layers with both one-way and two-way drainage. The governing Eq. (2.1), which is highly nonlinear was reduced to a linear form, Eq. (2.3), by assuming the variable terms – finite strain coefficient of consolidation (g(e)) and variable coefficient (λ(e)) to be constant. The nonlinearity of soil permeability and compressibility were retained.

$$\frac{\partial^2 e}{\partial z^2} \mu \lambda(\rho_s - \rho_f)\frac{\partial e}{\partial z} = \frac{1}{g}\frac{\partial e}{\partial t} \tag{2.3}$$

$$g(e) = -\frac{k(e)}{\gamma_w(1+e)}\frac{d\sigma'}{de} \tag{2.4}$$

$$\lambda(e) = -\frac{d}{de}\left(\frac{de}{d\sigma'}\right) \tag{2.5}$$

The void ratio and effective stress relation was implicit in Eq. (2.4), integration of which gives

$$e = (e_{oo} - e_{\infty})\exp(-\lambda\sigma') + e_{\infty} \tag{2.6}$$

where e_{oo} and e_{∞} are the void ratios at the beginning ($\sigma' = 0$) and end ($\sigma' = \infty$) of consolidation.

The governing Eq. (2.3) was normalized and solved using finite difference numerical technique. A comparison with conventional theory has shown that conventional theory seriously overestimates the time of consolidation and underestimates the excess pore water pressure in a soft layer.

Cargill (1984) presented a simplified hand-calculation procedure for the calculation of one-dimensional primary consolidation of very soft fine-grained material such as dredged fill based on charts developed from linear finite strain consolidation theory by Gibson et al., (1981). The solution charts for self-weight consolidation of dredged fill, with both one-way and two-way drainage, and technique for handling the case of multiple consolidating loads i.e. the periodic deposition of fill hydraulically placed over the previously placed and partially consolidated layers were also presented. Comparison of predicted settlements from linear finite strain theory with measured data for the sites Canaveral Harbor disposal area and Craney Island disposal were in very close agreement. Possible reasons for the deviation of predicted settlements from the measured were attributed to desiccation, approximations in hand-calculation procedure etc. The small strain theory seriously under predicts the settlements even before desiccation effects were possible.

Saito et al., (2001) proposed an analytical model based on Bjerrum's hypothesis to deduce the depth wise distribution of void ratio and other soil parameters. Difference in plasticity index values i.e compression index, C_c (Eq. 2.7), was reflected in the

distribution of parameters – void ratio, unit weight, overburden pressure, apparent preconsolidation and OCR (overconsolidation ratio) with depth.

$$C_c = (0.015+0.007PI)/0.434 \qquad\qquad (2.7)$$

On the other hand depositional rate has shown considerable effect on OCR but almost no effect on void ratio and unit weight. The results compared well with the field data reported by Meade (1963) and Velde (1996), for soils with PI in the range of PI from 10 to 100.

Morris (2002) derived analytical solutions for linear finite strain one-dimensional consolidation (Gibson *et al.*, 1981), small-strain consolidation and self-weight consolidation with both one-way and two-way drainage. The analytical solutions were only marginally more accurate than the numerical solutions by given Gibson *et al.*, (1981) and Cargill (1984). The degree of consolidation, U, values from numerical method were slightly more at the beginning and less at the end of consolidation than the exact values. Maximum difference in degrees of consolidation between numerical and exact values was less than 6%.

CHAPTER 3

EXPERIMENTAL STUDIES

3.1 GENERAL

Generally, most of the fly ash produced by Thermal Power Plants is disposed off in slurry form in to ponds / lagoons / ash dykes. The fly ash in slurry form undergoes sedimentation and excess water is drained out. Fly ash deposit formed through sedimentation process undergoes consolidation under its own weight and will be in a soft state. The properties of this sedimented and consolidated deposit of fly ash could be very different from those of compacted fly ash about which considerable literature exists (Gray and Lin, 1972; Leonards and Bailey, 1982; Web and Hughes, 1987; Martin and Collins, 1990; Capco, 1990; Singh, 1994; Sinha, 1998). As the land requirement as well as the cost of land is increasing day by day, it is essential to reclaim or improve the ash ponds so that they can be used for the construction of light to medium heavy structures. In view of this, it becomes necessary to study the compressibility and consolidation properties of these sedimented and consolidated fly ash deposits.

3.2 EXPERIMENTAL STUDIES

Fly ash directly collected from the hopper of Panki Power Plant is used for the present study. Fly ash is thoroughly mixed with water and made in to slurry. The following experiments are performed on the samples prepared from this fly ash slurry – Settling limit, Large-scale consolidation tests (Simulation of sedimentation and consolidation process of fly ash beds), Large-scale Radial Consolidation tests (Simulation of infiltration), Consolidation Tests, Double Oedometer Tests (for Collapse potential) and Grain size analysis. Table 3.1 presents some of the characteristics of the fly ash.

3.2.1 Settling Limit (Sridharan and Prakash, 1998)

The state of soil-water system at conventional liquid limit does not necessarily nor precisely correspond to a stress-free reference state. As such Sridharan and Prakash (1998) propose a simple procedure for the determination of the settling limit (real liquid limit) of natural soils. Settling limit represents the maximum water holding capacity of

the soil that corresponds to the stress-free reference state. Following is the procedure to determine the settling limit.

1. A sample of 25g of fly ash (soil) is placed in each of about seven to eight 100 ml jars.

2. With the same amount of fly ash in each of the jars, fly ash-water suspensions of different initial water contents (w_i) are prepared by adding varying quantities of distilled water to the jars.

3. Each of the fly ash-water suspension prepared is thoroughly mixed and left undisturbed.

4. The sediment equilibrium volume (V_f) in each of the jars is noted after about 24 hrs.

5. Knowing the dry weight (w_s) of the fly ash taken, the final sediment volume (V_f) and the specific gravity of the fly ash (G_s), the final equilibrium water contents (w_f) of each of the sediments are calculated as follows.

Volume of solids $= V_s = \dfrac{w_s}{G_s \gamma_w}$ where γ_w is the unit weight of water.

$\Rightarrow$ Weight of water held by the sediment $= w_w = (V_f - V_s)\, \gamma_w$

$\therefore$ Final equilibrium water content, $w_f = w_w / w_s$.

Table 3.2 presents initial and final water contents obtained for series 1 and 2

6. The results are plotted in the form w_f versus $\log_{10} w_i$ (Fig. 3.5).

7. The final equilibrium water content corresponding to the intersection of the best-fit line encompassing the experimental points with the $w_f = w_i$ line is noted as the 'settling-limit water content' of the fly ash.

Table 3.1 Some Characteristics of Fly Ash

Colour	Grey
Physical State	Powder
Specific Gravity	2.05
Particle Size	
Sand (0.4 – 0.075 mm)	26%
Silt (0.075 – 0.002 mm)	70%
Clay (<0.002 mm)	4%
Settling Limit (Real Liquid Limit)	60%

Table 3.2 Initial and Final Water Contents

Series 1		Series 2	
w_i %	w_f %	w_i %	w_f %
60	59.22	65	63.22
70	63.22	75	69.22
80	69.22	90	75.22
100	75.12	110	77.22
125	79.22	140	79.22
150	81.22	170	83.22
200	87.22	230	85.22
250	89.22	-	-

3.2.2 Preparation of the Samples for Sedimentation

The dry fly ash, collected from the hopper, from the Panki Power Plant is mixed with water content that is more than its settling limit of 60 %. The fly ash-water mixture is thoroughly mixed and made into slurry. The slurry is left for 24 hrs for uniform distribution of water content. The average water content of the slurry varied from 74% to 81%.

3.2.3 Simulation of Sedimentation and Consolidation Process of Fly Ash in Ponds

Self-weight consolidation of fly ash slurry hydraulically placed/deposited into a lagoon/ash pond/ash dyke has been simulated in the laboratory. The prepared slurry is poured into tanks, sides of which are greased to reduce the friction during loading. The tanks (Fig. 3.1c) have a perforated base and are of size 38.5 cm in diameter and 20 cm in height. Initially slurry undergoes sedimentation and excess water is collected through the perforated base. The top of the soft deposit is covered with perforated Perspex sheet and loaded as shown in Figure 3.1a, up to a maximum stress that varied from 20 to 35 kPa, to represent the self-weight consolidation of a layer at depth, z (Fig. 3.1b). The settlements are measured by three dial gauges placed on the top of the plate. Figures 3.1c and 3.1d represent the layers at shallow and deep depths. Each load is kept for a sufficiently long period until the rate of settlement becomes negligible and the final near

constant settlements are obtained. The average water contents of these sedimented and consolidated deposits varied from 53 % to 57 %. A total number of four tanks, series 1 to 4, are filled with fly ash slurry, loaded and thus prepared.
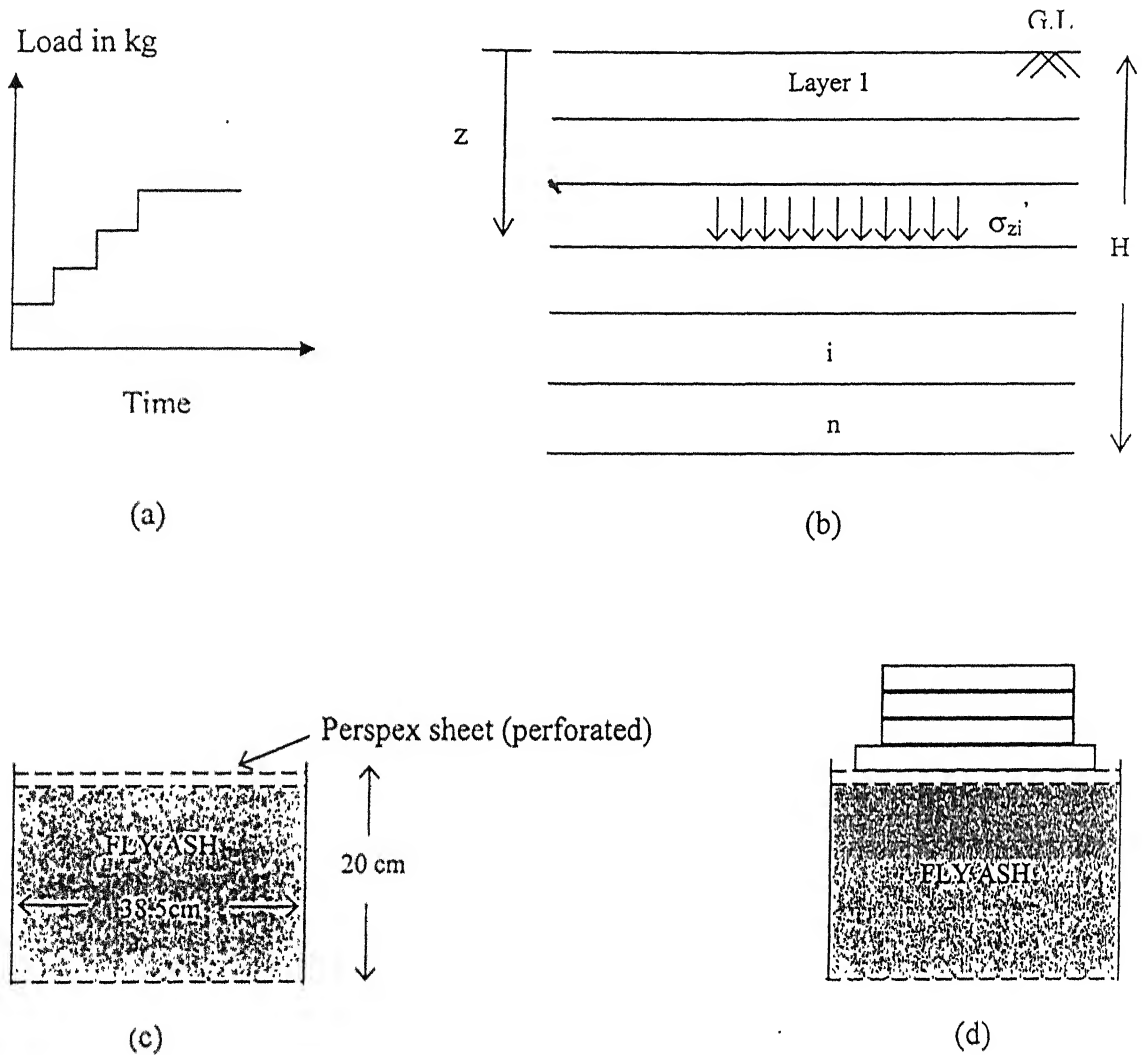
Figure. 3.1 Simulation of Self-Weight Consolidation of Fly Ash, Deposited in Ash Pond/Lagoon. a) Loading b) Deposition c) Self-Weight Consolidation, Shallow Depth d) Loading to Simulate Layers at Depth.

In the wet disposal system, pollution of ground water may occur because of the leachate percolating through foundation of the ash pond into the ground water (Fig. 3.2). The rate of percolation depends on the permeability of the foundation medium. Harmful effects due to this leachate can be prevented by lining the ash ponds with suitable non-permeable layers to prevent infiltration of leachate in to the ground or by providing infiltration galleries to collect the leachate for remediation and treatment

before discharging in to natural streams. Water collected in these galleries is pumped out and either let off into nearby stream / river or recirculated back to the plant where it is treated and used again in the preparation of fly ash slurry.
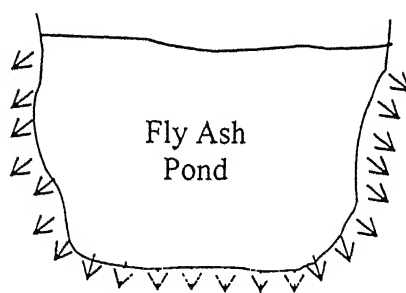

Fig. 3.2 Percolation of Leachate into the Ground from Fly Ash Pond

The infiltration is simulated in the laboratory by providing a metallic tube of internal diameter 5 cm inside the tank of size 38.5 cm in diameter and 20 cm in height. In the present study two cases are studied. In first case, infiltration galleries are without radial fins. In the second case, infiltration galleries are provided with radial fins of size 5 mm in diameter and 5 cm in length. The openings in infiltration gallery and on radial fins are covered with filter paper to prevent the movement of fly ash particles into the gallery. Water from these infiltration galleries is collected as shown in Figure 3.3.

3.2.4 Consolidation Tests

After the sedimented fly ash is consolidated under the applied stress in the tanks, samples from different depths, top, middle and bottom layers, are taken out and tested for compressibility and consolidation characteristics by conducting conventional oedometer tests.

3.2.5 Collapse Potential

The fly ash particles in the sedimented deposit are often relatively in loose packing as compared to those in compacted state (Fig. 3.4). Hence reclaimed fly ash may exhibit collapse phenomenon. The same is studied by conducting double oedometer tests in the laboratory. Two of the three samples collected from each layer are dried, by keeping them open to atmosphere to simulate the field conditions, and oedometer tests are performed. The dry ash samples are initially loaded to certain normal stress. After the completion of the initial compression, the ash samples are
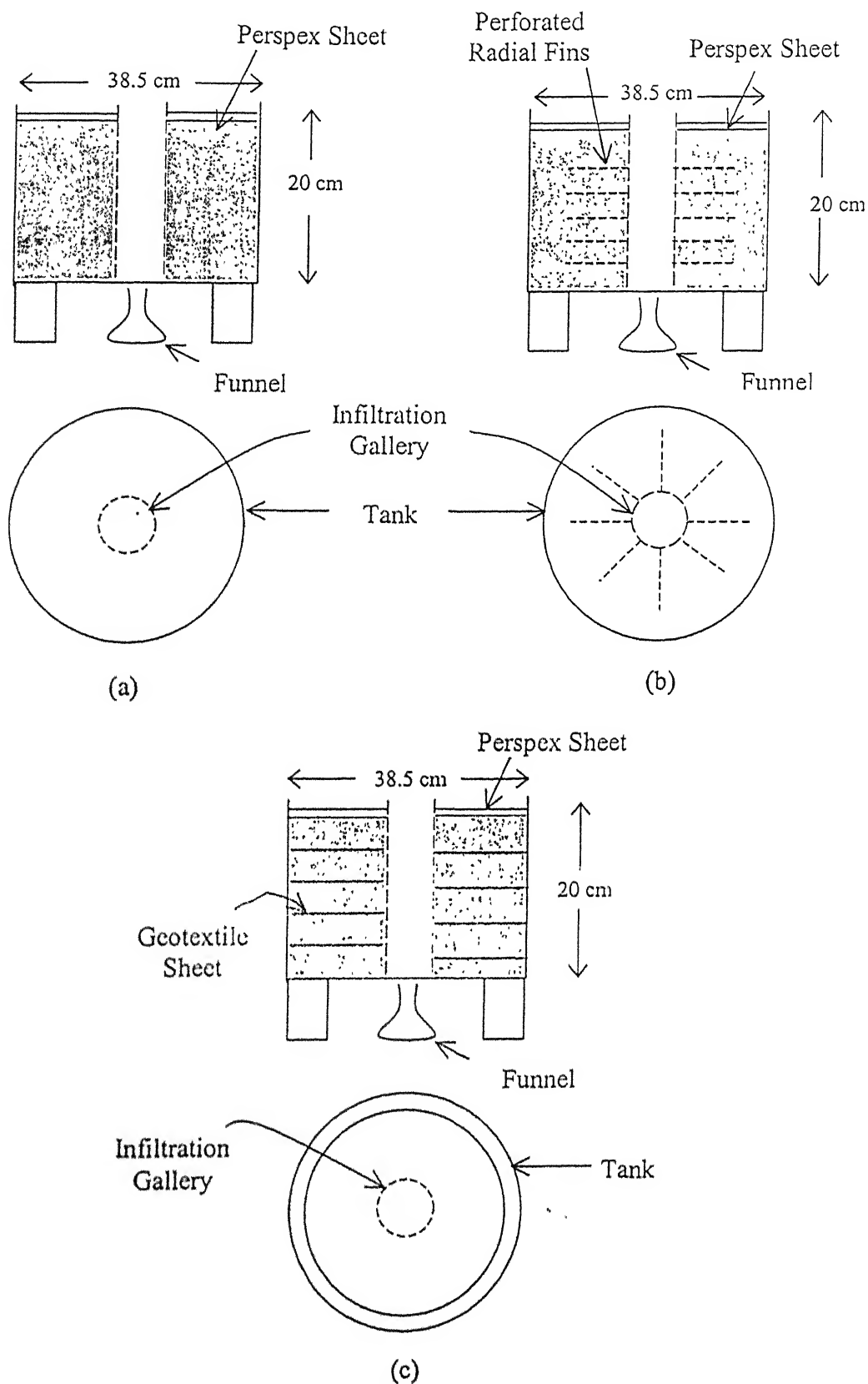
Fig. 3.3 Simulation of Infiltration Galleries in Fly Ash Deposits a) without Radial Fins
b) with Radial Fins c) with Geotextiles.

flooded with water and the collapse potential (C_p) is obtained as follows

$$C_p = (e_1 - e_2) / (1+e_o) \tag{3.1}$$

$$or = (\Delta H_2 - \Delta H_1) / H_i. \tag{3.2}$$

where, e_1 and e_2 are void ratios before and after flooding and e_o is the natural void ratio of the ash sample or ΔH_1 and ΔH_2 are respective vertical displacements before and after flooding and H_i is the initial thickness of the ash sample.

(a)   (b)

Figure. 3.4 Arrangement of Particles in a) Sedimented and b) Compacted Deposits of Fly Ash Samples

3.2.6 Gradation Analysis

Grain size distribution analyses are performed on the samples from top and middle layers of the sedimented deposits (Series 3), before and after consolidation, to evaluate the changes in them, if any. Maximum stresses applied on samples during consolidation are 392.4, 784.4, 1569.6 and 3139.2 kPa.

3.3 RESULTS AND DISCUSSION

Results obtained from the experimental studies on Panki fly ash are presented and discussed here.

3.3.1 Settling Limit of Fly Ash

Two series of tests are conducted as per the procedure given by Sridharan and Prakash (1998). The results are depicted in Fig. 3.5. Settling limit of Panki fly ash is found to be 60%. The liquid limit determined by the fall cone test was about 56% (Madhav and Ghosh, 2000).
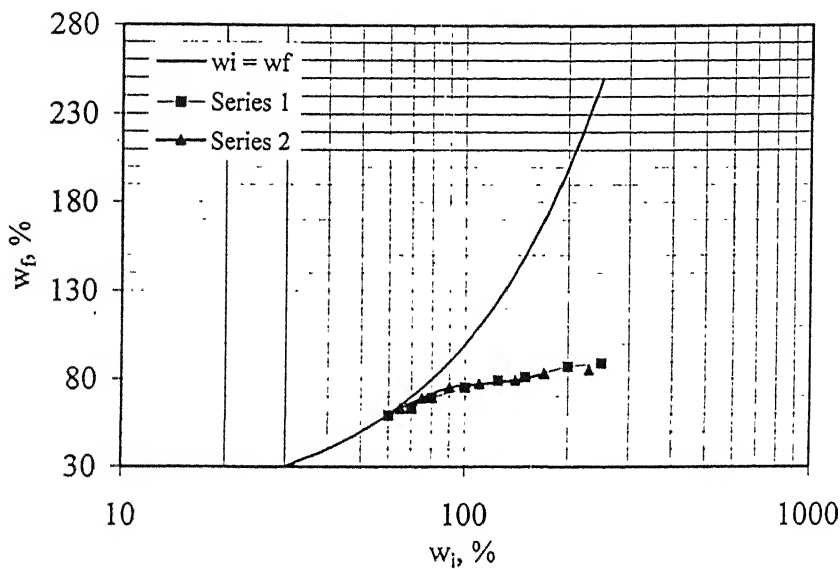
Fig.3.5 Determination of Settling Limit of Fly Ash

3.3.2 Simulation of Sedimentation and Consolidation Process of Fly Ash in Ponds

The loading sequence and settlements of fly ash deposits under each stress applied that occurred with time are depicted in Figure 3.6. Results show that the settlements (Fig. 3.6b) follow the applied stresses (Fig. 3.6b). Settlements occur very rapidly with time immediately after applying load and subsequently increase marginally with time. Results on the compressibility of fly ash deposits in the tanks (series 1 to 4) are depicted in Figure. 3.7 as strain (ε) versus log (σ') to avoid effect of the variation in the initial void ratio. Even though the deposits are not subjected to any pre- or overconsolidation all the curves depict responses similar to those of over consolidated soils. The pseudo-overconsolidation stress (σ'_{cs}) is determined from the three methods, viz., e versus log (σ'), log e versus. log (σ') and log (1+e) versus. log (σ') and tabulated in Table 3.3. A linear void ratio – log (effective stress) is to be expected for sedimented deposits. However all the samples exhibited a change in slope at an effective stress in the range 6 to 12 kPa even though none of them are subjected to any such stress. This pseudo-overconsolidation effect may be due to the pozzolanic activity possessed by the fly ash in the presence of calcium oxide in small amounts. Plots of e versus log (σ'), log e versus. log (σ') and log (1+e) versus. log (σ') are also shown in Fig. 3.8. Results show that there is hardly any rebound of fly ash during unloading except for series 1, which may be due to some disturbance. Compression Index (C_c) and

swell index (C_s) of the samples sedimented in the tanks varies from 0.08 to 0.16 and 0.003 to 0.28 (Table 3.4) with average values of 0.114 and 0.01 respectively.

Table 3.3 Values of the Pseudo-Overconsolidation (σ'_{cs} in kPa) Stress exhibited by Sedimented Samples.

| Method	Series 1	Series 2	Series 3	Series 4
e vs. log σ	11.3	7	6.5	7
log e vs. log σ	10	5.6	6	6
log (1+e) vs. log σ	10	5.6	5	6

Table 3.4 Virgin Compression Index (C_c) of Sedimented Samples

Series	Compression Index (C_c)	Swell Index (C_s)	Stress Range kPa
1	0.167	0.008 – 0.028	10 – 26
2	0.101	-	6 – 20
3	0.08	0.004	7 – 26
4	0.102	0.0037	7 – 35

Results of simulation of infiltration into galleries for the cases 1) without fins 2) with fins are depicted in Figures 3.9 to 3.12. The maximum stress applied is 26 kPa and 21 kPa respectively for cases 1 and 2. The water content of the slurry varied from 72% to 75%. Results show that settlements in case 2 are more (Figs. 3.9 and 3.10) compared to those for case 1. The volume of water collected is more for case 2, as expected, and the corresponding settlements are also more (Fig. 3.10). Settlements and volume of water collected under each stress with time are depicted in Fig. 3.11. Settlements and volumes of water collected follow the stresses applied The stress versus strain plot (Fig. 3.12) of fly ash deposits with infiltration galleries does not show a clear pseudo preconsolidation effect.
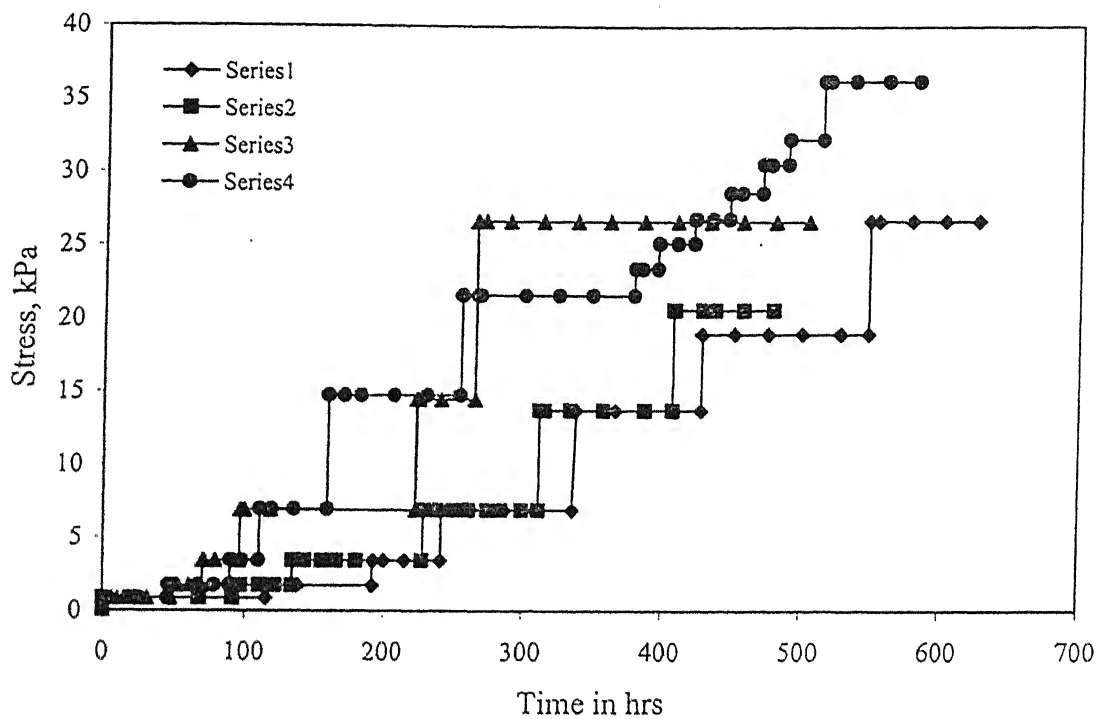
(a)
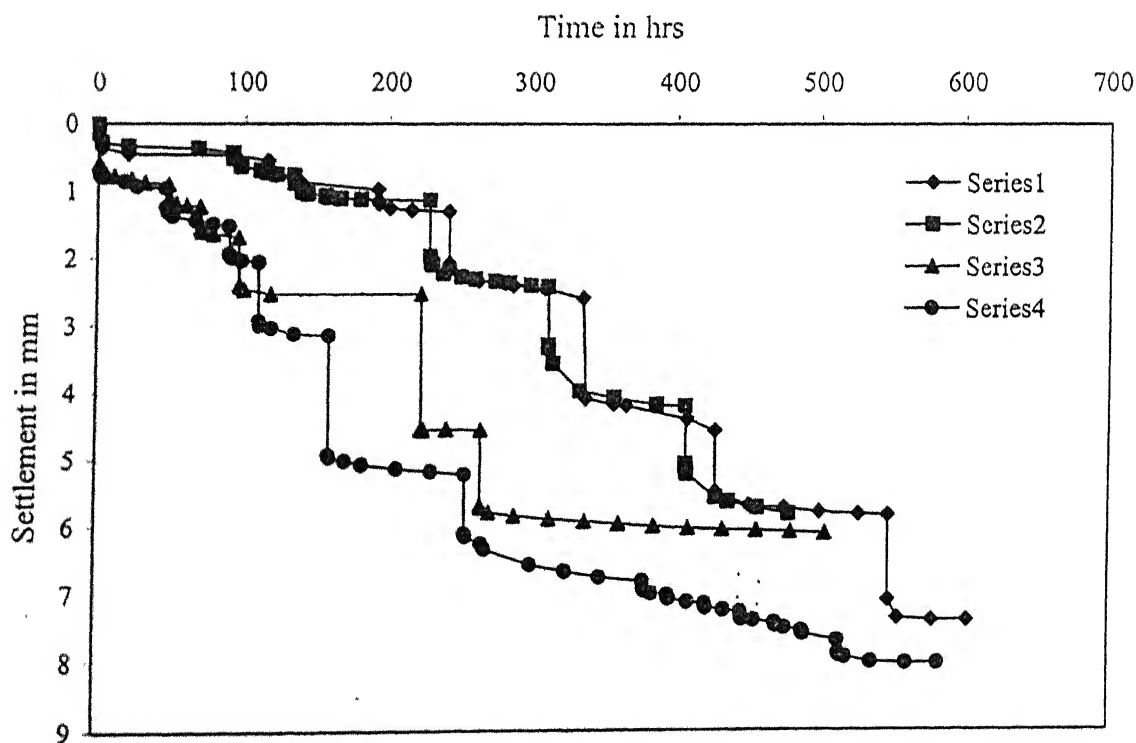
(b)

Fig. 3.6 Settlements of Fly Ash Deposits of Series 1 to 4 with Time under Each Stress a)
Stress versus Time b) Settlement versus Time.

Figure 3.7. Strain (ε) versus Log (σ') of Loading of Fly Ash Samples in Series 1 to 4

(a)

(b)

(c)
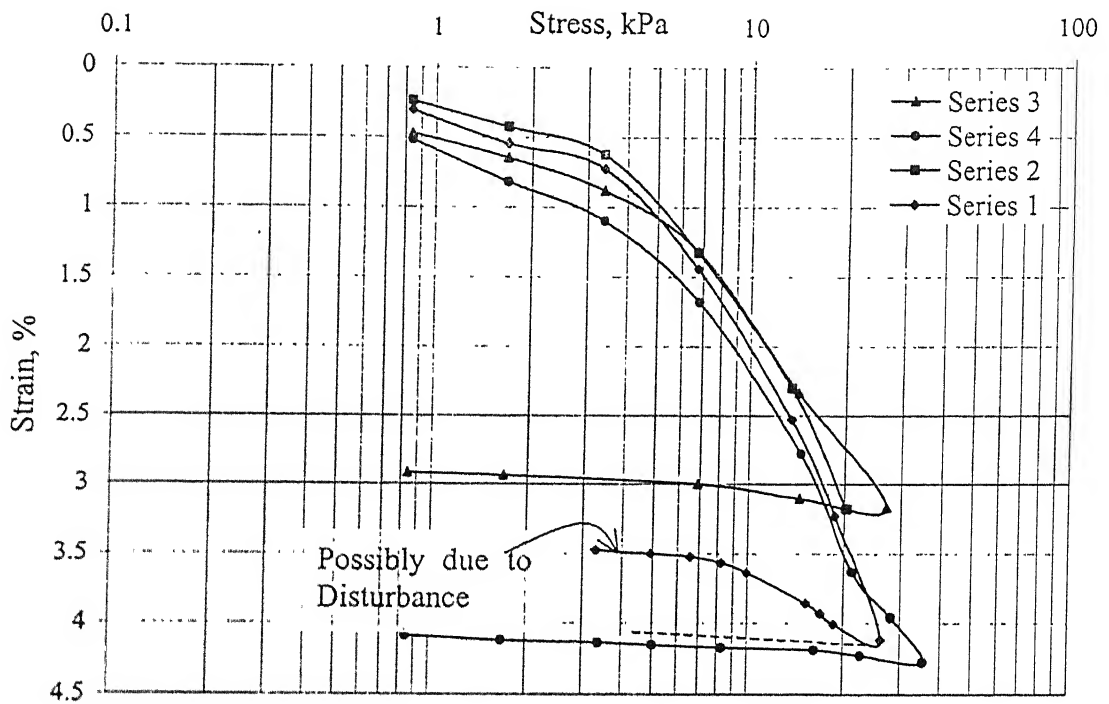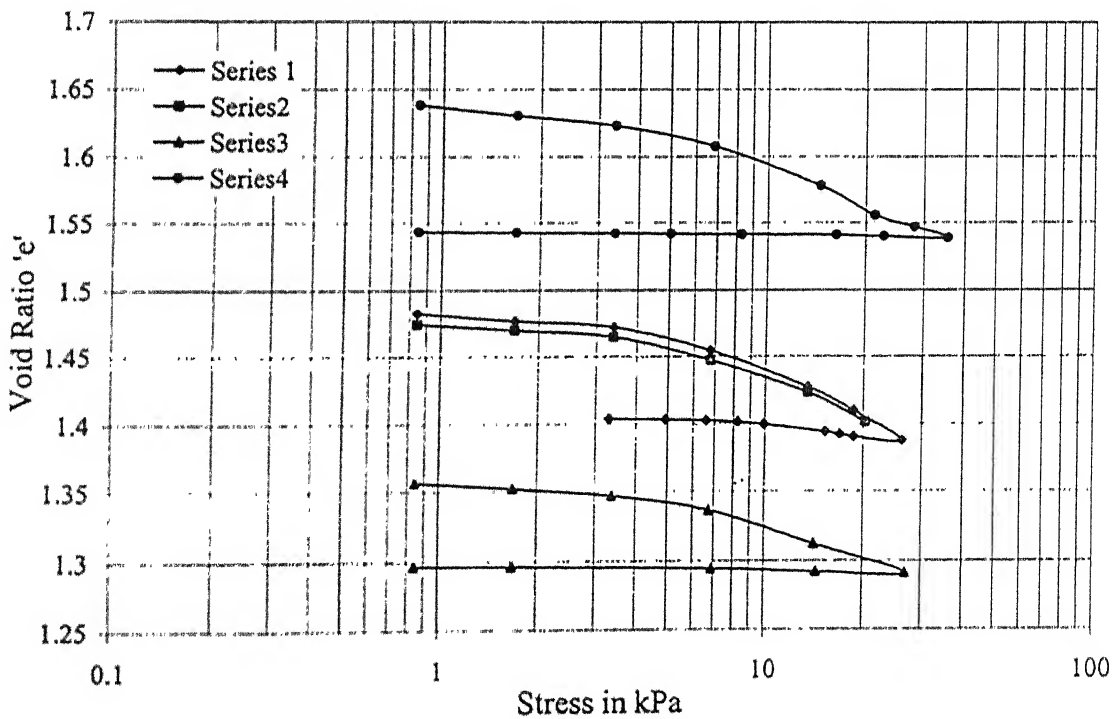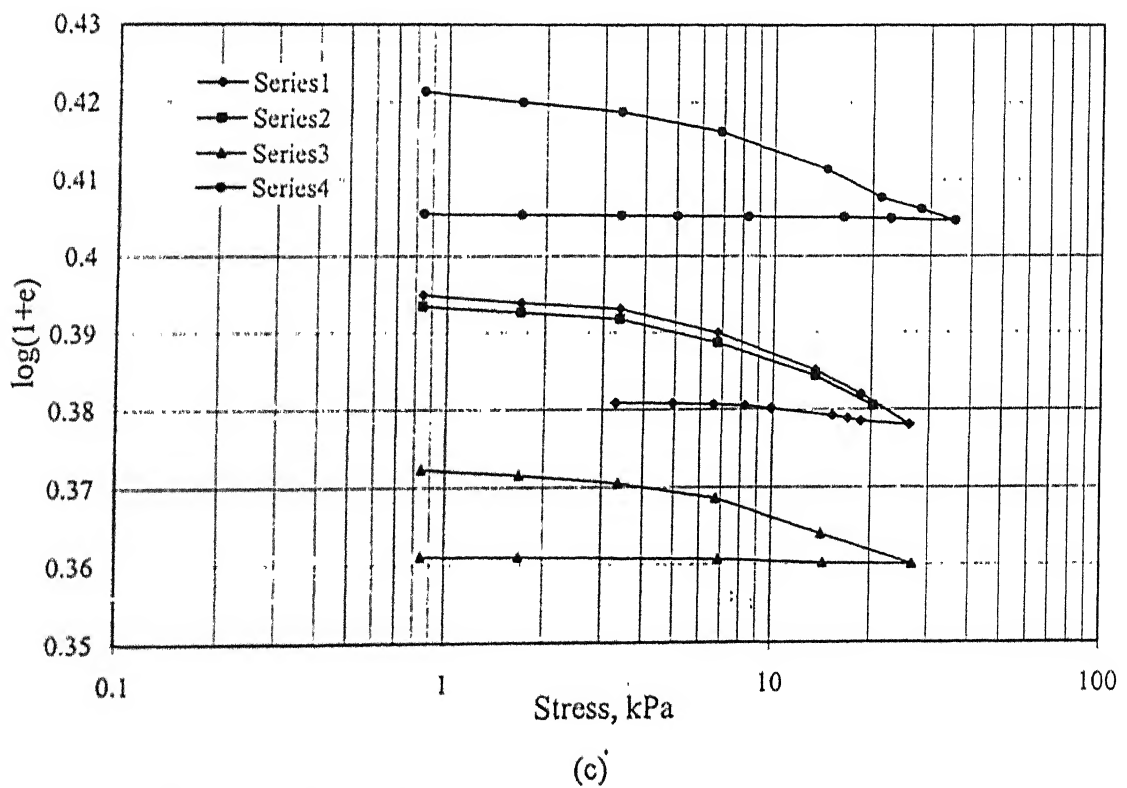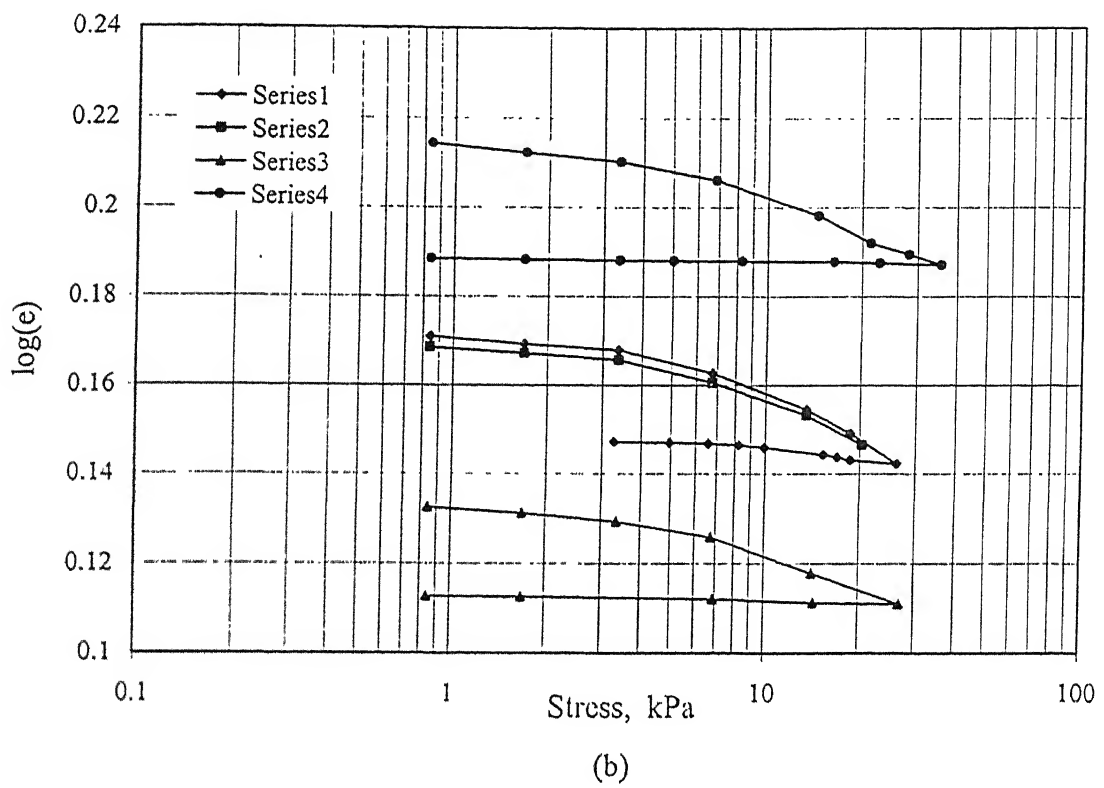
Figure 3.8. a) e versus. log (σ') b) log e versus. log (σ') c) log (1+e) versus. log (σ') of Loading of Fly Ash Samples in Series 1 to 4
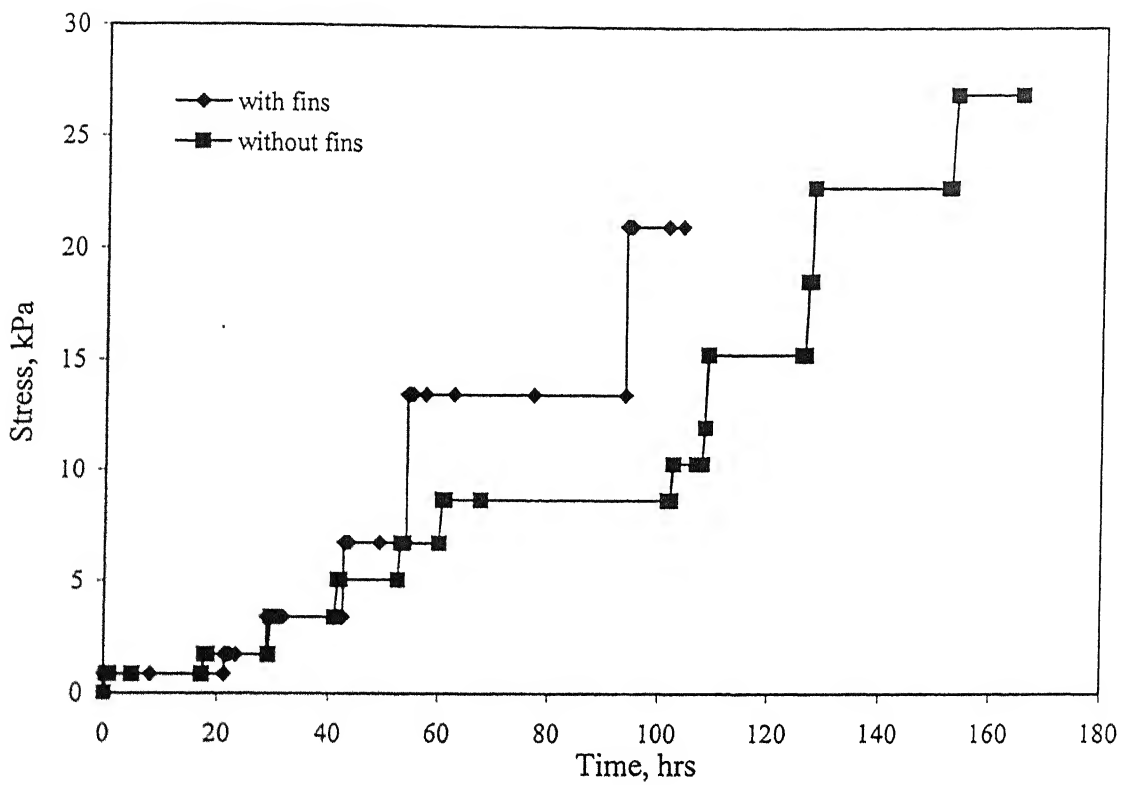
(a)
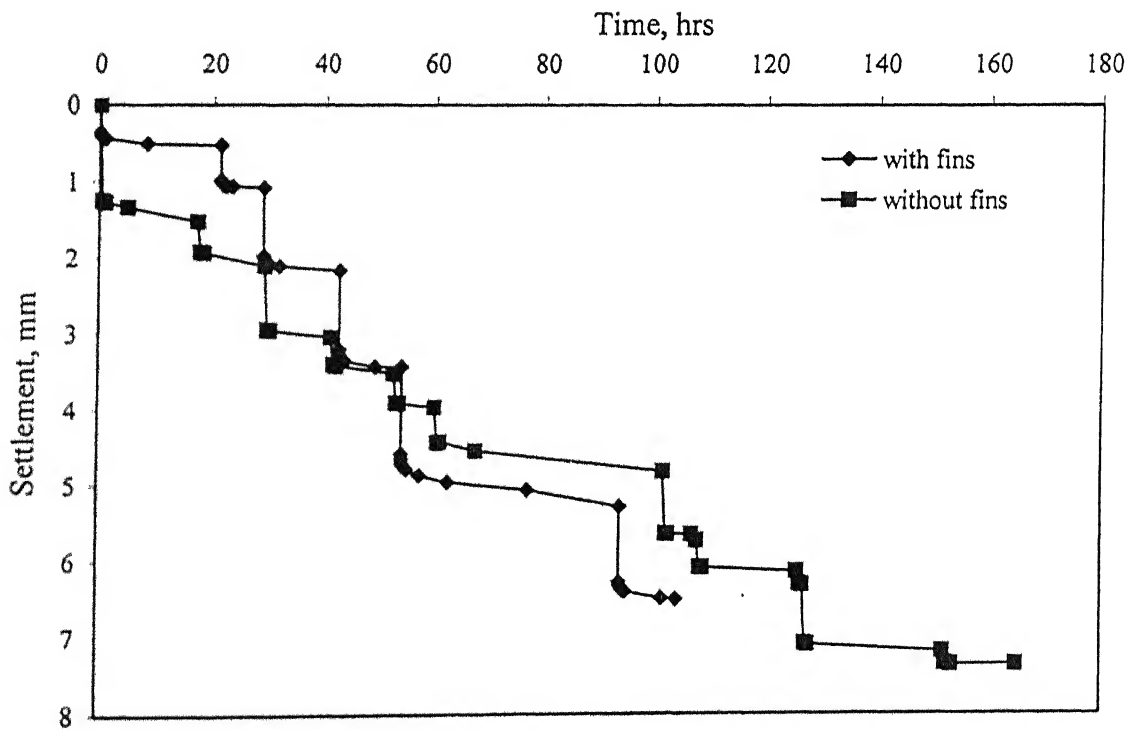
(b)

Fig. 3.9 Fly Ash Deposits with Infiltration Galleries a) Stress versus Time b) Settlement versus Time.
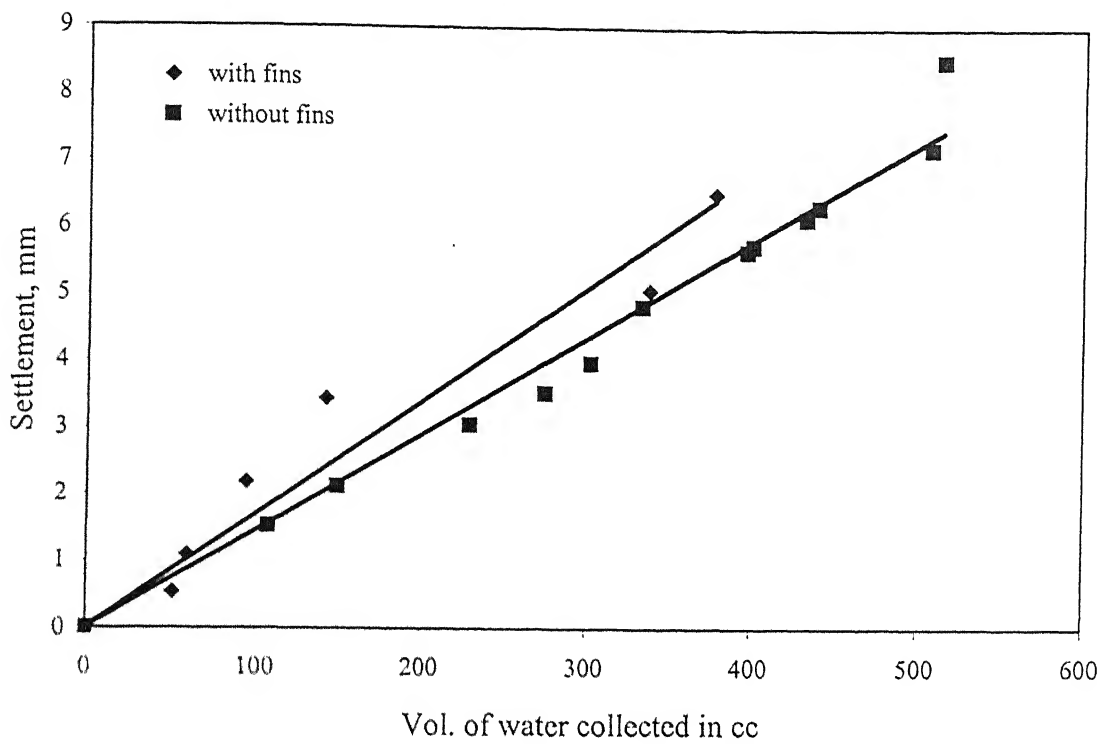
Fig. 3.10 Volume of Water Collected from Fly Ash Deposits and Corresponding Settlements

(a) With fins

31
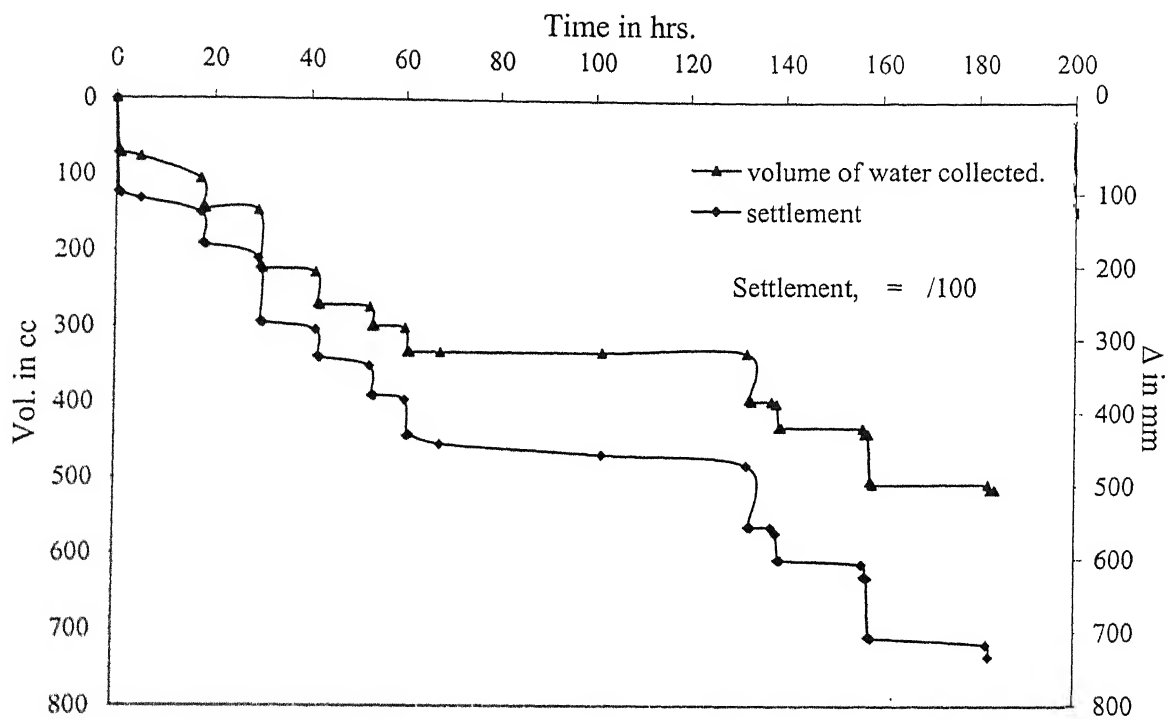
(b) Without fins

Fig. 3.11 Settlements of Fly Ash Deposits with Time Under Each Stress a) with fins b) without fins.
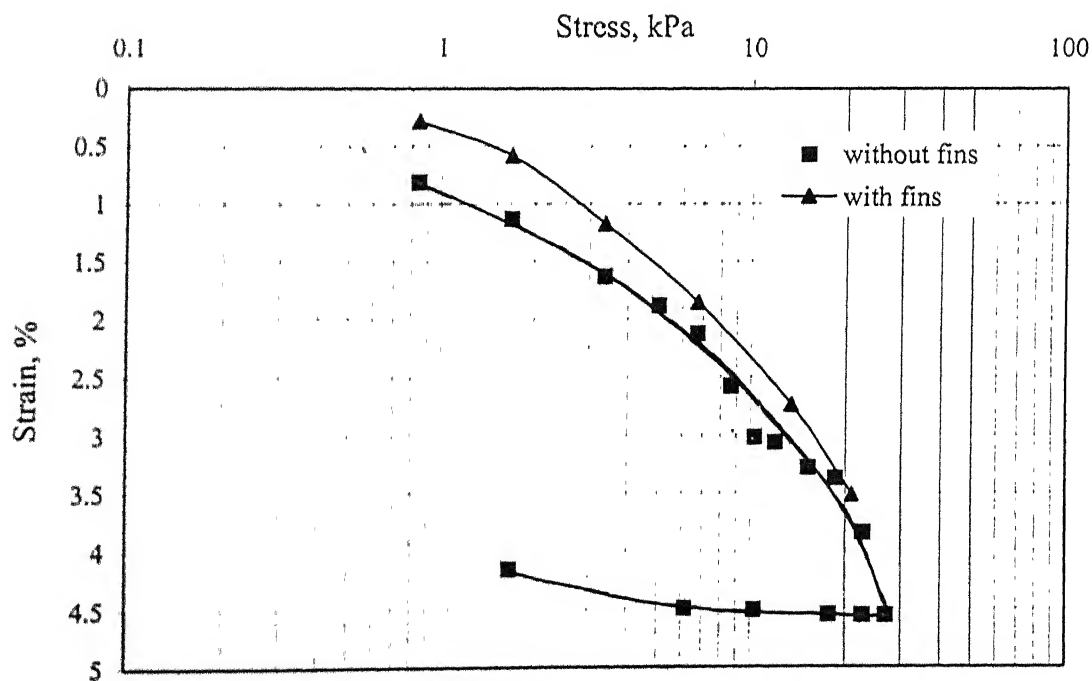
Fig. 3.12 Stress versus. Strain of Fly Ash Deposits with Infiltration Galleries.

3.3.3 Consolidation Characteristics

One-dimensional consolidation tests are conducted on samples collected from different depths - top, middle and bottom layers from sedimented and consolidated fly ash deposits (Series 1 and 2). Typical results are depicted in Fig. 3.13. The results compared with consolidation tests on compacted fly ash (Kaniraj and Havanagi, 1999; Raza *et al.*, 2000; Kolay, 2000; Singh, 1994) are presented as strain (%) versus log (σ'), to circumvent the influence due to the variation in initial void 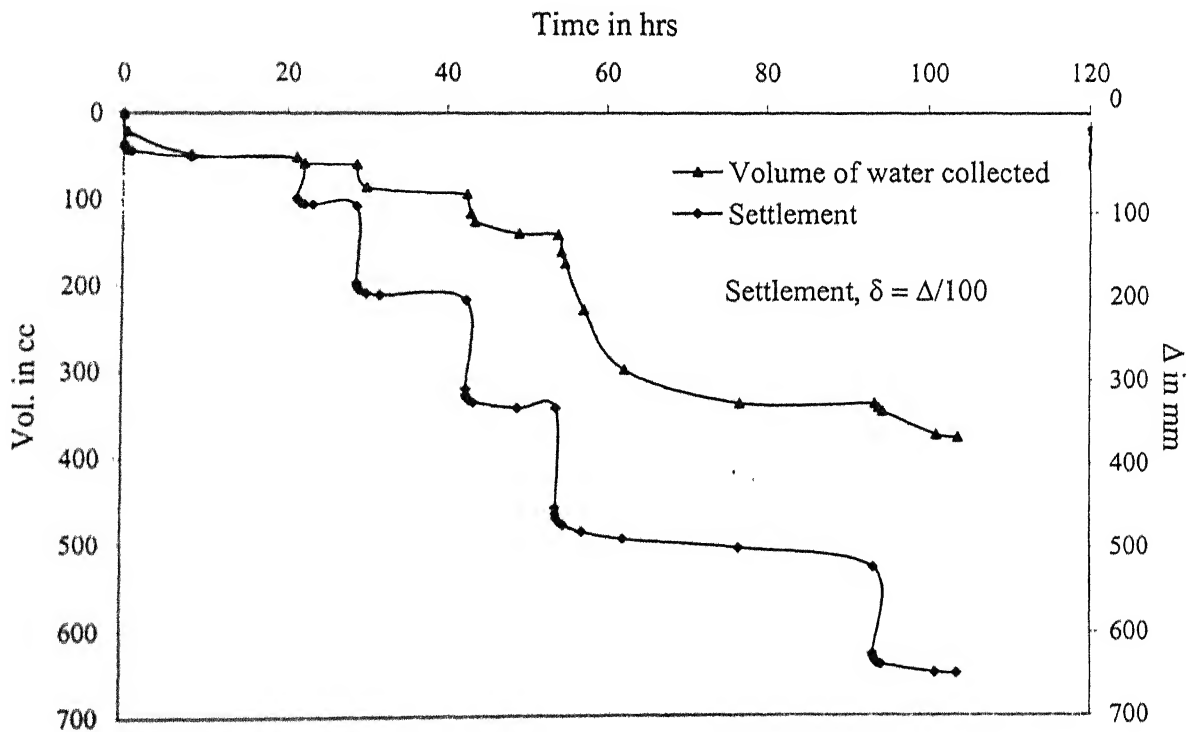ratio, in Fig. 3.14. From the figure it is clear that the compression of sedimented fly ash is much more than that of compacted fly ash.

The void ratio, e, versus log (σ') plots did not show any linear relation over the stress range investigated. C_c values have been computed for each stress increment much like the coefficient of volume change, m_v, in conventional oedometer tests. The compressibility of fly ash deposits appears to increase with normal stress, as the e versus log (σ') curves are steeper at higher stresses. Figure 3.15 shows typical variation of the compression index, C_c, of the samples collected from the sedimented deposit from series 2 with the average applied stress. In the stress range of 15 to 100 kPa, C_c increases rapidly with average effective stress (σ'). The rate of increase of C_c decreases with σ' at higher stresses. C_c values continue to increase linearly with σ' even at stresses as high as 1 MPa. The increase in C_c with σ' may be because of breakdown of weak structural bonds between the packets (Fig. 3.16) under the stress. Simultaneously, under the same stress the particles may be bonding again resulting in larger size of packets as revealed by the grain size analysis (Fig. 3.19).

The compression index values for samples from sedimented deposits are high (Table 3.5) compared to those of compacted samples (Kolay, 2000; Kaniraj and Havanagi, 1999; Raza, *et al.*, 2000; MacLaren, *et al.*, 1987; Sinha *et al.*, 1998). The C_c values of sedimented Panki fly ash are in the same range as those reported for normally consolidated fly ash reported by McLaren and Digioia (1987) but much higher than those of compacted samples (Kaniraj and Havanagi, 1999; Raza *et al.*, 2000; Kolay, 2000). C_c values of compacted samples reported by Sinha *et al.*, (1998) are higher than those of other compacted samples, even though the void ratios of these samples are

smaller.
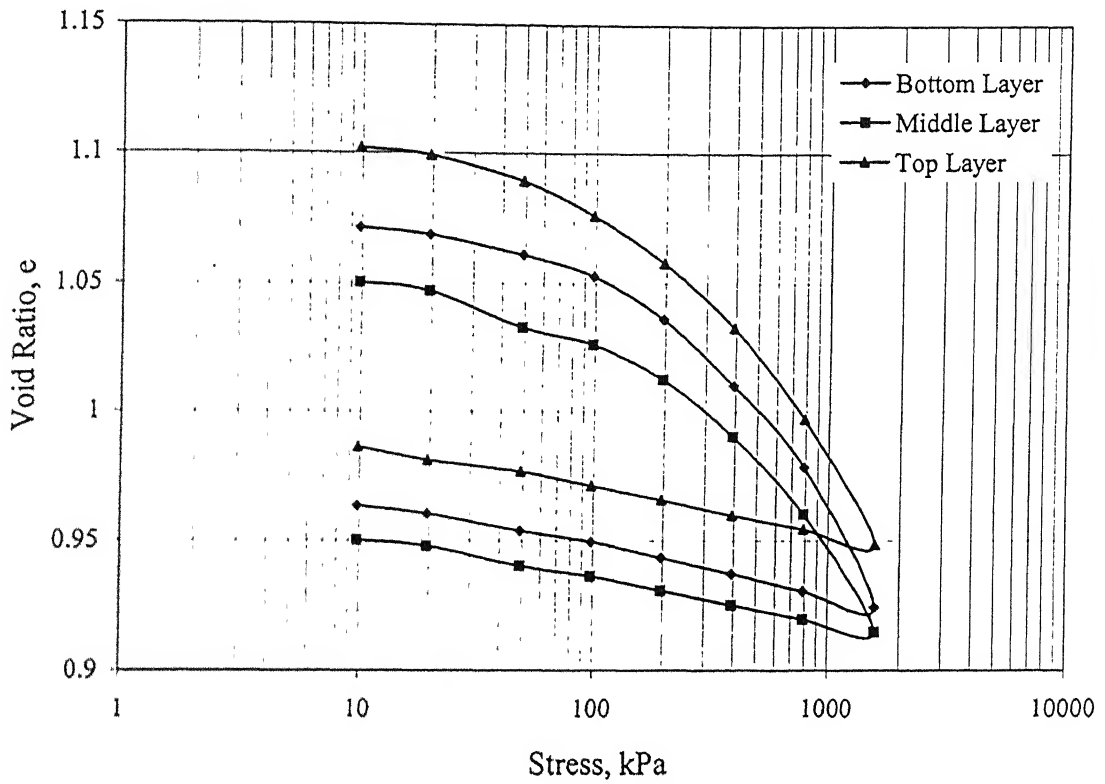
(a)
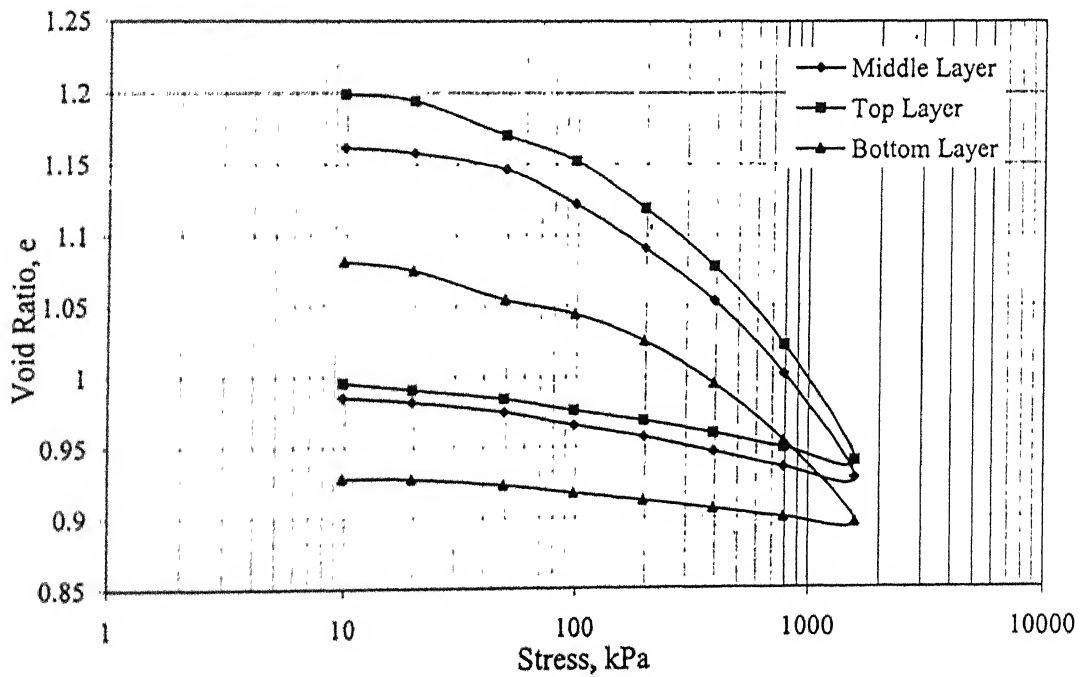
(b)

Fig. 3.13 Consolidation Characteristics of Sedimented Fly Ash from a) Series 1 b) Series 2.

34
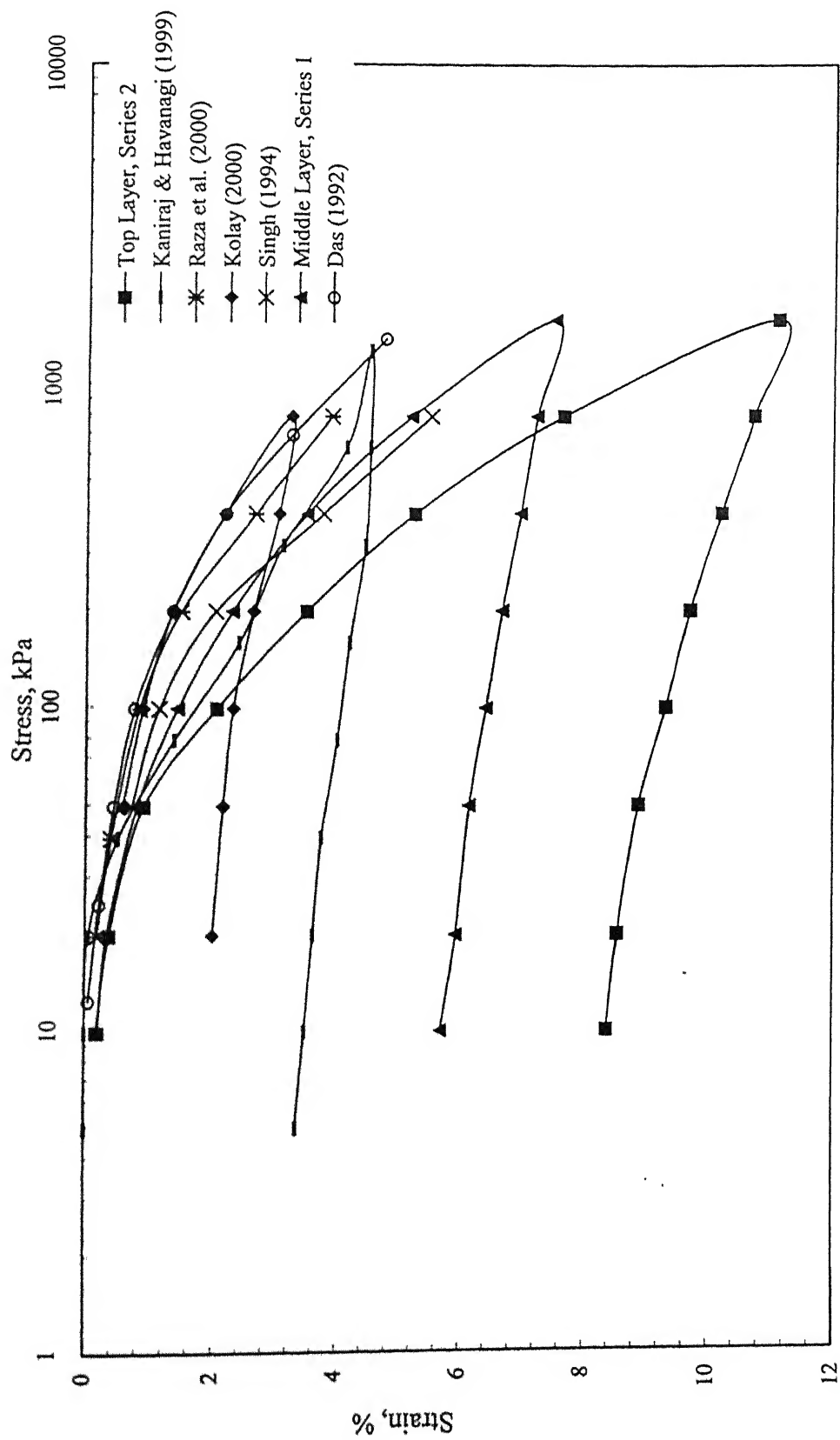
Fig. 3.14 Consolidation Characteristics of Sedimented and Compacted Fly Ash

35
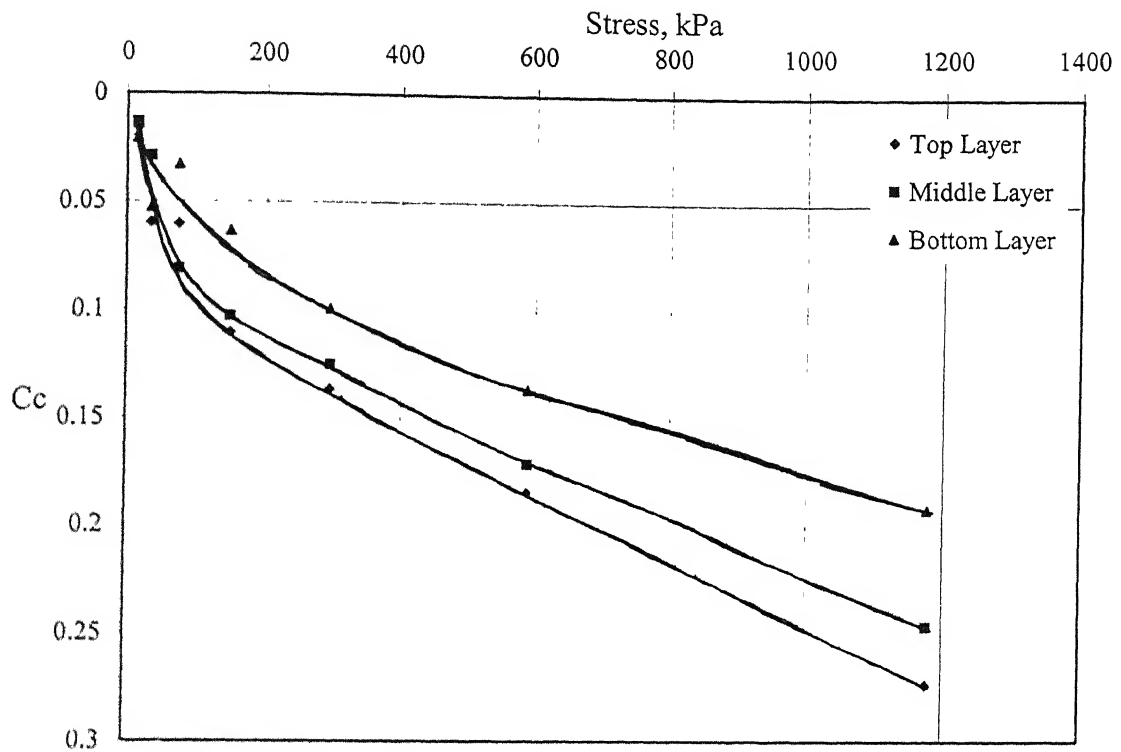
Fig. 3.15 Variation of Compression Index with Average Effective Stress of Sedimented Fly Ash Samples from Series 2.
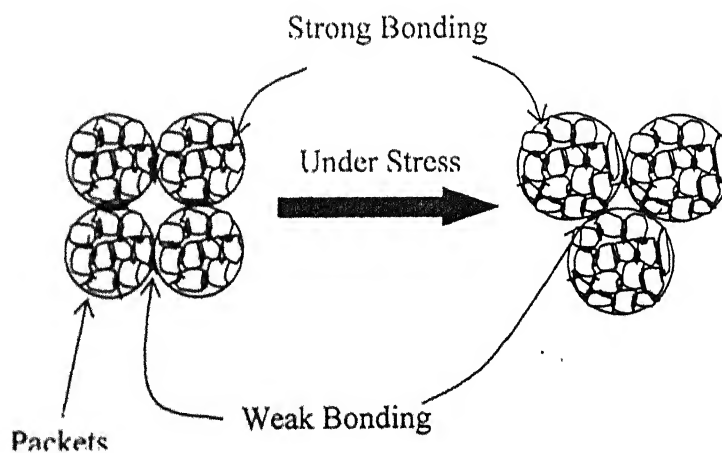
Fig. 3.16 Definition Sketch for Mechanism of Increase in Compressibility with Effective Stress.

Table 3.5. Comparison of C_c of Sedimented Deposits with Compacted Fly Ash.

	Compression Index, C_c	Initial Void Ratio, e_o	C_r	Remarks
Present Study	0.1 (100 kPa) – 0.2 (1 Mpa)	1.1 to 1.2	0.01 - 0.04	Sedimented deposits
McLaren and Digioia (1987)	0.13 ± 0.088	0.8 ± 0.2	--	Normally Consolidated
Kaniraj and Havanagi (1999)	0.072	1.17	0.017	Statically compacted at OMC and MDD
Raza et al. (2000)	0.1158	1.755	—	Compacted to 76.5% of MDD at OMC
Kolay (2000)	0.0328	0.9	0.016	Compacted at OMC.
Sinha, et al. (1998)	0.12 to 0.31	0.71 – 1.145	—	Compacted to 85%, 90% and 95% of MDD.
Yudbhir and Honjo (1991)	0.225 ± 0.16 (Medium dense) to 0.4 ± 0.21 (Loose)	1.0 – 2.0	—	Hydraulically placed in Lagoons

3.3.4 Collapse Potential

The results of double oedometer tests on the samples collected from different depths from series 1 and 2 are plotted as strain (ε) versus log (σ') in Figures. 3.17 and 3.18 respectively. Plots are presented in the form of vertical strain, ε, vs. log σ' curves rather than in the form of e vs. log σ' to avoid the effect of variation of initial water content/void ratio of the samples (Table 3.6). Initially, dried samples are loaded to a

certain predetermined stress, σ'_c, (Table 3.7) and flooded with water subsequently. The samples are kept under this stress until the settlements become negligible. The samples are further loaded similar to the wet samples. Collapse potential (C_p) of the fly ash is determined using Eq. 3.1.

Table 3.6. Variation of the Initial Water Content (%) of the Samples from Series 1 and 2

Sample from	Series 1	Series 2
Top Layer	55.71	57.85
Middle Layer	51.87	54.69
Bottom Layer	51.8	54.67

The slope of the (Figs. 3.17 and 3.18) curves is varying and more with stress. In some dry samples strains after collapse i.e. after flooded with water are more by approximately by 0.5% (Fig. 3.18 c, Dry Sample 1) to 3% (Fig. 3.17 b, Dry Sample 1) compared to those of wet samples. Table 3.7 presents the collapse potential values of the samples from sedimented deposits and of samples compacted at their OMC (Kolay, 2000). The average collapse potential of the sedimented samples is found to be of order of 0.5% and more as compared to the compacted samples. Collapse potential of compacted sample decreases with increase in effective stress.

The collapse potential of samples from sedimented fly ash beds range between 0.4 and 0.8 except for one (Table 3.7). All the values measured being less than 1.0 (Table 2.2), the severity of collapse on foundations is negligible. The collapse potential of sedimented fly ash beds is considerably higher than that of compacted samples (Kolay, 2000).

3.3.5 Gradation Analysis

Grain size distributions are evaluated before and after consolidation on samples from top and middle layers of series 3 to evaluate the changes that occur during the consolidation process. The results presented in Figure. 3.19 reveal that grain size distributions of particles subjected to higher stresses move to the right, showing that the

particle sizes of the samples are more compared to those of the samples before consolidation and reveal that bonding might have taken place between the fly ash particles under stress. This bonding may be due to the presence of calcium in small amounts.
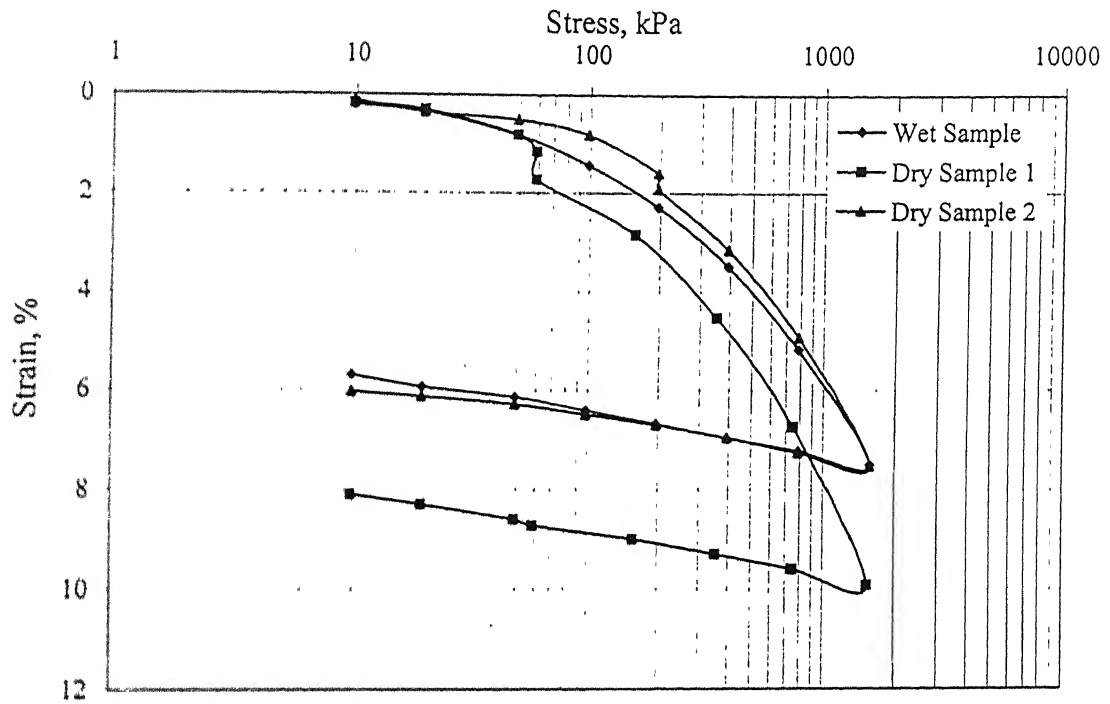
(b)
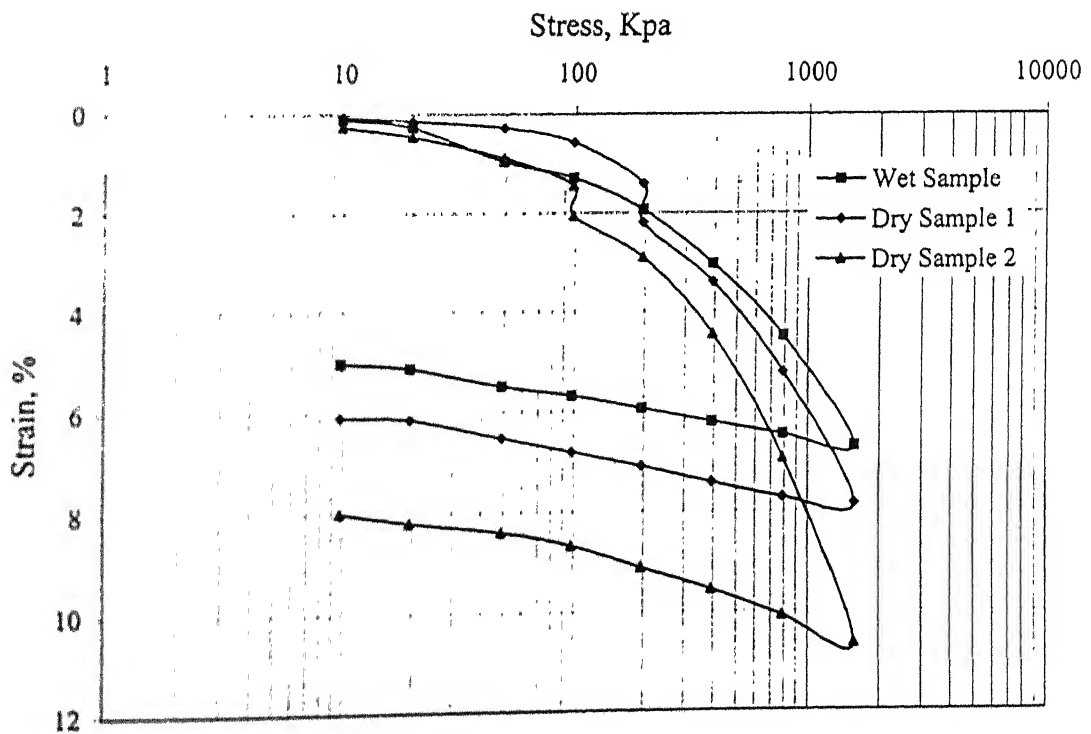
(b)
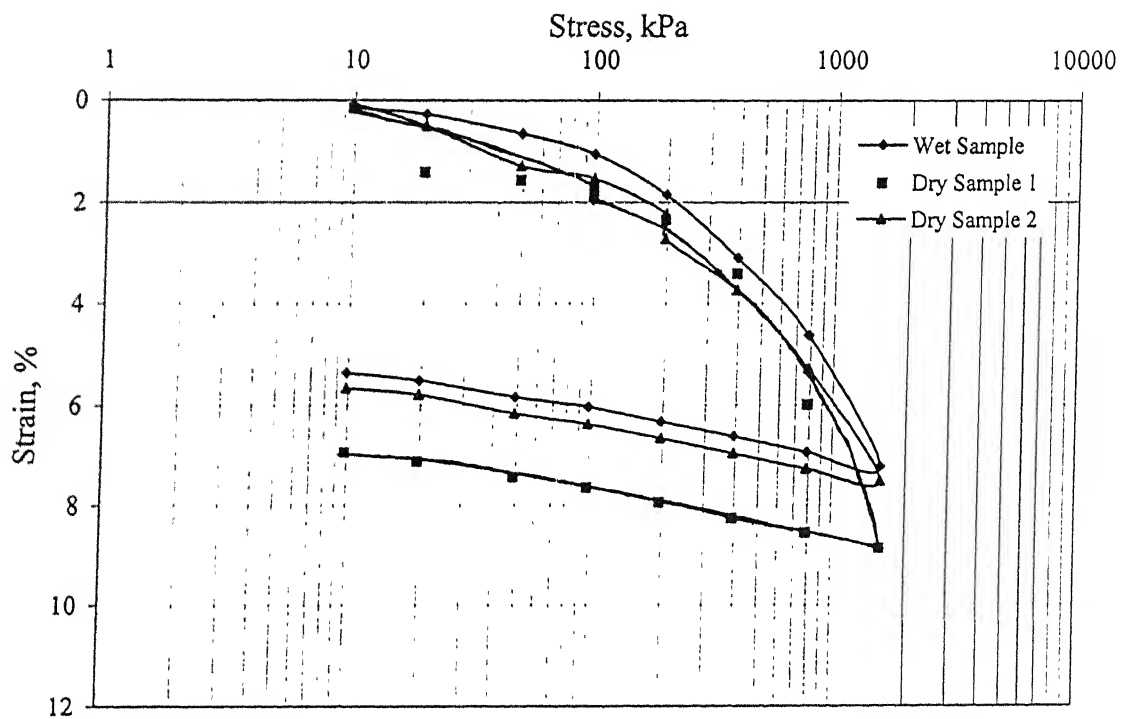
(c)

Fig. 3.17 Results of the Double Oedometer Tests on Samples from Series 1. (a) Top Layer; (b) Middle Layer and (c) Bottom Layer.
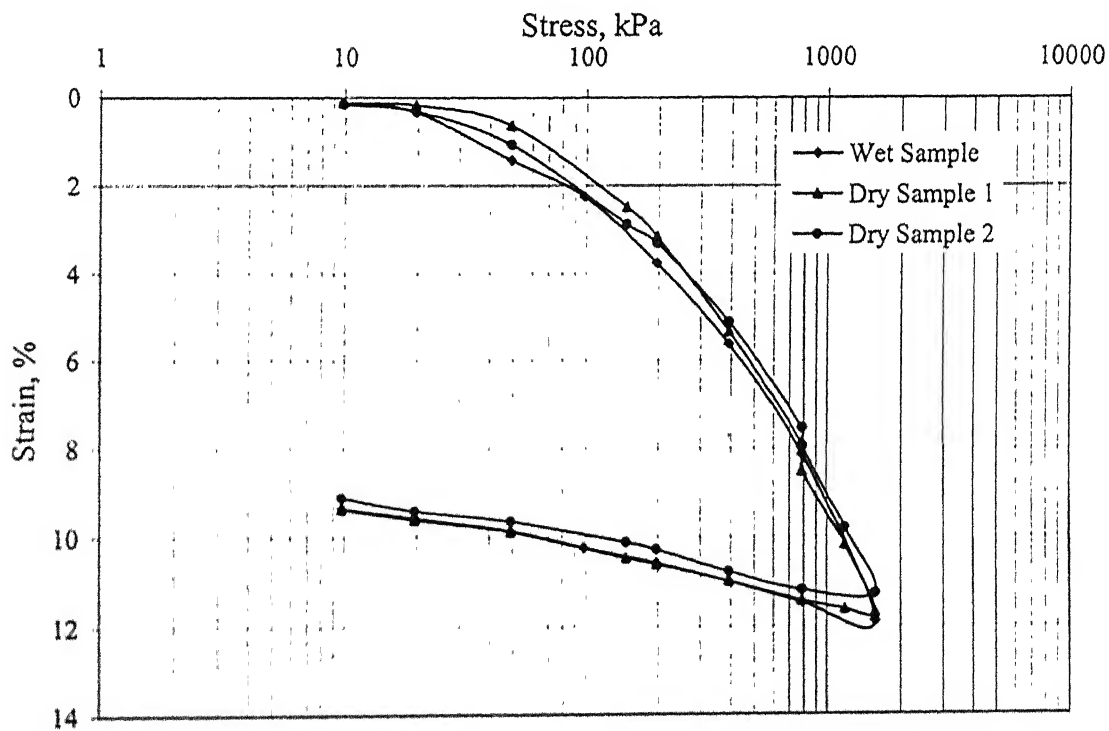
(a)
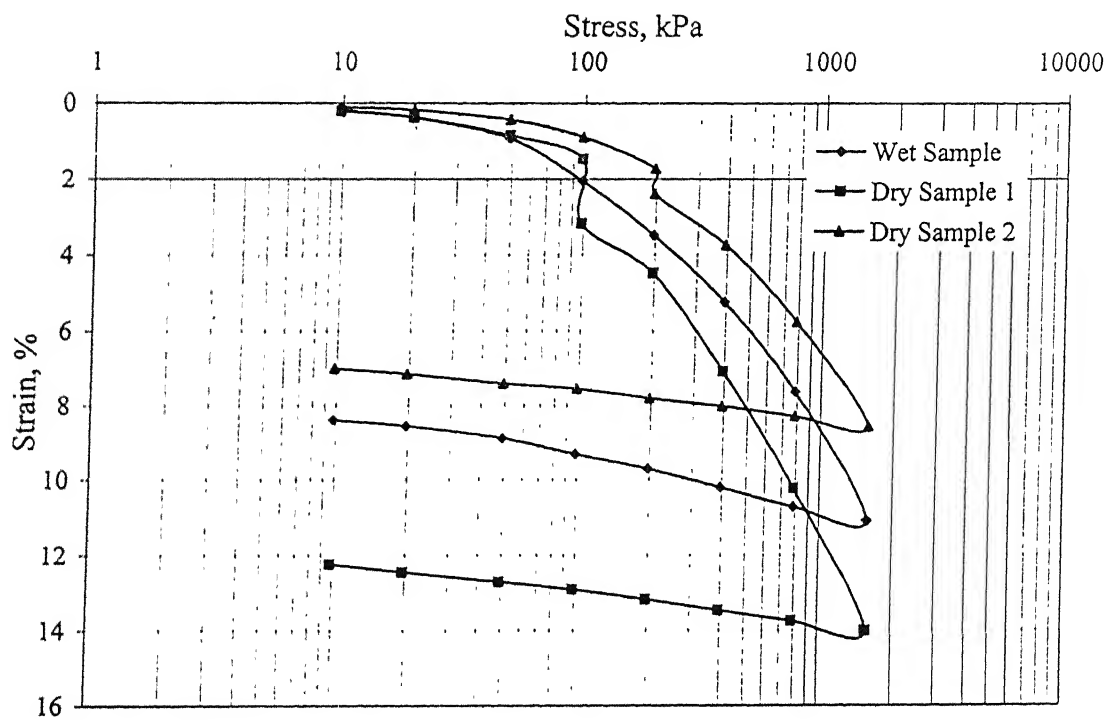
(b)
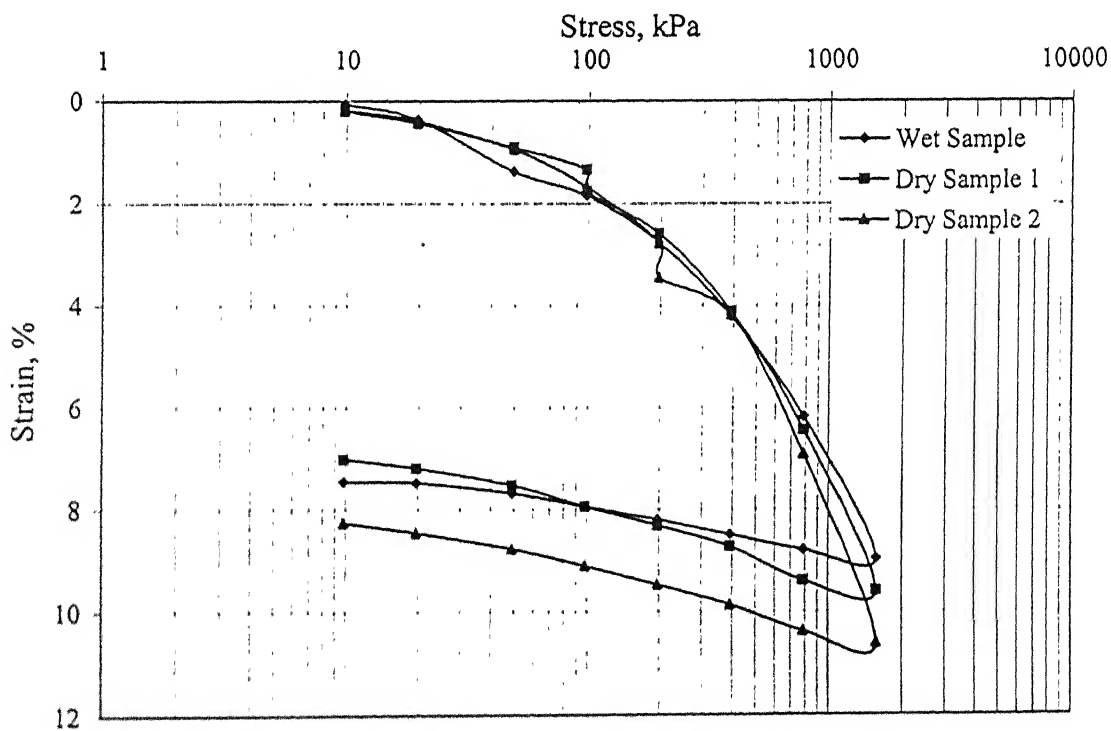
(c)

Fig. 3.18 Results of the Double Oedometer Tests on Samples from Series 2. (a) Top
Layer; (b) Middle Layer; (C) Bottom Layer.

Table. 3.7 Collapse Potential (Cp in %) of the Fly Ash Samples from Sedimented Deposits

Sample from (Sedimented Deposit)		Series 1				Series 2			
		Sample 1		Sample 2		Sample 1		Sample 2	
		Cp	σ_c'	Cp	σ_c'	Cp	σ_c'	Cp	σ_c'
Top Layer		0.61	60 kPa	0.41	200 kPa	0.57	800 kPa	0.33	800 kPa
Middle Layer		0.67	100 kPa	1.72	200 kPa	0.79	100 kPa	0.60	200 kPa
Bottom Layer		0.41	100 kPa	0.67	200 kPa	0.16	100 kPa	0.51	200kPa
Compacted sample (Kolay, 2000)	σ_c',kPa	20		50		100		200	400
	C_P	0.29		0.046		0.047		0.042	0.015
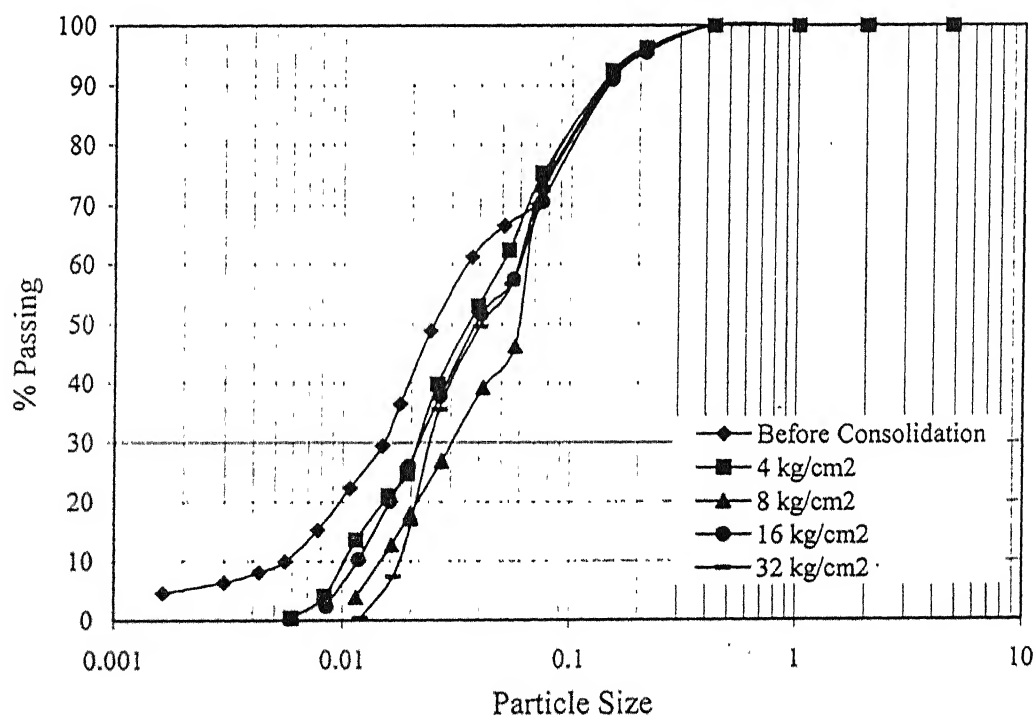
(a)
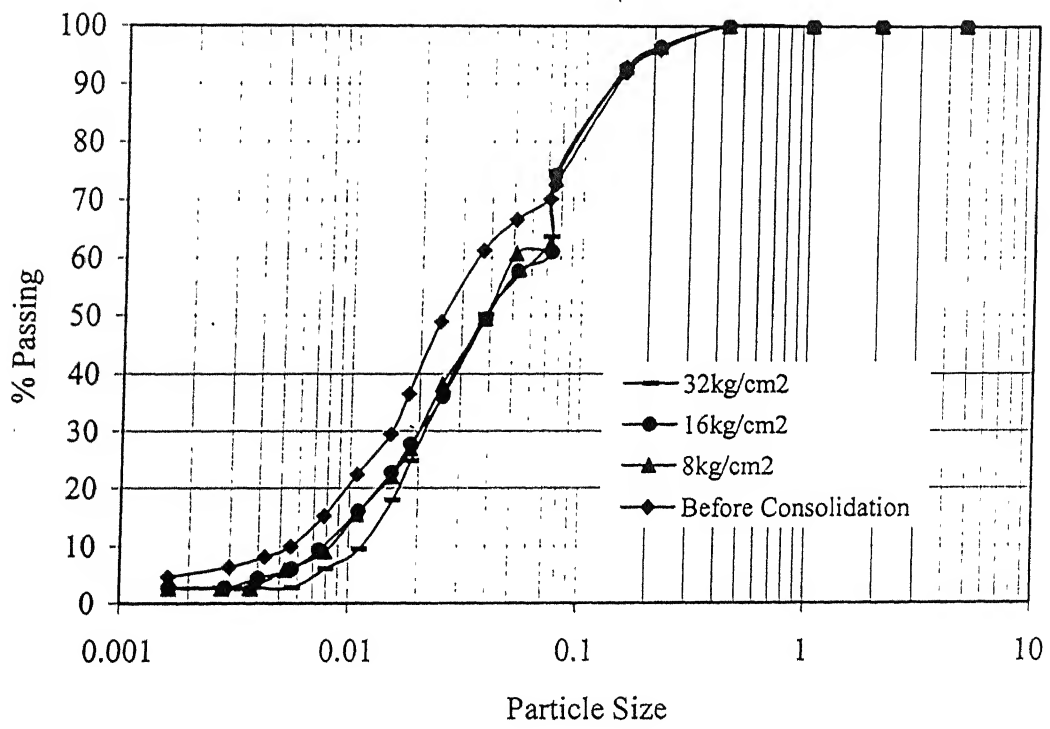
(b)

Fig. 3.19 Particle Size Distributions of Samples from Series 3 subjected to Consolidation. (a)Top Layer and (b) Middle Layer.

CHAPTER 4

ANALYTICAL STUDY

4.1 GENERAL

Fly ash released into the pond undergoes sedimentation through water, passing from a suspension to very soft state. The sediment then undergoes self-weight consolidation accompanied by large strains, stiffness increasing with depth or on additional loading. Many models for one-dimensional consolidation were developed neglecting the stresses due to self-weight. Gibson *et al.,* (1967) proposed a theory, which accounts for large strains and the variation of compressibility and permeability during consolidation. Lee and Sills (1981) applied this theory to consolidation during and after deposition. The important aspect in Lee and Sill's approach is the consideration of self-weight during the consolidation process as it has significant effect in case of soft soils and fly ash deposited in fluidized form. In the above theories the initial void ratio, e_i, of the deposit is assumed to be constant. Saito *et al.,* (2001) proposed an analytical model to deduce the depth wise distribution of void ratio and other soil parameters by applying Bjerrum's (1967) hypothesis.

4.2 PROBLEM STATEMENT

A new theory is proposed to determine the in situ variation of void ratio, unit weight and effective stress with depth of sedimented and normally consolidated fly ash deposit. In practice fly ash slurry is deposited in layers into the ash ponds or lagoons. Each layer undergoes sedimentation and then consolidation under its own weight and also under the weight of the layers placed above it. It is assumed that the water table is at ground surface i.e. effect of desiccation is neglected. The Final state of the deposit is considered in the proposed theory.

4.2.1 FORMULATION

Figure 4.1 shows the schematic diagram of sedimentation followed by consolidation. The co-ordinate 'h' (Fig 4.1 a) represents the depth of the deposit prior to sedimentation while 'z' represents the depth after the completion of consolidation (Fig.

44

4.1 b). It is assumed that the sedimented deposit is initially of uniform submerged density 'γ_{bo}' and the rate of deposition 'V (= dh/dt)' is constant. T_o is the total time of sedimentation and consolidation. The process of consolidation is assumed to begin from an infinitesimal initial effective stress of $\sigma_o = \gamma_{bo}Vt_c$ attained in time t_c. It is assumed that the water table is at ground surface i.e. the effect of desiccation is neglected. The final state of the deposit is estimated by the proposed theory.
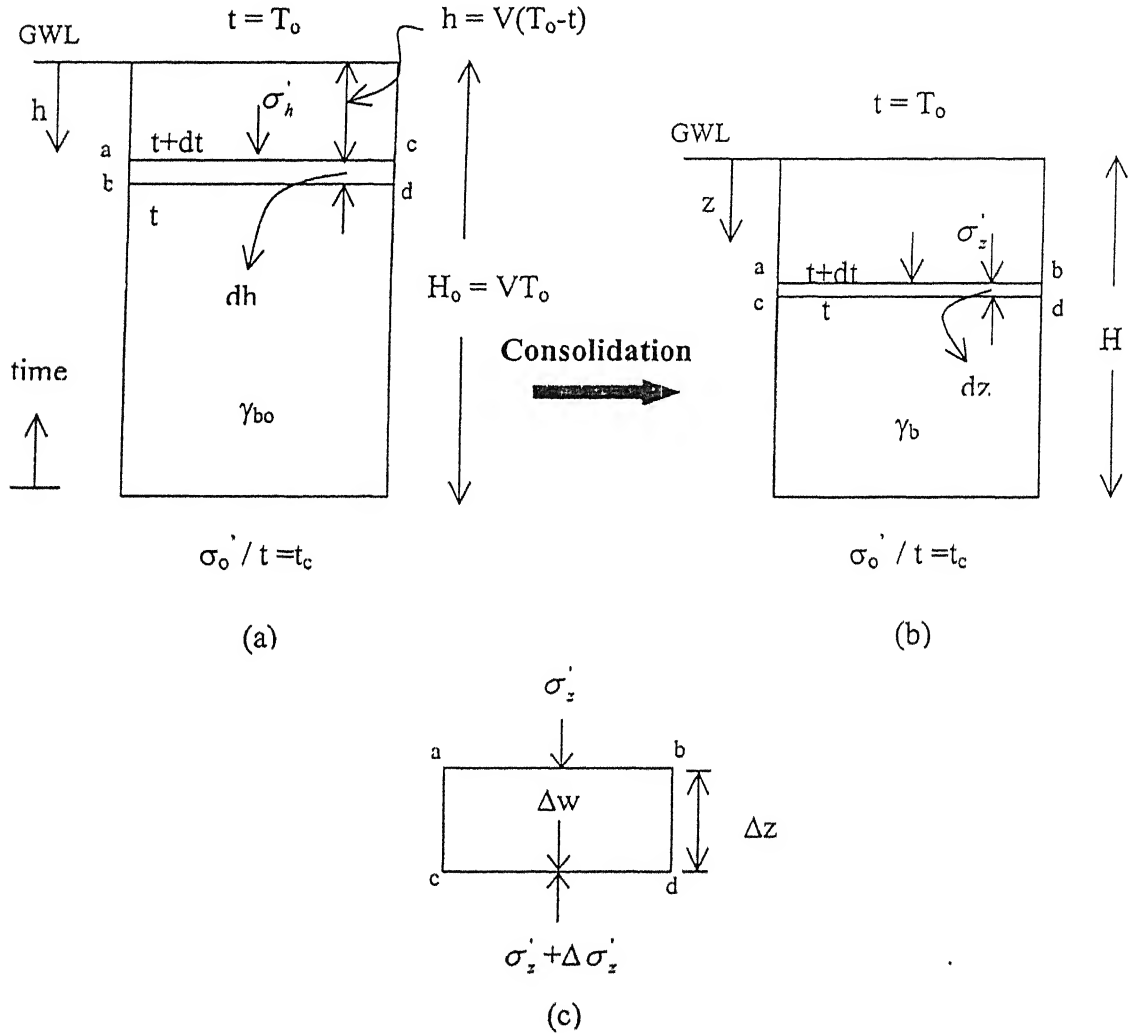

Fig. 4.1 Problem Definition a) As Deposited b) Final State c) Element 'abcd'.

Considering vertical equilibrium of the element 'abcd' at time, t (Fig. 4.1 b) one gets.

$$\frac{d\sigma_z'}{dz} = \gamma_b(z) \tag{4.1}$$

where σ_z' is the effective stress and $\gamma_b(z)$ is submerged unit weight of fly ash at depth, z.

As the void ratio is a function of 'z', the unit weight is also a function of 'z' and is given by the following expression.

$$\gamma_b(z) = f(z) = \frac{(G_s - 1)\gamma_w}{1 + e(z)} \tag{4.2}$$

Substitution of Eq. (4.2) in (4.1) gives

$$\frac{d\sigma_z'}{dz} = \frac{(G_s - 1)\gamma_w}{1 + e(z)} \tag{4.3}$$

where e (z) is the void ratio at depth 'z' and G_s is the specific gravity of solids. Linear relationship between void ratio, e, and log of effective stress, σ' is considered. Hence the change in void ratio for primary compression, Δe_p, is

$$\Delta e_p = C_c \log \frac{\sigma_z'}{\sigma_o'} \tag{4.4}$$

C_c is the compression index and σ_o' is the initial effective stress from which state consolidation is initiated. Change in void ratio due to secondary compression or creep, Δe_s, following Mesri (1973) and Mesri & Godlewski (1977) is

$$\Delta e_s = C_\alpha \Delta \log t \tag{4.5}$$

where 'C_α' is the secondary compression index and t is time.
The total change in void ratio, Δe, is

$$\Delta e = \Delta e_p + \Delta e_s = C_c \log \frac{\sigma_z'}{\sigma_o'} + C_\alpha \log \frac{(T_o - t)}{t_c} \tag{4.6}$$

The number of soil particles above the element 'abcd' before and after consolidation, at depth 'h' in sedimented deposit (Fig 4.1 a) equal to V(T_o-t), at time 't' are the same. Hence the effective stress on it before consolidation, σ_h', (Fig. 4.1 a) should equal the effective stress after consolidation, σ_z', (Fig 4.1 b).

i.e. $\sigma_z' = \sigma_h' = \gamma_{bo}h = \gamma_{bo}V(T_o-t)$ \hfill (4.7)

Substituting Eq. (4.7) in Eq. (4.6), one gets

$$\Delta e = C_c \log \frac{\gamma_{bo} V (T_o - t)}{\sigma_o'} + C_\alpha \log \frac{(T_o - t)}{t_c}$$

$$\Rightarrow e(z) = e_i - (C_c \log \frac{\gamma_{bo} V (T_o - t)}{\sigma_o'} + C_\alpha \log \frac{(T_o - t)}{t_c}) \tag{4.8}$$

where 'e_i' is the initial depositional void ratio of the deposit.

Substituting Eqs. (4.7) and (4.8) in Eq. (4.3), one gets

$$\frac{-dT^*}{d\bar{z}} = \frac{a}{b - C_c \log \frac{\gamma_{bo} V t_c (T_o^* - T^*)}{\sigma_o'} - C_\alpha \log (T_o^* - T^*)} \tag{4.9}$$

where $a = \frac{(G_s - 1)\gamma_w H_o}{\gamma_{bo} V t_c}$; $b = (1 + e_i)$; $T^* = \frac{t}{t_c}$; $T_o^* = \frac{T_o}{t_c}$ and $\bar{z} = \frac{z}{H_o}$.

Equation (4.9) is in normalized form and in finite difference form is

$$-\frac{(T_i^* - T_{i+1}^*)}{\Delta \bar{z}_i} = \frac{a}{b - C_c \log \frac{\gamma_{bo} V t_c (T_o^* - T_i^*)}{\sigma_o'} - C_\alpha \log (T_o^* - T_i^*)} \tag{4.10}$$

where T_i^*, T_{i+1}^* and $\Delta \bar{z}_i$ are normalized times of ith, $(i+1)^{th}$ layer and thickness of ith layer respectively.

Substituting $\sigma_o' = \gamma_{bi} V t_c$ in Eq. (4.10), one gets

$$-\frac{(T_i^* - T_{i+1}^*)}{\Delta \bar{z}_i} = \frac{a}{b - c \log (T_o^* - T_i^*)} \tag{4.11}$$

where $c = C_c + C_\alpha$.

Solving Eq. (4.10) or (4.11) for $\Delta \bar{z}_i$, one gets

$$\therefore \Delta \bar{z}_i = \frac{(T_{i+1}^* - T_i^*)\{b - C_c \log \frac{\gamma_{bo} V t_c (T_o^* - T_i^*)}{\sigma_o'} - C_\alpha \log (T_o^* - T_i^*)\}}{a} \tag{4.12}$$

47

$$\text{or } \Delta \bar{z}_i = \frac{(T^*_{i+1} - T^*_i)\{b - c \log(T^*_o - T^*_i)\}}{a} \qquad (4.13)$$

$$\Rightarrow \Delta z_i = \Delta \bar{z}_i \times H_o$$

$$\text{and } z = \sum_{i=1}^{n} \Delta z_i \qquad (4.14)$$

$$\sigma'_z = \sum_{i=1}^{n} \gamma_{b_i} \times \Delta z_i \qquad (4.15)$$

where γ_{b_i} is computed from Eq. (4.2).

The coordinate, z, is determined using Eq. (4.12) and the corresponding void ratio, submerged unit weight and effective stress are calculated using Eqs. (4.8), (4.2) and (4.15) respectively. A parametric study is carried out by varying the parameters – initial depositional void ratio, e_i, from 1.0 to 3.0, compression index, C_c, from 0.1 to 0.3, the specific gravity of fly ash particles, G_s, from 1.9 to 2.1, σ'_o from 0.01 to 0.3 kPa, the ratio C_α/C_c from 0 to 0.05, depositional rate 'V' from 0.5 to 2.0 m/year and T_o from 15 to 75 years. Results are presented in the form of variations of void ratio, total unit weight and effective stress of the deposit with depth.

4.3 VARIATION OF COMPRESSION INDEX, C_c, WITH VOID RATIO

The e versus log σ' plots of one-dimensional consolidation tests conducted on samples collected from different depths – top, middle and bottom layers of sedimented and consolidated fly ash beds, do not show any linear relation over the stress range investigated. The compression index, C_c, of fly ash increases with normal stress (Fig.3.15) as e versus log σ' curves are steeper at higher stresses (Fig. 3.13), in the range of stress considered. The same is plotted with respect to average void ratio, e_{avg}. C_c is found to vary linearly with e_{avg} (Fig. 4.2). This linear variation of compression index is incorporated in e versus σ' relationship to study its effect on the variation of void ratio with depth. Following is the expression is proposed for linear variation of C_c based on results shown in Fig. 4.2

$$C_c = C_{c_o} + \mu(e_i - e) \qquad (4.16)$$

where C_{c_o} is the compression index at $e=e_i$ and μ is the slope of C_c versus e_{avg}.
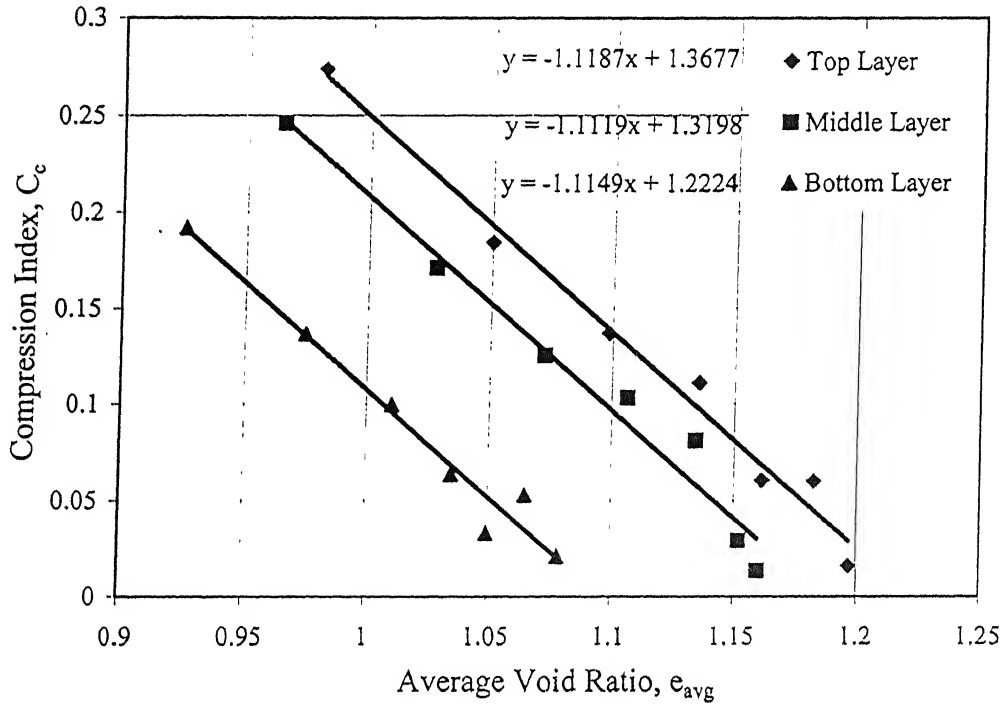
Fig. 4.2 Variation of Compression Index with Average Void Ratio of Sedimented Fly Ash Samples from Series 2.

4.3.1 RELATIONSHIP BETWEEN VOID RATIO AND EFFECTIVE STRESS FOR C_c VARYING LINEARLY WITH VOID RATIO

From Figs. 3.8 and 4.2 it is evident that

$$\frac{de}{d(\log \sigma')} = -C_c = -\left\{ C_{c_o} + \mu(e_i - e) \right\} \tag{4.17}$$

$$\Rightarrow \frac{de}{\left\{ C_{c_o} + \mu(e_i - e(z)) \right\}} = -0.434 d(\ln \sigma'(z)) \tag{4.18}$$

Integrating both sides of Eq. 4.18 with limits e_0 at σ_o' to $e(z)$ at $\sigma'(z)$, one gets

$$\left\{ \frac{C_{c_o} + \mu(e_i - e(z))}{C_{c_o}} \right\} = \left(\frac{\sigma'(z)}{\sigma_o'} \right)^{0.434\mu} \tag{4.19}$$

Solving Eq. 4.19 for $e(z)$, one gets

49

$$e(z) = \frac{1}{\mu}\left\{(C_{c_o} + \mu e_i) - C_{c_o}\left(\frac{\sigma'}{\sigma_o'}\right)^{0.434\mu}\right\}$$ (4.20)

Neglecting the secondary compression and substituting Eqs. (4.7) and (4.20) in Eq. (4.3), one gets

$$\frac{-dT^*}{d\bar{z}} = \frac{a}{1 + \frac{1}{\mu}\left\{(C_{c_o} + \mu e_i) - C_{c_o}\left(\frac{\gamma_{bo} Vt_c (T_o^* - T^*)}{\sigma_o'}\right)^{0.434\mu}\right\}}$$ (4.21)

Eq. (4.21) is in normalized form and in finite difference form is

$$-\frac{(T_i^* - T_{i+1}^*)}{\Delta \bar{z}_i} = \frac{a}{1 + \frac{1}{\mu}\left\{(C_{c_o} + \mu e_i) - C_{c_o}\left(\frac{\gamma_{bo} Vt_c (T_o^* - T_i^*)}{\sigma_o'}\right)^{0.434\mu}\right\}}$$ (4.22)

Substitution of $\sigma_o' = \gamma_{bo} Vt_c$ in Eq. (4.22), one gets

$$-\frac{(T_i^* - T_{i+1}^*)}{\Delta \bar{z}_i} = \frac{a}{1 + \frac{1}{\mu}\left\{(C_{c_o} + \mu e_i) - C_{c_o}\left(T_o^* - T_i^*\right)^{0.434\mu}\right\}}$$ (4.23)

Solving Eq. (4.22) or (4.23) for $\Delta \bar{z}_i$, one gets

$$\therefore \Delta \bar{z}_i = \frac{(T_{i+1}^* - T_i^*)\left(1 + \frac{1}{\mu}\left\{(C_{c_o} + \mu e_i) - C_{c_o}\left(\frac{\gamma_{bo} Vt_c (T_o^* - T_i^*)}{\sigma_o'}\right)^{0.434\mu}\right\}\right)}{a}$$ (4.24)

$$\text{or } \Delta \bar{z}_i = \frac{(T_{i+1}^* - T_i^*)\left(1 + \frac{1}{\mu}\left\{(C_{c_o} + \mu e_i) - C_{c_o}\left(T_o^* - T_i^*\right)^{0.434\mu}\right\}\right)}{a}$$ (4.25)

$$\Rightarrow \Delta z_i = \Delta \bar{z}_i \times H_o$$

$$\text{and } z = \sum_{i=1}^{n} \Delta z_i$$ (4.26)

The coordinate 'z' is computed using Eq. (4.26) and the corresponding void ratio and compression index are determined using Eqs. (4.20) and (4.16) respectively.

4.4 RESULTS AND DISCUSSION

Results obtained from analytical studies are presented and discussed here

4.4.1 WITH CONSTANT C_c

The present study is validated with Saito *et al.* (2001) who determined the variations of void ratio, unit weight, effective stress, apparent preconsolidation, overconsolidation ratio, etc. with depth of sedimented and consolidated clay deposits, whose lowermost formation is T_o years old. The initial conditions, i.e. initial depositional void ratio, e_i, submerged unit weight, γ_{bi}, at the time of deposition and compression index, C_c, are computed from the present conditions - plasticity index, PI, and average unit weight, $\bar{\gamma}'$, Eqs (4.27) and (4.28).

$$\bar{\gamma}' = \frac{G_s - 1}{1 + G_s \dfrac{a(1.79PI + 13.8)}{100}} \gamma_w \tag{4.27}$$

$$C_c = (0.015 + 0.007PI)/0.434. \tag{4.28}$$

The rate of deposition, V, is computed from Eq. (4.29)

$$V = \frac{H}{T_o} / \left\{ 1 - \frac{\lambda + \alpha'}{1 + e_i} (\ln T_o - \ln t_c - 1) \right\} \tag{4.29}$$

where a = ratio of w_n (natural water content) / w_L (liquid limit), H is the present thickness of the deposit, $\lambda = 0.434 C_c$ and α' is the secondary compression index.

Variation of void ratio with depth is obtained for a deposit whose lowermost formation is 5000 years (T_o) old, present thickness is 20 m (H), a = 0.87, G_s = 2.7 and PI = 20 i.e C_c = 0.35. In the present study variation of void ratio, unit weight and effective with depth of sedimented and consolidated deposit, that will form after T_o

पुरुषोत्तम काशीनाथ केलकर पुस्तकालय

years from now, are determined assuming the initial conditions – initial depositional void ratio, submerged unit, compression index and rate of deposition. For validation purposes the variation of void ratio with depth for the same initial conditions and data (Saito *et al.,* 2001) are determined. Results obtained are depicted in Fig. 4.3. The two approaches agree closely.

Effect of initial depositional void ratio on the variation of void ratio with depth is depicted in Fig. 4.4. Very sharp decrease of void ratio occurs in the top 2 to 3 m of the deposit. Thereafter the variation is very gradual for all depositional void ratios. The total depth of the deposit increases with increase in initial depositional void ratio. As the initial depositional void ratios are high the unit weight of the deposit will be low resulting in effective stresses that are less in value compared to those resulting from low initial depositional void ratio, of say 1.5. Therefore the compression will be less for deposits with high initial void ratios, which is reflected in Fig 4.4. Since the variation of void ratio with depth is similar for all initial void ratios a normalized plot in which the void ratio, e, is normalized with initial void ratio, e_i, is also shown in Fig. 4.4 b.

Fig. 4.5 depicts the effect of initial depositional void ratio on the variation of unit weight with depth, z. In the top 2 to 3 m the unit weight increases rapidly with depth. There after it increases gradually from 15.5 to 16.7 kN/m^3, 14.2 to 15 kN/m^3 and 13.3 – 14 kN/m^3 from approximately 2.5 m to the bottom of the deposit for void ratios 1.5, 2.0 and 2.5 respectively. Increase in the unit weight is more for deposit with low initial depositional void ratio. From Figs. 4.4 and 4.5 it is evident that the variation of effective stress with depth will be more for deposits with low initial depositional void ratios (Fig. 4.6). The variations in effective stress with depth are nonlinear.

A sediment transforms into a solid once particles come into contact with each other and transfer stresses from one to the other. An infinitesimal initial effective stress, σ_o', is required, to initiate primary compression (Eq. 4.4). A parametric study is carried out to quantify the effects initial stress, σ_o'. Sridharan et al. (1998) proposed the yield shear strength for clayey soils at settling limit to be around 7 Pa. Initial stress, σ_o', in the present study is varied from 0.01 to 0.03 kPa. The effect of initial stress, σ_o', on the variation of void ratio with depth is depicted in Fig. 4.7. The decrease in void ratio in

top 2 to 3 m is very high for low initial stresses (0.01 to 0.05 kPa), which is very unlikely. Therefore a mean value of $\sigma_o{'} = 0.1$ kPa is considered throughout the analysis.

Effect of initial stress, $\sigma_o{'}$, on the variations of unit weight and effective stress with depth are depicted in Figs. 4.8 and 4.9. The unit weights corresponding to low values of initial effective stresses, 0.01 to 0.05 kPa are high as the compression is more (Eq. 4.8) i.e. void ratios are less compared to void ratios with high initial stresses, 0.15 to 0.3 kPa (Fig. 4.7). Final thickness (H) of the deposit increases with increase in initial effective stress, $\sigma_o{'}$, but the effective stresses at the bottom of the deposits with different final thickness are the same (Fig. 4.9) as the number soil particles are the same.

From the experiments conducted on fly ash slurry, with water content and initial void ratio varying from 74 to 81% and 1.35 to 1.65 respectively, the compression index is found to range from 0.1 to 0.17 (Table 3.3). Yudbhir and Honjo (1991) gave the range of compression index to be 0.24 to 0.61 for hydraulically placed fly ash with void ratio in the range of 1.0 to 2.0. In the present study compression index is varied from 0.1 to 0.3. Fig. 4.10 depicts the effect of compression index on the variation of void ratio with depth, z. For the compression index, C_c, of 0.1 and 0.15 the decrease in void ratio in the top 2 top 3 m is from 2.0 to 1.8 and 1.7 respectively, which is relatively low, while for $C_c = 0.3$ the decrease is from 2.0 to 1.3. Below the top 2 to 3 m, the variation of void ratio with depth is marginal for $C_c = 0.1$ and 0.15 while for $C_c = 0.3$ variation of void ratio with depth is significant.

Figs 4.11 and 4.12 depict the effect of compression index on the variation of unit weight and effective stress with depth, z. Unit weights are more and increase considerably with depth for compression index of 0.3 while the increase is almost constant with depth for compression index of 0.1 and 0.15. The effective stress (Fig 4.12) at the bottom of the deposit will be the same irrespective of the value of the compression index as the initial void ratio, depositional rate and time for sedimentation and consolidation are the same for all C_c values.

Effect of secondary compression index, C_α, on the variation of void ratio, unit weight and effective stress are depicted in Figs 4.13, 4.14 and 4.15 respectively. Mesri

and Godlewski (1977) suggested the range of the ratio C_α/C_c to be $0.025 - 0.1$. In the present study the ratio C_α/C_c for fly ash is varied from 0 to 0.05. $C_\alpha/C_c = 0.0$ corresponds to the case where secondary compression is negligible. The void ratios (Fig. 4.13) and unit weights (Fig 4.14) are almost the same in top 2 to 3 m, for all values of C_α/C_c. Thereafter the effect of secondary compression index becomes significant with depth, z. This is because the bottom layers are having a long duration of time compared to the layers near top. Fig 4.15 shows that the effect of secondary compression index in negligible on the variation of effective stress with depth, z, possibly because 50 years is too short a time for the effect of secondary compression to be significant on effective stress.

The rate of deposition, V, and time for sedimentation and consolidation, T_o, have no effect on the variations of void ratio, unit weight and effective stress with depth. But to show their effects on total thickness of the deposit, variations of unit weights with depth are presented in Figs. 9 and 10. To show the effect of 'V', each curve in Fig. 9 is shifted to the right by 0.5, 1.0, 1.5 kN/m^3 for V = 1.0, 1.5 and 2.5 m/yr respectively with respect to the curve for V = 0.5 m/yr. For showing the effect of T_o, each curve in Fig. 10 is shifted by 0.5, 1.0, 1.5 and 2.0 kN/m^3 for T_o = 30, 45, 60 and 75 years respectively with respect to the curve for T_o = 15 yrs.

Effect of specific gravity of fly ash particles, G_s, on the variations of unit weight and effective stress with depth, z are depicted in Figures 4.18 and 4.19 respectively. Unit weight for all the deposits increase sharply in the top 2 to 3 m. The increase is more for higher values of specific gravity. The increase in unit weights is gradual below 2 to 3 m. Effective stresses increases non-linearly with depth.

4.4.2 C_c VARYING LINEARLY WITH VOID RATIO

Considering the initial conditions, i.e. e_i and σ_o', same as the values for the top layer (TL) of series 2 (Fig. 3.13 b) i.e. 1.2 and 10 kPa respectively, C_{c_o} and μ are 0.03 and 1.11 respectively for the same sample (Fig. 4.2). The variation of void ratio is determined with depth for T_o = 50 yrs, G_s = 2.05 and V=1.0 m/yr. From the e $-$ log σ' relationship obtained from the consolidation test for top layer, series 2 (Chap. 3) the

effective stresses are converted to the corresponding depths, z. Both the experimental and predicted void ratios are plotted and the results depicted in Fig. 4.20. The predicted values agree closely with the measured ones.

Effect of variable compression index on the variation of void ratio with depth is depicted in Fig. 4.22. Compression index varies from an initial value of 0.03 at the top (e_i = 1.2) to 0.6 at the bottom (e = 0.65) of the deposit (Fig. 4.21). For comparison purpose variation of void ratio for an average value C_c of 0.25 (from Fig. 4.21) is also plotted in Fig. 4.21. In the top 2 to 3 m of deposit the void ratio does not decrease sharply as the compression index is very low in top few meters, but the decrease in void ratio increases with depth. In contrast the decrease in void ratio with depth is very sharp in top 2 to 3 m, thereafter the decrease in void ratio with depth is very much less for constant C_c. Void ratios at all the depths for a deposit with variable C_c are more compared to those with constant C_c.
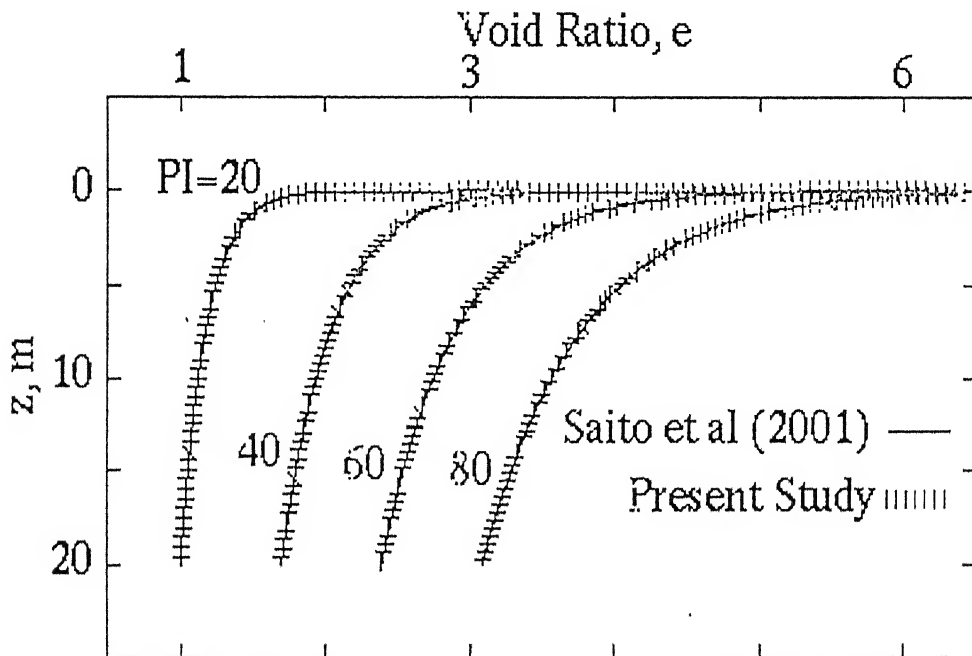

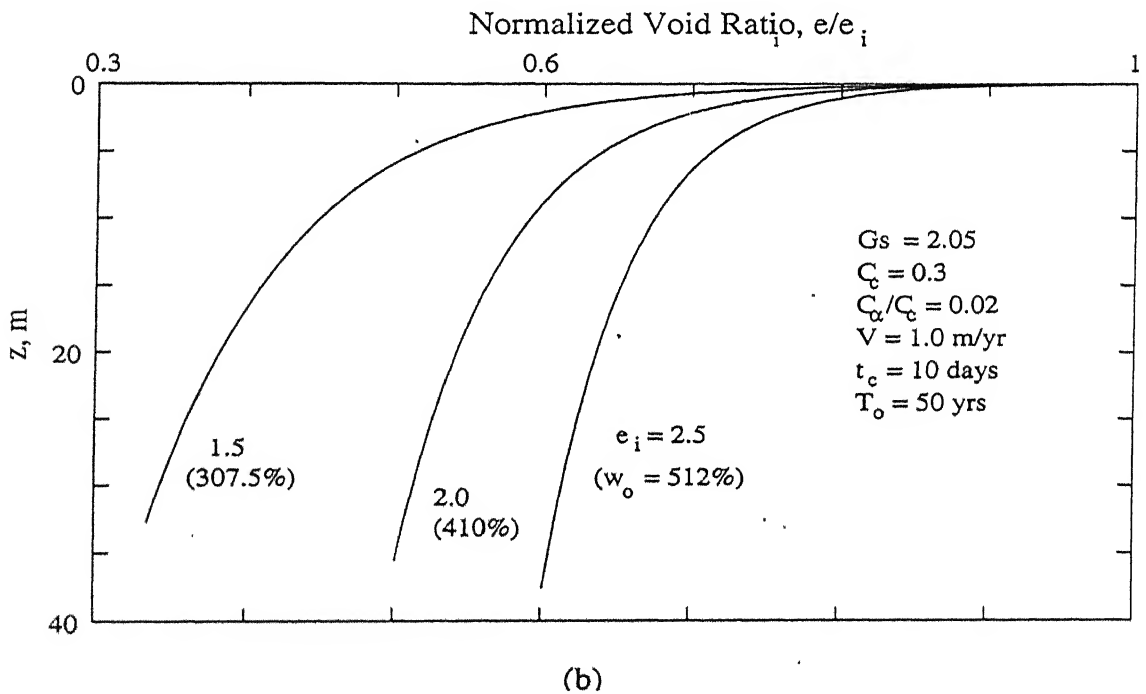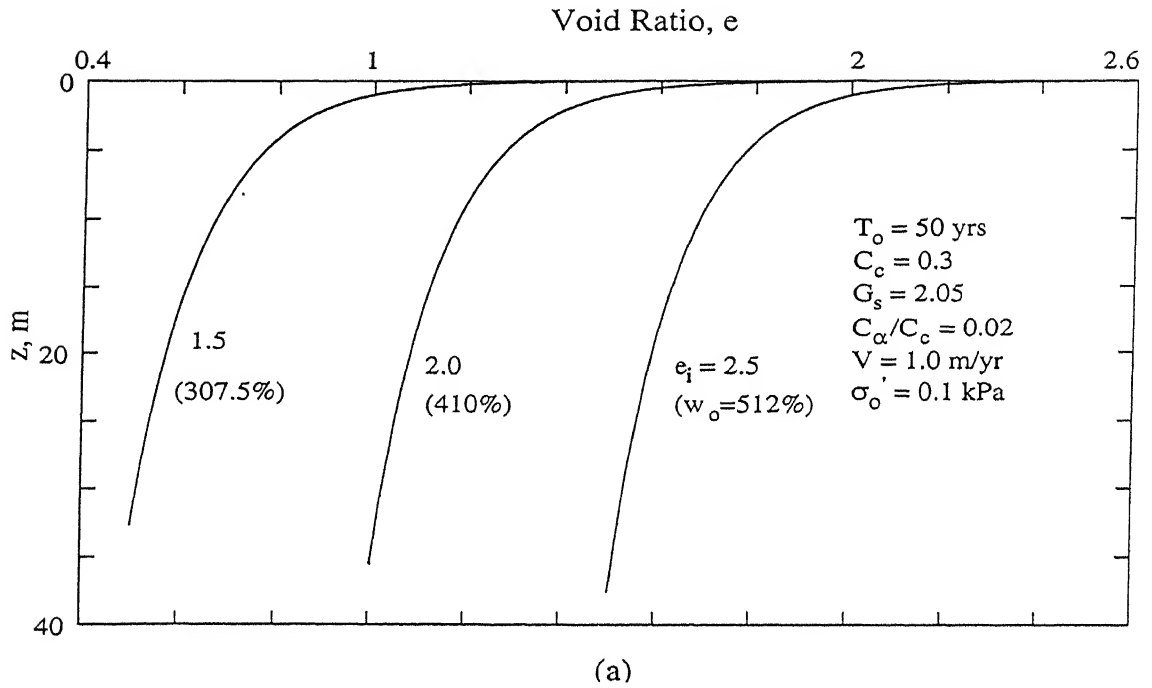Fig. 4.3 Comparison of Results of Present Study with those Based on Saito et al. (2001).

Figure 4.4: Effect of Initial Depositional Void Ratio on Varaition of a) Void Ratio and b) Normalized Void Ratio with Depth.
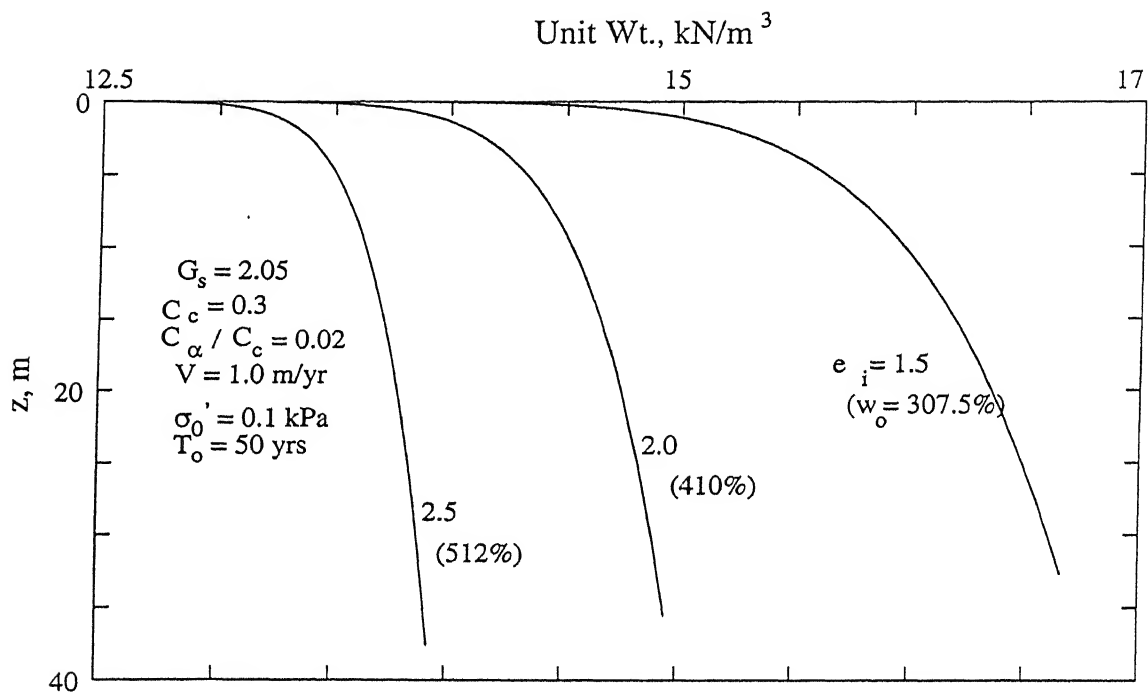
Unit Wt., kN/m^3

12.5   15   17

G$_s$ = 2.05
C$_c$ = 0.3
C$_\alpha$ / C$_c$ = 0.02
V = 1.0 m/yr

σ_0' = 0.1 kPa
T$_o$ = 50 yrs

e$_i$ = 1.5
(w$_o$ = 307.5%)

2.0
(410%)

2.5
(512%)

z, m

20

40

Figure 4.5: Effect of Initial Depositional Void Ratio on the Variation of Unit Weight with Depth.

EffectiveStress, kPa

0   100   200

e$_i$ = 1.5 (w$_o$ = 307.5%)

G$_s$ = 2.05
C$_c$ = 0.3
C$_\alpha$ / C$_c$ = 0.02
T$_o$ = 50 yrs

σ_0' = 0.1 kPa
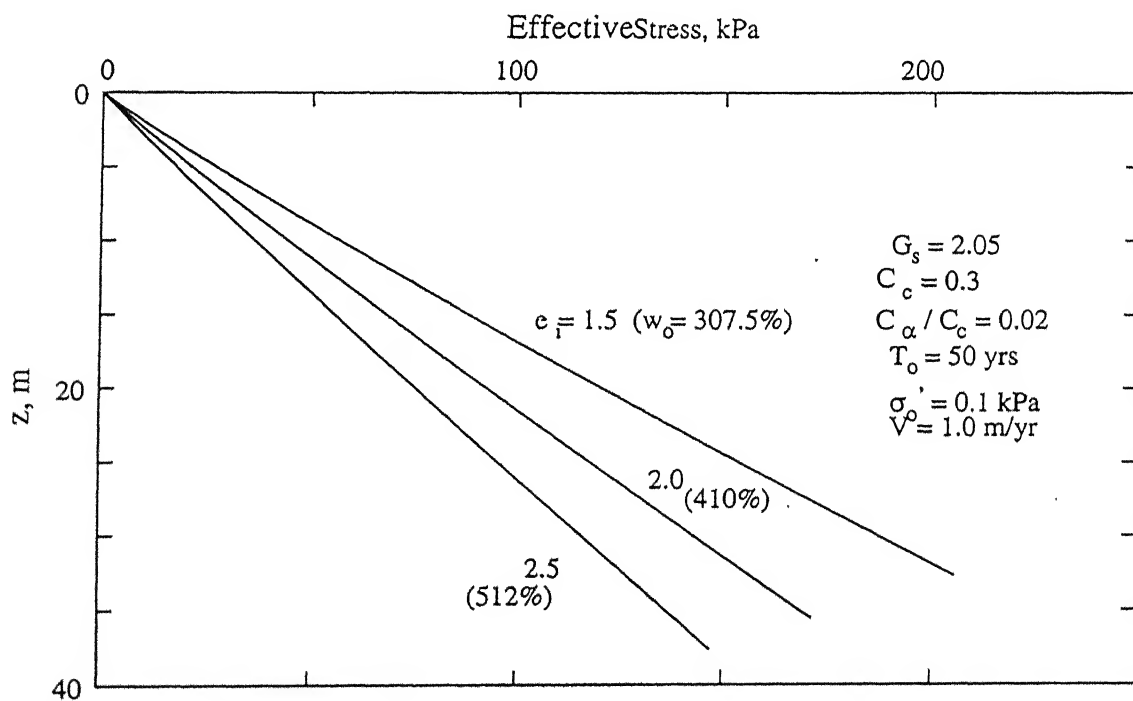V = 1.0 m/yr

2.0 (410%)

2.5
(512%)

z, m

20

40

Figure 4.6: Effect of Initial Depositional Void Ratio on the Variation of Effective Stress with Depth.

57

Figure 4.7: Effect of Initial Stress, σ_o', on the Variation of Void Ratio with Depth.

Figure 4.8: Effect of Initial Stress, σ_o', on the Variation of Unit Weight with Depth

58

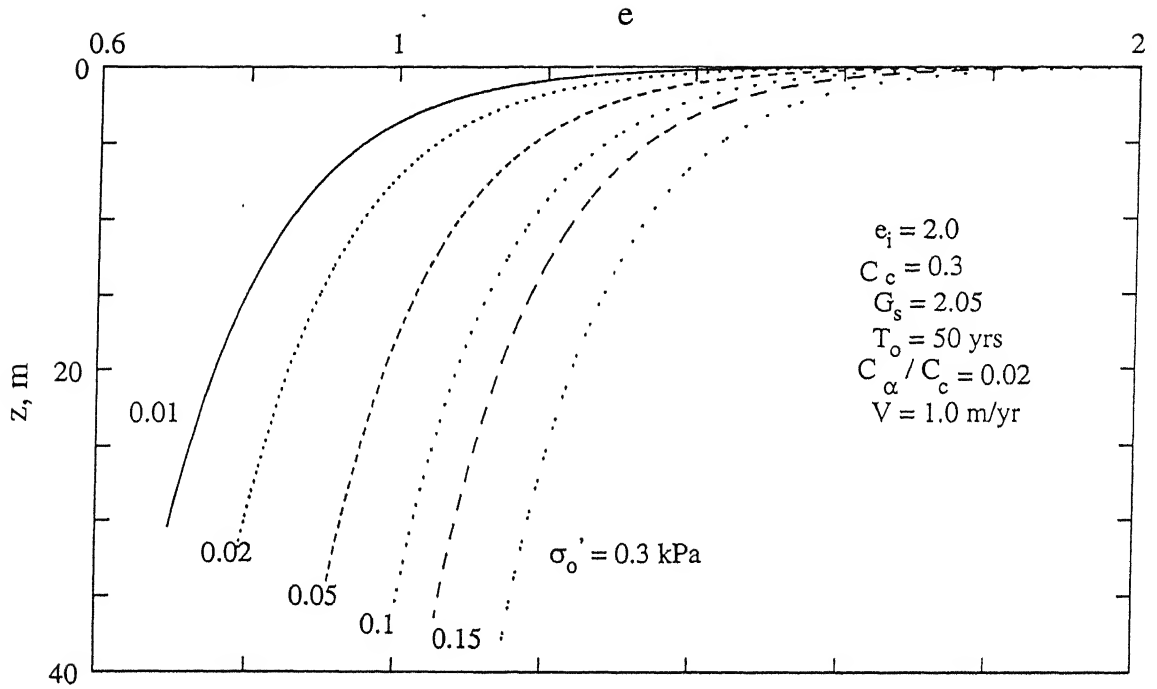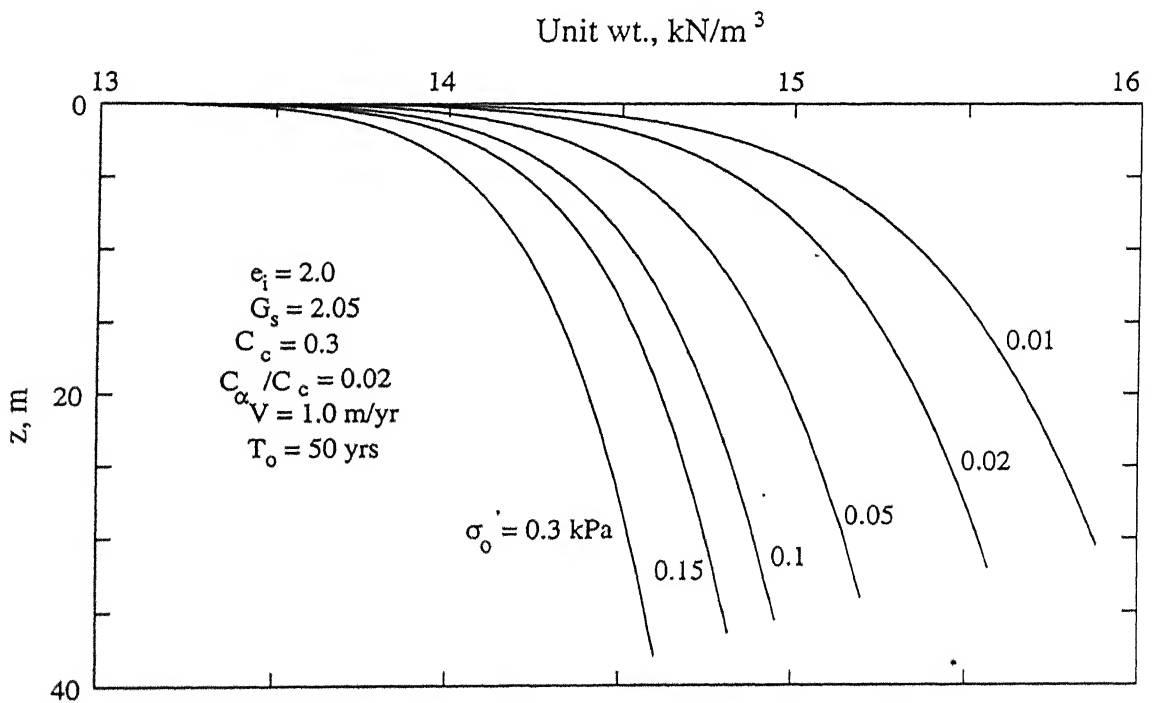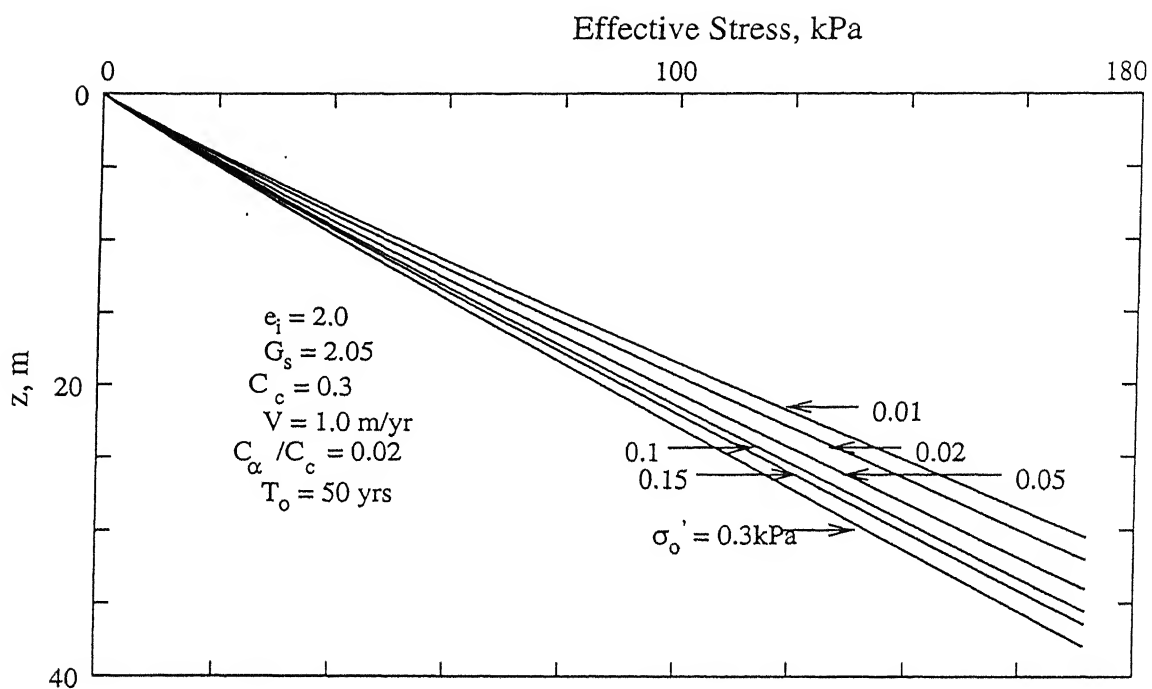Figure 4.9: Effect of Initial Stress, σo, on the Variation of Effective Stress with Depth.
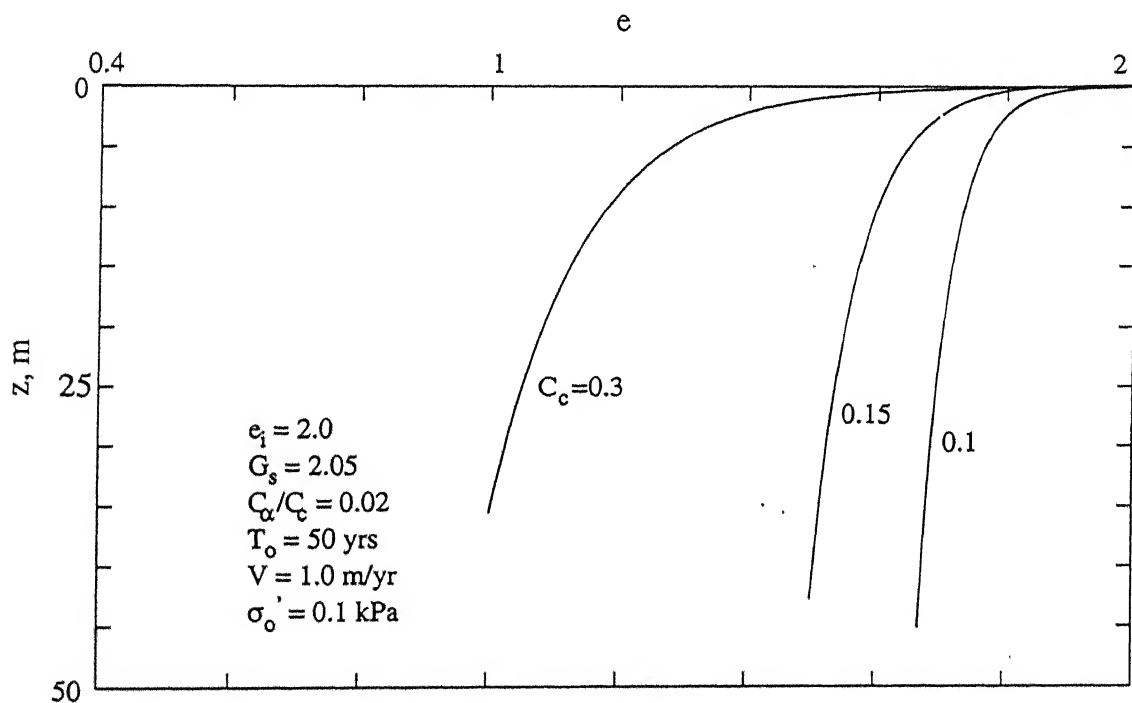

Figure 4.10: Effect of Compression Index, C_c, on the Variation of Void Ratio with Depth.
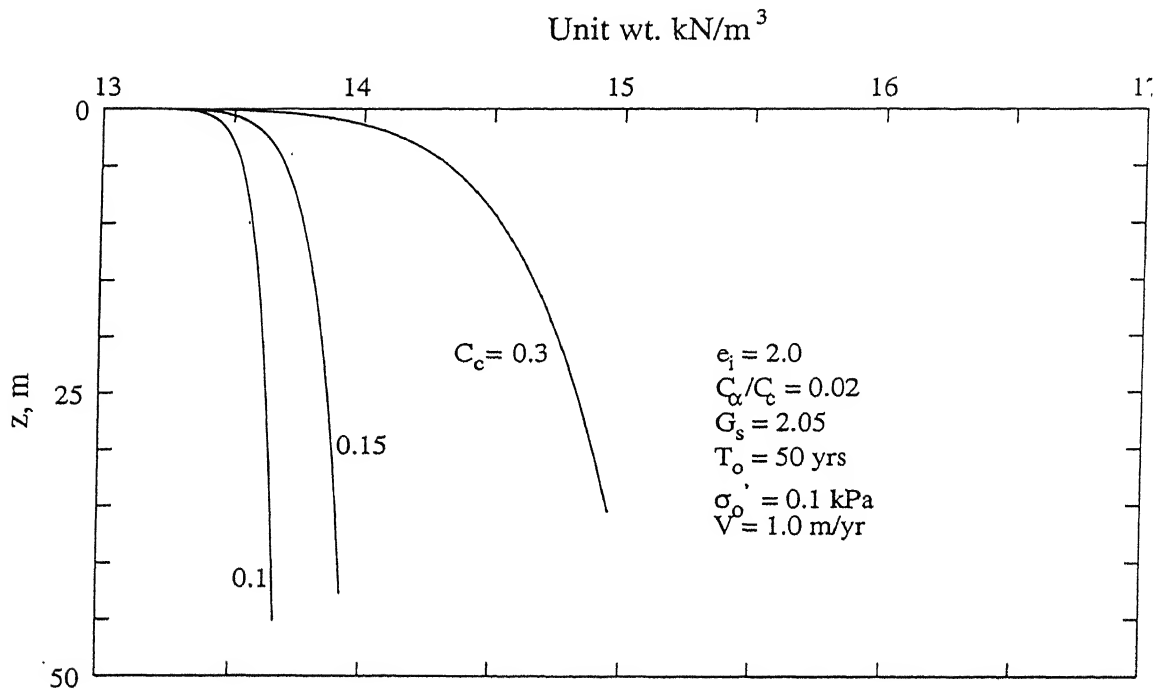
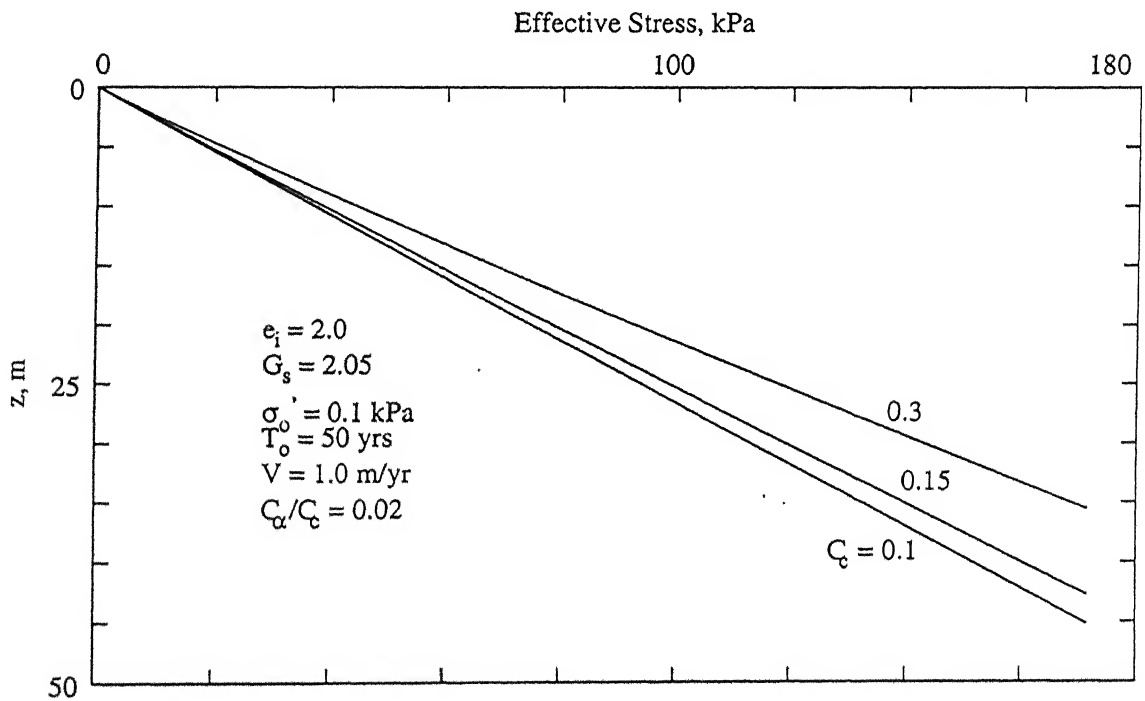Figure 4.11: Effect of Compression Index, C_c, on the Variation of Unit Weight with Depth.

Figure 4.12: Effect of Compression Index, C_c, on the Variation of Effective Stress with Depth.
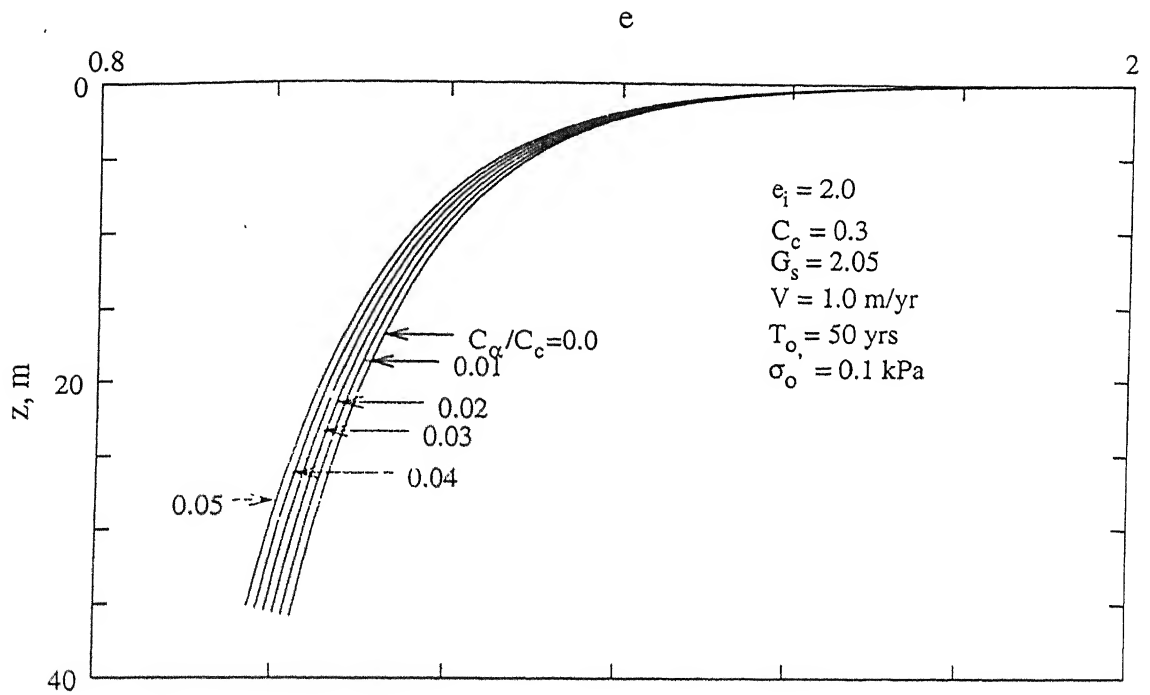
60

Figure 4.13: Effect of Secondary Compression Index, C_α, on the Variation of Void Ratio with Depth.
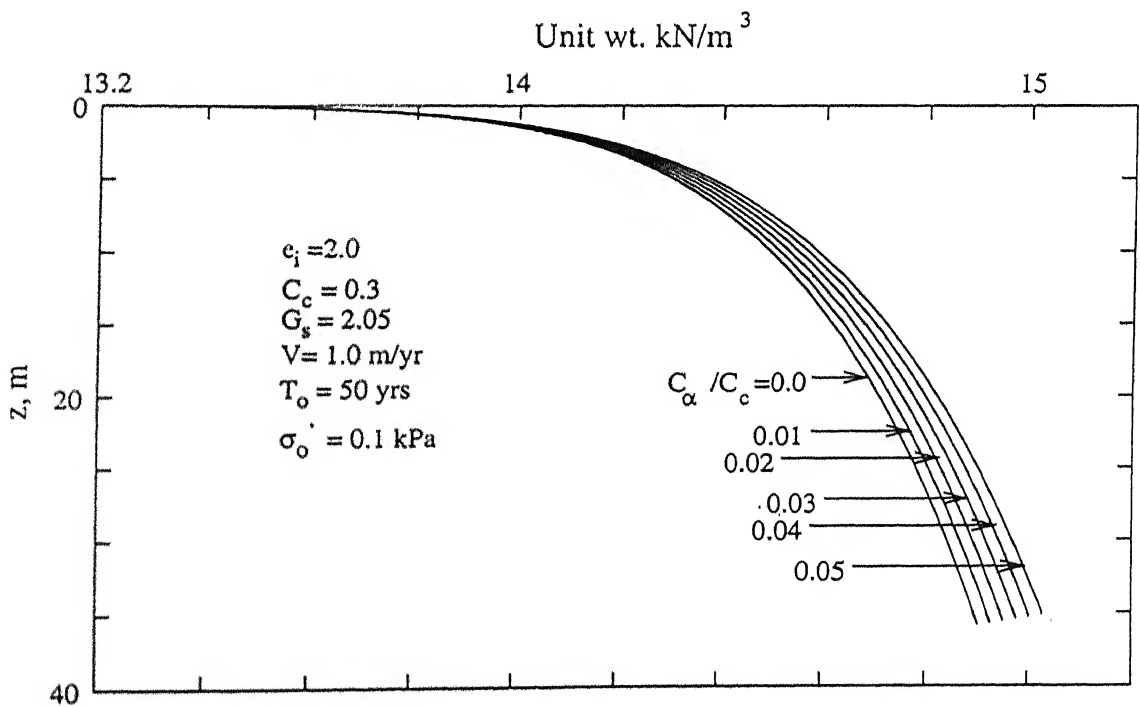
Figure 4.14: Effect of Secondary Compression Index, C_α, on the Variation of Unit Weight with Depth.

Figure 4.15: Effect of Secondary Compression Index, C_α, on a) Void Ratio b) Unit Weight and c) Effective Stress
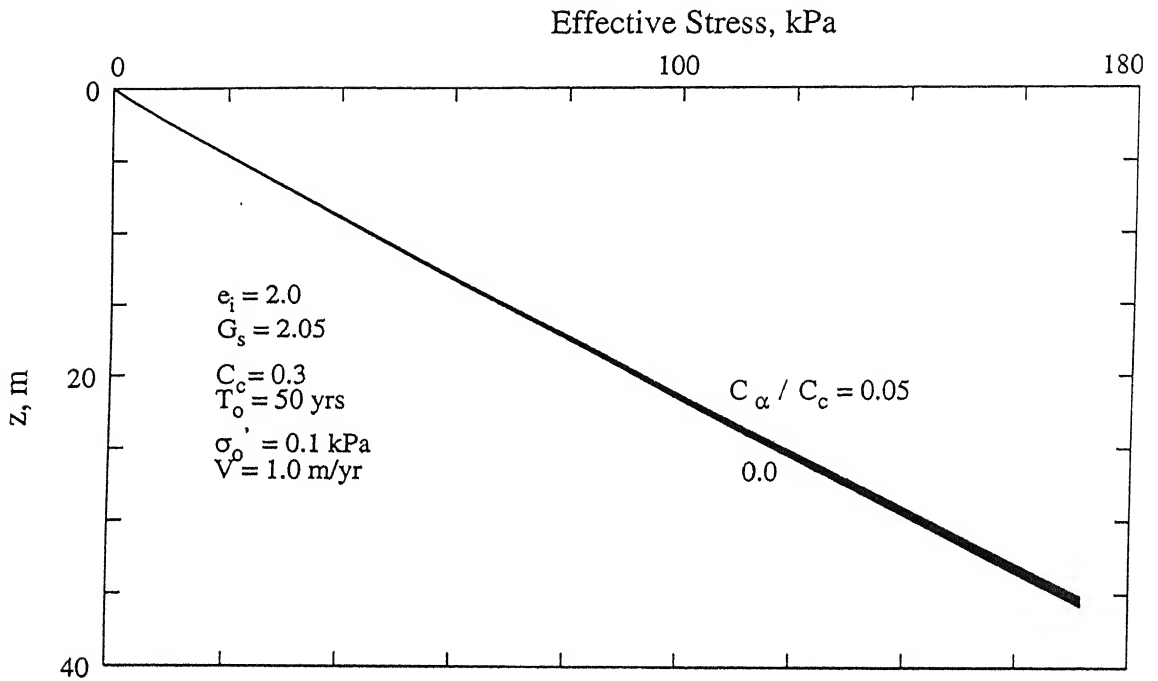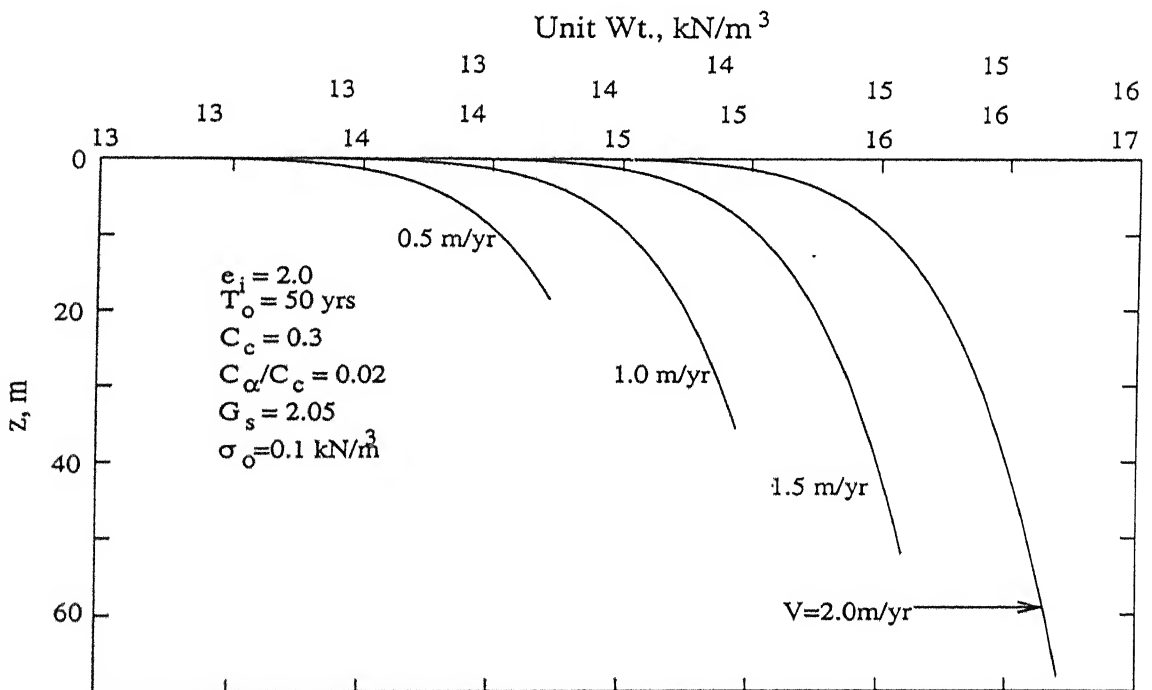

Figure 4.16: Effect of Rate of Deposition, V, on the Variation of Unit Weight with Depth.
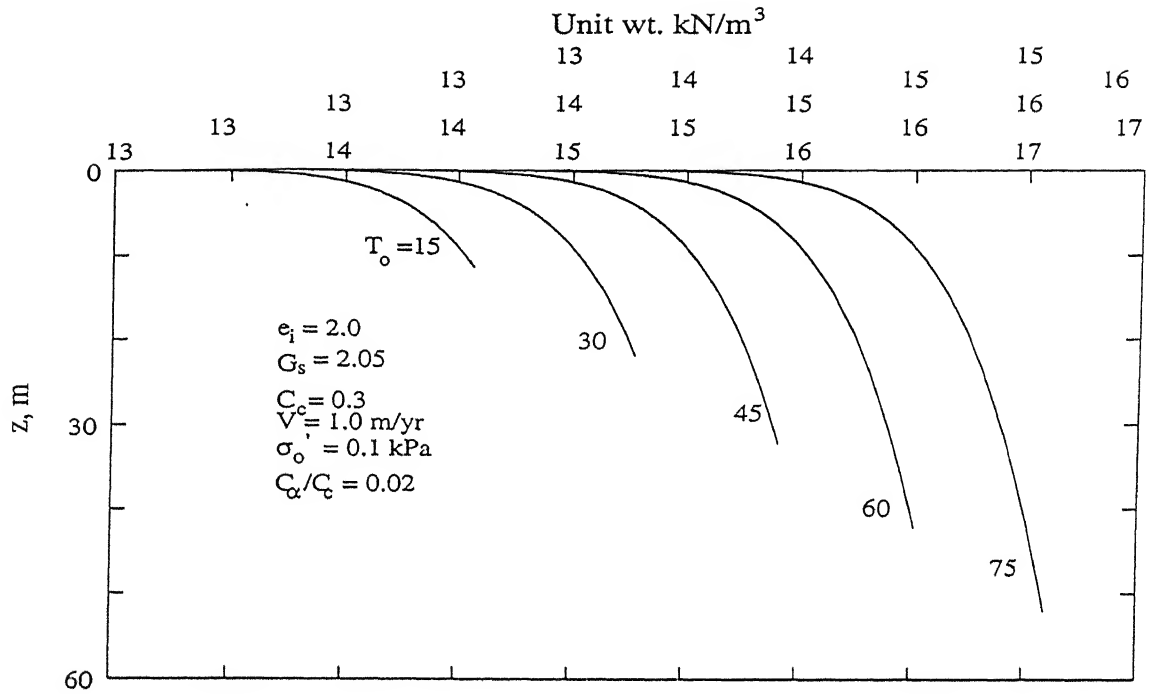
Figure 4.17: Effect of T_o, Time for Sedimentation on the Variation of Unit Weight with Depth.
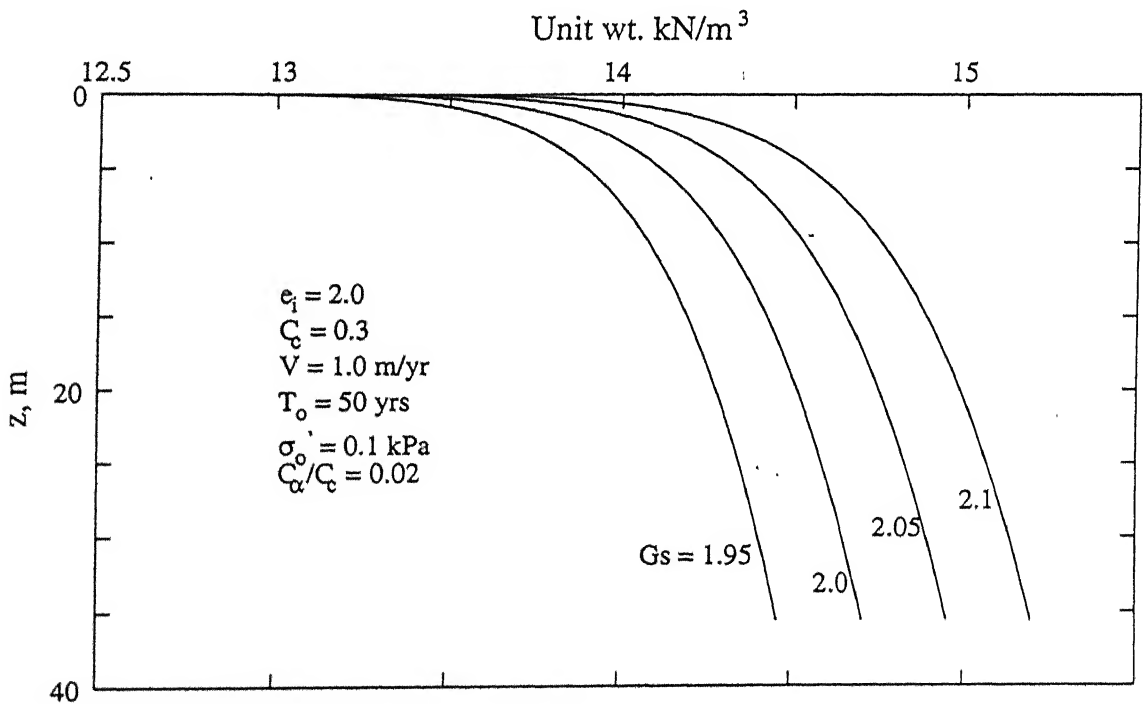
Figure 4.18: Effect of Specific Gravity on the Variation of Unit Weight with Depth

Effective Stress, kPa

0   100   180

0

z, m

20

$e_i = 2.0$
$C_c = 0.3$

$C_\alpha/C_c = 0.02$
$V = 1.0 m/yr$
$T_o = 50$ yrs
$\sigma_o' = 0.1$ kPa

$G_s = 2.1$
2.05
2.0

1.95

40
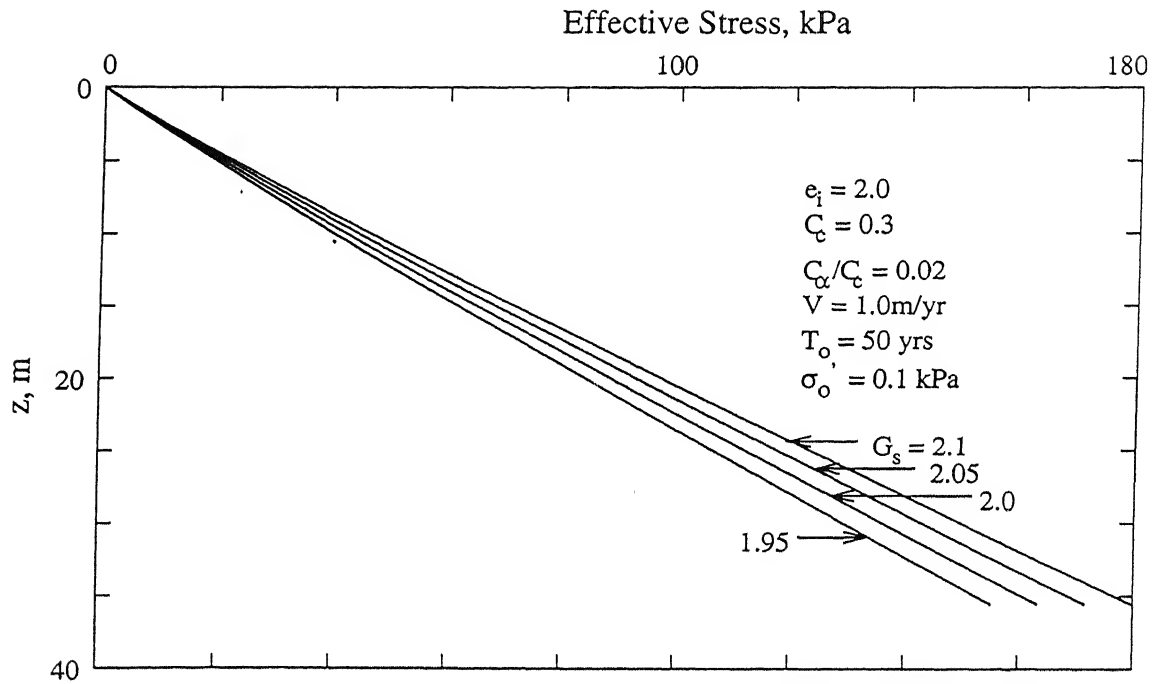
Figure 4.19: Effect of Specific Gravity on the Variation of Effective Stress with Depth

Void Ratio, e

0.5   1   1.2

0

Theoritical ⎯⎯
Experimental ◇

$e_i = 1.2$
$T_o = 50$ yrs
$G_s = 2.05$
$\sigma_o' = 10$ kPa
$V = 1.0$ m/yr
$C_{c_o} = 0.028$
$\mu = 1.11$

z, m

25

50

Figure 4.20: Comparison of Predicted and Experimental Void Ratios for Variable C_c

Figure 4.21: Variation of Compression Index, C_c, with Void Ratio

Figure 4.22: Effect of Variable C_c on the Variation of Void Ratio with Depth

65

CHAPTER 5

CONCLUSIONS

Based on the studies reported in chapters 3 and 4 following conclusions are made.

5.1 EXPERIMENTAL STUDY

1. The sedimented fly ash deposit exhibits a pseudo-overconsolidation effect possibly because of the pozzolanic activity.

2. Collapse Potential of fly ash is found could be of order of 1 % but much higher than that of compacted fly ash

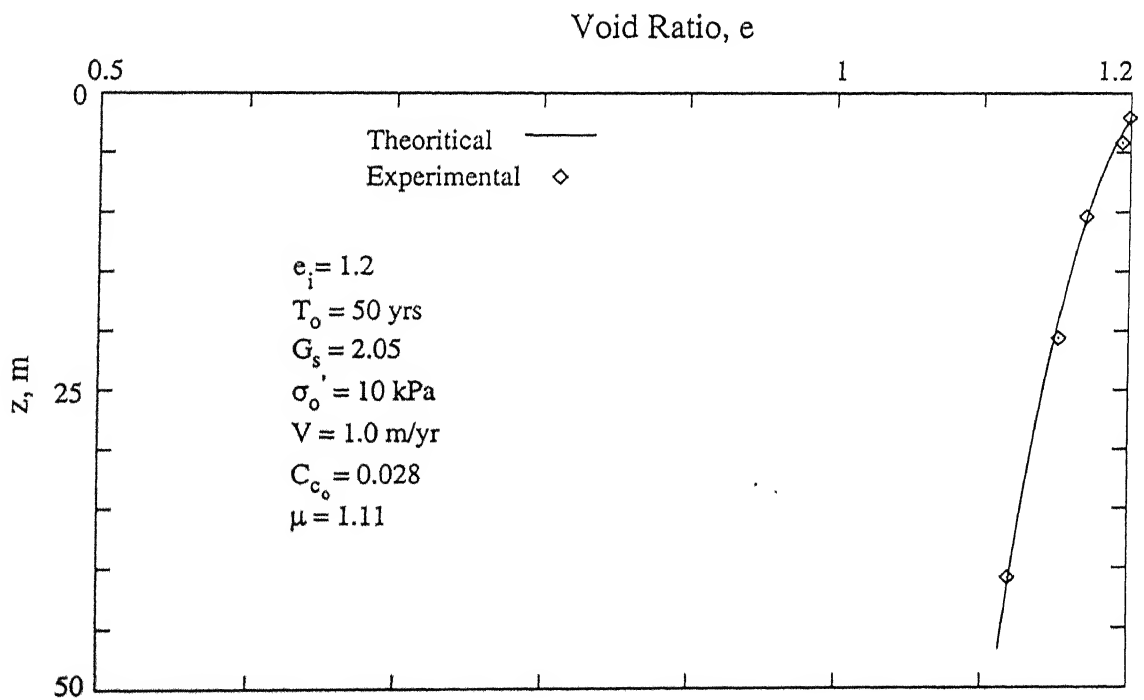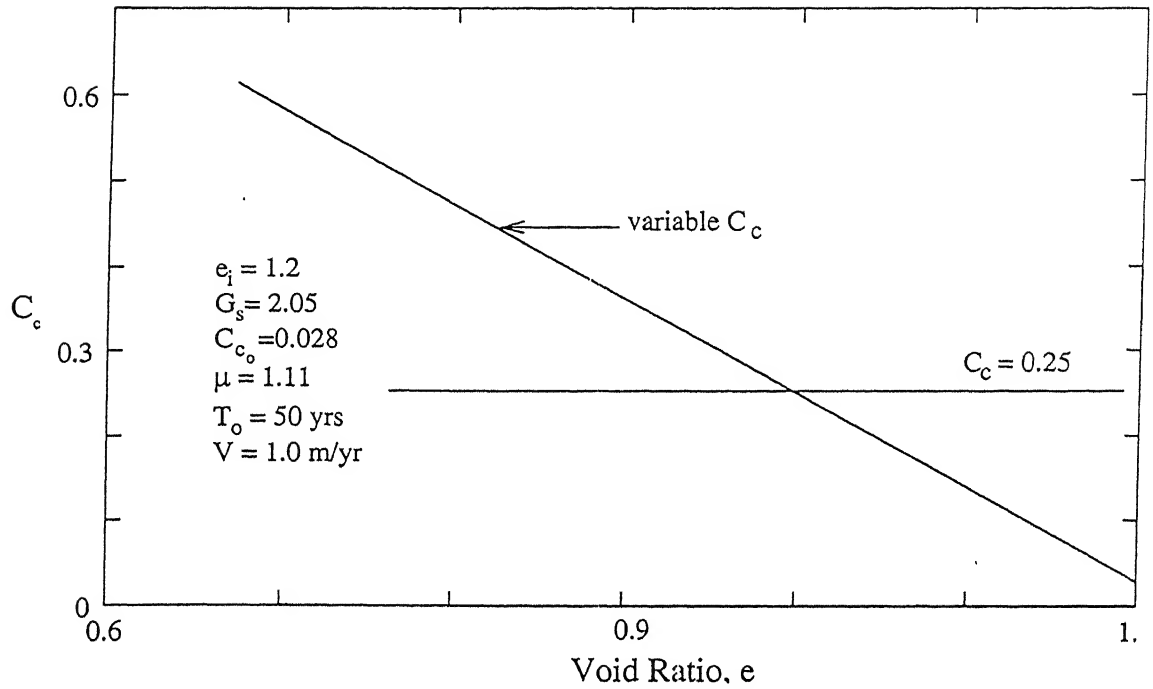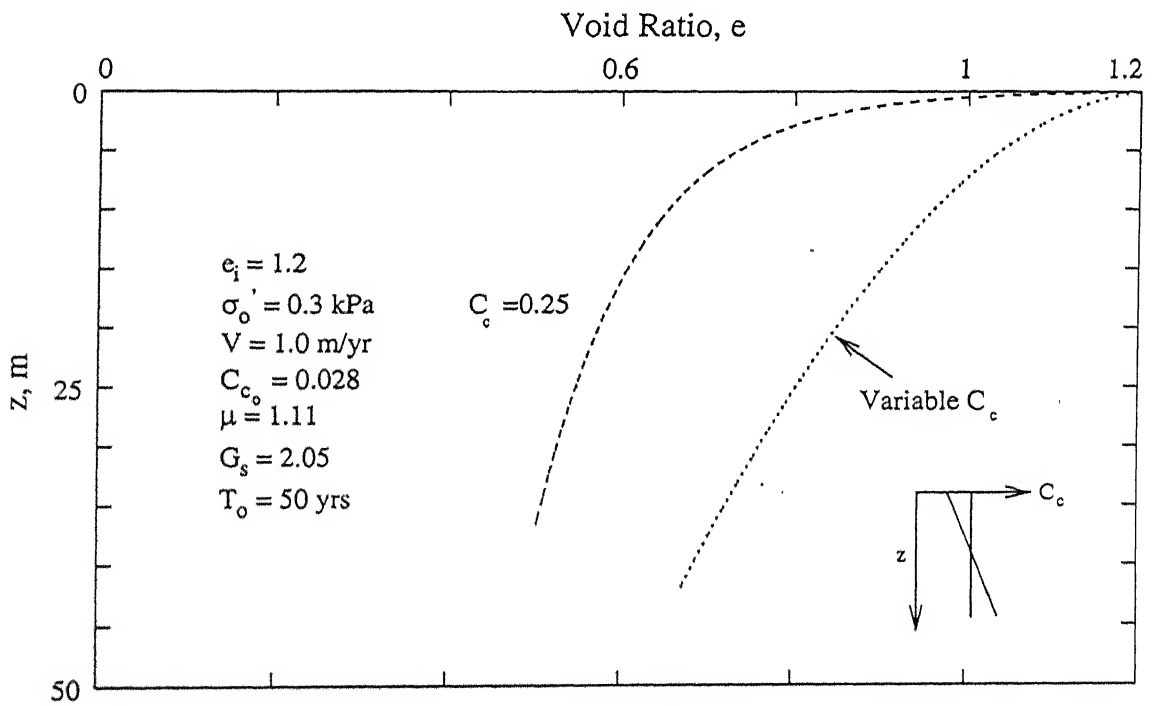3. Fly ash particles bond under high stresses may be due to pozzolanic activity as revealed through grain size distributions before and after compression under high stress.

4. Compression Index (C_c) of samples from the sedimented deposits increases with the average effective stress. The increase is sharp at smaller stresses and gradual at higher stresses.

5. Compressibility of sedimented fly ash deposits is more compared to that of compacted fly ash.

6. The average values of compression index of sedimented fly ash deposits are in the range of 0.1 to 0.2.

5.2 ANALYTICAL STUDIES

A new theory is proposed to estimate the variations of void ratio, unit weight and effective stress with depth of sedimented and consolidated deposit. Following are in the conclusions drawn based on the parametric study.

1. In the final stage, the void ratio decreases while the unit weight increases sharply with depth in the top 2 to 3 m. The effective stress increases non-linearly with depth.

2. Depositional rate has no effect on the variations of void ratio, unit weight and effective stress with depth, except that for a given period of deposition, the final thickness of the deposit increases with rate of deposition.

3. It is noted that the final profiles are sensitive to the initial effective stress from which compression and consolidation are initiated.

3. In the final stage, the void ratios at all the depths for the deposit with compression index, C_c, increasing with decrease in void ratio, e, are more while the corresponding unit weights and effective stresses are less compared to those in a deposit with compression index, C_c, constant with e.

4. The final thickness for the deposit with varying compression index is more than the deposit with C_c constant with e. The predicted void ratios for the deposit with varying C_c agree closely with predictions based on experimental results from one-dimensional consolidation tests.

REFERENCES

Ballisager, C. C. and Sorensen, J. L. (1981). "Fly Ash as Fill Material." *Proc., 10th Int. Conf. on Soil Mech. and Found. Engrg.,* (2), 297 – 301.

Been, K. and Sills, G. C. (1981). "Self-Weight Consolidation of Soft Soils: An Experimental and Theoretical Study." *Geotechnique,* 31(4), 519 – 535.

Bjerrum, L. (1967). "Engineering Geology of Norwegian Normally-Consolidated Marine Clays as Related to Settlements of Buildings." *Geotechnique,* 17, 81 – 118.

Capco (1990). "Pulverized Fuel Ash as a Reclamation fill." Report of the China Light and Power Co. Ltd., Hong Kong, 1 – 34.

Cargill, K. W. (1984). "Prediction of Consolidation of Very Soft Soil." *Journal of Geotechnical Engineering,* ASCE, 110 (6), 775 – 795.

Clemence, S. P. and Finbarr, A. O. (1981). "Design Consideration for Collapsible Soils." *Journal of Geotechnical Engineering Division,* ASCE, 107(3), 305 – 317.

Consoli, N.C. and Sills, G.C. (2000). "Soil Formation from Tailings: Comparison of Predictions and Field Measurements." *Geotechnique,* 50 (1), 25 –33.

Das, S.K. (1992). "Morphological, Chemical and Mineralogical Characterization of Some Indian Fly Ashes." *M.Tech Thesis,* Indian Institute of Technology, Kanpur

DiGioia, A. M. Jr. and Nuzzo, L.W. (1972). "Fly Ash as Structural Fill." *Journal of the Power Division,* ASCE, 98, 77-92.

Gandhi, S.R., Ashim, K.D. and Selvam, S. (1999). "Densification of Pond Ash by Blasting." *Journal of Geotechnical and Geoenvironmental Engrg.,* ASCE, 125(10), 889-899.

Gandhi, S. R. (2000). "Densification of Deposited Ash Slurry." *Management of Ash Ponds for Human Settlements.* Narosa Publishing House, New Delhi, 94 – 106.

Ghosh, A. and Bhatnagar, J. M. (1999). "Reclamation of Abandoned Fly Ash Ponds for Human Settlements: A Case Study." *Fly Ash Disposal and Deposition Beyond 2000 A.D.* Narosa Publishing House, New Delhi, 162 – 172.

Ghosh, A., Singh, A., Dinesh., Kumar, D., Misra, S. K., Bhatnagar, J. M. and Singh, J. (1997). "Geotechnical Investigations on Abandoned Fly Ash Pond for Human Settlemments." *Indian Geotechnical Conference,* Vadodara, 379 – 378.

Gibson, R. E., England, G. L. and Hussey, M. J. L. (1967). "The Theory of One-Dimensional Consolidation of Saturated Clays. I. Finite Non-linear Consolidation of Thin Homogeneous Layers." *Geotechnique*, 17, 261 – 273.

Gibson, R. E., Schiffman, R. L. and Cargill, K.W. (1981). "The Theory of One-Dimensional Consolidation of Saturated Clays. II. Finite Non-linear Consolidation of Thick Homogeneous Layers." *Canadian Geotechnical Journal*, 18(2), 280 – 293.

Gray, D.H. and Lin, Y.K. (1972). "Engineering Properties of Compacted Fly Ash." *Journal of Soil Mechanics and Foundations Division*, ASCE, 98 (4), 361 – 379.

Havukainen, J. (1983). ``The Utilization of Compacted Coal Ash in Earth Works.'' *Proc. 8th Euro. Conf. on Soil Mech. and Found. Eng.*, (2), 773 – 776.

Kaniraj, S. R. and Havanagi, V. G. (1999). "Geotechnical Characteristics of Fly Ash-Soil Mixtures." *Journal of South East Asian Geotechnical Society*, 30(2), 129 – 147.

Kolay, P. K. (2000). "Characterization, Water-Interaction and Zeolitization of a Lagoon Ash." *Ph. D Thesis*, Indian Institute of Technology, Bombay.

Koppula, S. D., and Morgenstern, N. R. (1982). ``On the Consolidation of Sedimenting Clays.'' *Candian Geotechnical Journal*, 19, 260 – 268.

Lee, K. and Sills, G. C. (1981). "The Consolidation of A Soil Stratum, Including Self-Weight Effects and Large Strains." *Int. Journal for Numerical and Analytical Methods in Geomechanics*, 5, 405 – 428.

Leonards, G. A. and Bailey, M. B. (1982). "Pulverized Coal Ash as Structural Fill." *Journal of Geotechnical Engineering Division*, ASCE, 108 (4), 517 – 531.

Madhav, M. R. and Ghosh, A. (1999). "Reclamation of Fly Ash Beds with Granular Piles." *Fly Ash Disposal and Deposition Beyond 2000 A. D.* Narosa publishing House, New Delhi, 122 – 129.

Martin, J. P., Collins, R. A., Browning, J. S. and Biehl, F. J. (1990). "Properties and Use of Fly Ashes for Embankments." *Journal of Energy Engineering*, 116 (8), 71 – 86.

McLaren, R. J. and Digioia, A. M. Jr. (1987). "The Typical Engineering Properties of Fly Ash." *Proc. of the Conf. on Geotechnical Practice for Waste Disposal*, Geotechnical Special Publication No. 13, ASCE, 683 – 697.

Mesri, G. (1973). "Coefficient of Secondary Compression." *Journal of the Soil Mechanics and Foundation Division*, ASCE, 99 (1), 123 – 137.

Mesri, G. and Godlewski, P. M. (1977). "Time- and Stress-Compressibility Interrelationship." *Journal of the Geotechnical Engineering Division*, ASCE, 103 (5), 417 – 430.

Myint, B.W., Choa, V., Arulrajha, A. and Na, Y. M. (1999). "One-Dimensional Compression of Slurry with Radial Drainage." *Soils and Foundations*, 39(4), 9 – 17.

Morris, P. H. (2002). "Analytical Solutions of Linear Finite-Strain One-Dimensional Consolidation." *Journal of Geotechnical and Geoenvironmental Engineering*, ASCE, 128 (4), 319 – 326.

Pandian, N. S., Rajasekhar, C. and Sridharan. A. (1998). "Studies of the Specific Gravity of Some Indian Coal Ashes." *Journal of Testing and Evaluation*, ASTM, 26(3), No. 3, 177 – 183.

Raza, S. A., Khan, M. A., Ahmad, M. S. and Kumar, S. (1999). "Consolidation Behaviour of Treated and Reinforced Fly Ash." *Fly Ash Disposal and Deposition: Beyond 2000 A.D.* Narosa Publishing House, New Delhi, 216 – 222.

Saito, T., Lizuka, A., Kitamura, A. and Ohta, H. (2001). "Geological Approach to the Void Ratio of Aged Clays Based on Bjerrum's Hypothesis." *Journal of the Southeast Asian Geotechnical Society*, 32(3), 153 – 163.

Singh, D. N. (1989). "Engineering Properties of Compacted Panki Fly Ash." *M.Tech Thesis*, Indian Institute of Technology, Kanpur.

Sinha, U. N., Karthigeyan, S., Bhargava, S. N. and Sharma, A. K. (1998). "Compressibility Characteristics of Pond Ash used as Geomaterial." *Indian Geotechnical Journal*, 4, 377 – 387.

Skarzynska, K. M., Rainbow, A. K. M. and Zawisza, E. (1989). "Characteristic of Ash in Storage Ponds." *Proc. of the 12th Int. Conf. on Soil Mech. and Found. Eng.*, Rio de Janerio, 3, 1915 – 1918.

Sridharan, A. and Prakash, K. (1998). "Chracteristic Water Contents of a Fine-Grained Soil-Water System." *Geotechnique*, 48(3), 337 – 346.

Sridharan, A., Pandian, N. S. and Rajasekhar, C. (1996). "Geotechnical Characterization of Pond Ash." *Ash Ponds and Ash Disposal Systems*, Narosa Publishing House, 97 – 110.

Web, D. L. and Hughes, T. S. (1987). "The Consolidation Characteristics of Fly Ash. – A Valuable Resource." *Proc. of the CSIR Conference*. Pretoria, Republic of South Africa.

Yudhbir and Honjo, Y. (1991). "Applications of Geotechnical Engineering to Environmental Control." *Proc. of the 9th Asian Regional Conf. on Soil Mech. and Found. Eng.*, Bangkok, Thailand, 2, 431 – 469.

Znidarcic, D., Shiffman, R.L., Pane, V., Croce, P., Ko, H.Y. and Olsen, H.W. (1986) "The Theory of One-Dimensional Consolidation of Saturated Clays: Part V, Constant Rate of Deformation Testing and Analysis." *Geotechnique*, 36(2), 227-237.

APPENDIX

A-1 ANALYTICAL STUDY

Comparison of Predictions with Measured In Situ Results: The proposed method is used to predict the measured field data of bauxite tailings, usually called red muds, at the Ouro Perto site (Consoli and Sills, 2000). Specific gravity of the material is in the range 2.9 – 3.1, because of high iron content. The compression index, C_c, determined by a constant rate deformation test (Zinidarcic et al., 1986) is 2.8. Field measurements of void ratio with depth are made up to a depth of 7 m. The variation of void ratio with depth of bauxite tailings is predicted using the present approach with $G_s = 3.0$, $C_c = 2.8$ and assuming $V = 1.0$ m/yr, $T_0 = 15$ years, $C_\alpha/C_c = 0$ and $\sigma_o' = 1.5 - 5.6$ kPa. Good agreement between the predicted values and the field data over the depth of 7 m for $\sigma_o' = 2.8$ kPa can be noted (Fig. A1).
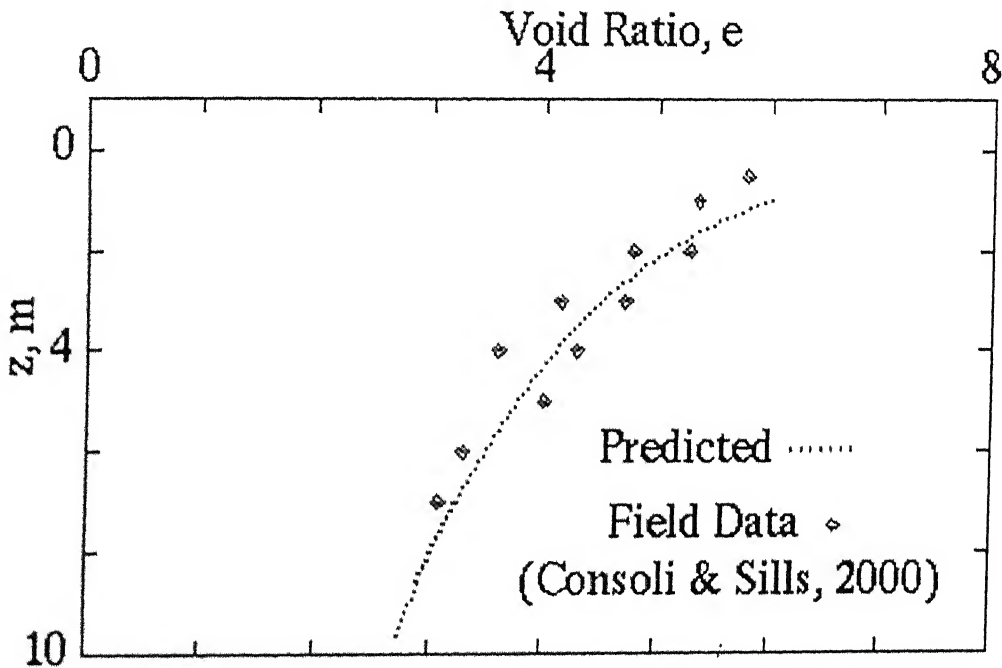

Figure A-1 Comparison of Field Data of Bauxite Tailings with Predicted Values